# Optimal Energy Management of Distribution Systems and Industrial Energy Hubs in Smart Grids

by

Sumit Paudyal

A thesis
presented to the University of Waterloo
in fulfillment of the
thesis requirement for the degree of
Doctor of Philosophy
in
Electrical and Computer Engineering

Waterloo, Ontario, Canada, 2012

© Sumit Paudyal 2012

I hereby declare that I am the sole author of this thesis. This is a true copy of the thesis, including any required final revisions, as accepted by my examiners.

I understand that my thesis may be made electronically available to the public.

## Abstract

Electric power distribution systems are gradually adopting new advancements in communication, control, measurement, and metering technologies to help realize the evolving concept of Smart Grids. Future distribution systems will facilitate increased and active participation of customers in Demand Side Management activities, with customer load profiles being primarily governed by real-time information such as energy price, emission, and incentive signals from utilities. In such an environment, new mathematical modeling approaches would allow Local Distribution Companies (LDCs) and customers the optimal operation of distribution systems and customer's loads, considering various relevant objectives and constraints.

This thesis presents a mathematical model for optimal and real-time operation of distribution systems. Thus, a three-phase Distribution Optimal Power Flow (DOPF) model is proposed, which incorporates comprehensive and realistic models of relevant distribution system components. A novel optimization objective, which minimizes the energy purchased from the external grid while limiting the number of switching operations of control equipment, is considered. A heuristic method is proposed to solve the DOPF model, which is based on a quadratic penalty approach to reduce the computational burden so as to make the solution process suitable for real-time applications. A Genetic Algorithm based solution method is also implemented to compare and benchmark the performance of the proposed heuristic solution method. The results of applying the DOPF model and the solution methods to two distribution systems, i.e., the IEEE 13-node test feeder and a Hydro One distribution feeder, are discussed. The results demonstrate that the proposed three-phase DOPF model and the heuristic solution method may yield some benefits to the LDCs in real-time optimal operation of distribution systems in the context of Smart Grids.

This work also presents a mathematical model for optimal and real-time control of customer electricity usage, which can be readily integrated by industrial customers into

their Energy Hub Management Systems (EHMSs). An Optimal Industrial Load Management (OILM) model is proposed, which minimizes energy costs and/or demand charges, considering comprehensive models of industrial processes, process interdependencies, storage units, process operating constraints, production requirements, and other relevant constraints. The OILM is integrated with the DOPF model to incorporate operating constraints required by the LDC system operator, thus combining voltage optimization with load control for additional benefits. The OILM model is applied to two industrial customers, i.e., a flour mill and a water pumping facility, and the results demonstrate the benefits to the industrial customers and LDCs that can be obtained by deploying the proposed OILM and three-phase DOPF models in EHMSs, in conjunction with Smart Grid technologies.

## Dedication

I dedicate this work to my parents, my brother Amit, and my wife Saru for their unconditional love, support, and encouragement.

# Contents

# List of Tables

# List of Figures

# Glossary of Terms

AMI        Advanced Metering Infrastructure

ANSI      American National Standards Institute

B&B        Branch and Bound

CDM      Conservation and Demand Management

CPU       Central Processing Unit

CVR       Conservation Voltage Regulation

DA         Distribution Automation

DER       Distributed Energy Resource

DLF       Distribution Load Flow

DOPF    Distribution Optimal Power Flow

DR         Demand Response

DSM       Demand Side Management

EA         Evolutionary Algorithm

EHMS    Energy Hub Management System

EV         Electric Vehicle

FIT        Feed-in-Tariff

GA         Genetic Algorithm

GAMS    General Algebraic Modeling System

GEA       Green Energy Act

GHG      Green House Gas

| | |
|---|---|
| HAN | Home Area Network |
| HOEP | Hourly Ontario Electricity Price |
| I/O | Input/Output |
| IESO | Independent Electricity System Operator |
| LDC | Local Distribution Company |
| LP | Linear Programming |
| LTC | Load Tap Changer |
| MILP | Mixed Integer Linear Programming |
| MINLP | Mixed Integer Non-linear Programming |
| NAN | Neighborhood Area Network |
| NLP | Non-linear Programming |
| OILM | Optimal Industrial Load Management |
| PSO | Particle Swarm Optimization |
| RTP | Real-time Pricing |
| SC | Switched Capacitor |
| SCADA | Supervisory Control and Data Acquisition |
| TOU | Time-of-Use |
| VR | Voltage Regulation |
| VVC | Volt/var Control |
| WAN | Wide Area Network |

# Chapter 1

# Introduction

## 1.1 Research Motivation

The economic growth and development of a country is reflected on its energy consumption patterns and per capita energy consumption. As reported by the U.S. Energy Information Administration, the world consumption of marketed energy is expected to increase by 44% over the period from 2006 to 2030, and the energy consumption from electricity usage is expected to increase by 77% [8]. Therefore, electric utilities need to meet this growing demand for electrical energy. In the context of Ontario, it has been determined that the province's total generation capacity will double by 2030, considering the retirement of 80% of its existing generation capacity [9].

The other facet of increased energy consumption is its impact on the environment. Several industrialized countries have committed themselves to agreements such as the Kyoto Protocol [10] and the Copenhagen Accord [11] to limit world greenhouse gas (GHG) emissions. After withdrawing from the Kyoto Protocol, Canada has set a new target of 17% reduction in GHG emissions from its 2005 levels by 2020, under the Copenhagen Accord [12].

In view of the above, there is a need to create new supply capacity in the system in order to meet the rapid growth in demand and also to reduce GHG emissions, at the same time. This can be partially achieved through energy conservation, energy management and deployment of renewable energy resources. In this context, the Green Energy Act (GEA) was enacted in Ontario in 2009, which has set the following objectives for the Ontario Energy Board and electric utilities in Ontario [13]:

- Promote investments in renewable energy resources.

- Promote conservation and energy management.

- Facilitate the implementation of Smart Grids.

The GEA has resulted in incentive programs such as the Feed-in-Tariff (FIT) and micro-FIT to motivate an increased integration of Distributed Energy Resources (DERs) in Ontario [14]. It is envisaged that the development of renewable energy based generation options in Ontario will help phase out coal-fired electricity generation by 2014, and increase the contribution of renewable energy in the total supply mix to 34% by 2025 [15].

Similarly, there are initiatives for energy conservation and management, as Ontario has set a goal to reduce the system peak demand by 6,300 MW by 2025 through Demand Side Management (DSM), Demand Response (DR), and demand control programs [15]. Among various customer sectors, the industrial sector has a large potential for peak demand reduction and other energy management activities, since it is the largest and an ever growing contributor to the energy demand in developed countries. For example, in Canada, the industrial sector accounted for 47% of the total energy consumption in 2008 (see Figure 1.1) [1]. To attain the peak demand reduction goals in Ontario, DR programs (such as DR 1, DR 2, DR 3) has been already enacted, with a target of 214 MW reduction in the peak demand and 640 GWh per year reduction in energy demand by 2014 from the industrial sector [16].
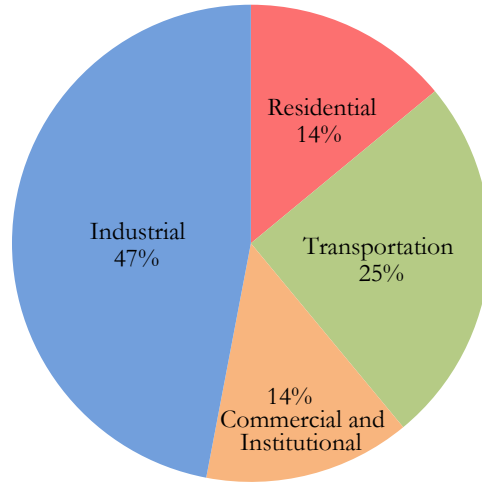
Figure 1.1: Share of energy consumption by sector in Canada in 2008 [1].

In order to help achieve the energy management objective set out by GEA, a pilot project has been initiated at the University of Waterloo in collaboration with other partners[1], to design and implement Energy Hub Management Systems (EHMSs) for different customer sectors in Ontario [17]. The EHMS is geared towards real-time management of energy activities at energy hubs, i.e., physical locations that produce, conserve, store, and consume energy for various customer sectors: residential, commercial and institutional, agricultural, and industrial [17, 18]. The EHMS is based on Smart Grid technologies such as Advanced Metering Infrastructure (AMI), improved communications and control infrastructure, and real-time information systems, which are gradually being incorporated in Ontario's grid [19, 20].

With the evolving concept of Smart Grids, Local Distribution Companies (LDCs) are gradually integrating advanced technologies in distribution systems. Also, because of environmental concerns and with incentives from regulators, Smart Grids are expected to accommodate high levels of DER and Electric Vehicle (EV) penetration. Furthermore, dynamic pricing schemes are expected to encourage LDCs to integrate into their systems

---

[1]Ontario Centres of Excellence (OCE), Hydro One Inc., Energnet Inc., Milton Hydro Distribution Inc., and Ontario Power Authority (OPA).

the customers participating in DSM, DR, and demand control programs, thereby turning distribution systems into smart networks, where intelligent operation and management of various resources will result in enhanced benefits to all involved entities [21–28].

The aforementioned developments have motivated the present research to propose and develop methodologies to optimally operate distribution systems and industrial loads, based on Smart Grid technologies, both at the LDC system and customer levels.

## 1.2   Literature Review

This section presents a review of the state-of-art research and developments reported in the technical literature in the following areas relevant to this work: Smart Grids, Distribution Automation (DA), distribution system operation, DSM, DR, and EHMS.

### 1.2.1   Smart Grids

Variations exist within the power industry regarding the definition of Smart Grids, as Smart Grid is neither a single concept nor a single technology. The U.S. Department of Energy states: "Think of the Smart Grid as the internet brought to our electric system. Devices such as wind turbines, plug-in-hybrid vehicles and solar arrays are not part of the Smart Grid. Rather Smart Grid encompasses the technologies that enables us to integrate, interface with and intelligently control these innovations and others" [22]. On the other hand, KEMA defines the Smart Grid as: "The Smart Grid is the networked application of digital technology to the energy delivery and consumption segments of the utility industry. More specifically, it incorporates advanced applications and the use of DERs, communications, information management, and automated control technologies to modernize, optimize, and transform the electric power infrastructure. The Smart Grid vision seeks to bring together these technologies to make the grid self-healing, more

reliable, safer, and more efficient, as well as to use intelligent meters and devices to empower customers to use electricity more efficiently. It also seeks to contribute to a sustainable future with improvements to national security, economic growth, and climate change" [29]. Thus, the Smart Grid can be viewed as a combination of various concepts and technologies, whose interpretations depend on the users [30]. However, the key functions of Smart Grid technologies are to improve flexibility, security, reliability, efficiency, and safety in electricity systems [20, 22].

Smart Grid encompasses all sorts of innovations, some of which are still in the development phase, while others are technologies already in use. Since communication and control infrastructure is prominently existent in transmission systems, the development of such infrastructure as well as technology and applications at distribution and customer levels are critical for the realization of Smart Grids. References [30, 31] list some of the many technologies of Smart Grids targeted at the customer level, such as Smart Meters, AMI, smart appliances, Home Area Network (HAN), home/building automation, process automation, etc. The EHMS pilot project also pertains to the development of a Smart Grid technology at the customer's end, which can be deployed for the benefits of both the customers and the LDC [17]. At the distribution system level, Smart Grid technologies include DA, technologies for selective load control, micro-grids, etc.

The province of Ontario has already initiated the integration of Smart Grid technologies in its distribution systems. For example, Ontario has completed the installation of Smart Meters in every home and small businesses in the province and a central "Meter Data Management and Repository" system, which is the first visible step towards a Smart Grid. LDCs in Ontario are actively participating in various Smart Grid pilot projects related to DR, self-healing grid, integration of EVs into the grid, and home/building automation systems. It is anticipated that by 2015, there would be a large-scale integration of energy management systems and smart appliances, feeder and substation automation technologies,

and implementation of projects involving energy storage, DR, and energy management programs [19]. By the year 2020, technologies for micro-grids and convenient charging of EVs is expected to be readily available. It is envisioned that the Smart Grid infrastructure in Ontario will support large penetration of DERs, EVs, and EHMSs, which can be deployed either at the system level or at the customer level for the optimal operation of distribution systems or customers' energy consumption [19, 20].

## 1.2.2   Distribution Automation (DA)

DA is a key technology for the realization of the benefits from a Smart Grid at the distribution system level. IEEE defines DA as: "A system that enables an electric utility to remotely monitor, coordinate and operate distribution components, in a real-time mode from remote locations" [32].

The concept of DA began in 1970s, when computer and communication technologies were evolving. Since then, implementation of DA in utilities has been governed by existent monitoring, control, and communication technologies. Some small pilot projects on DA were implemented by utilities in the 1970s, and there were several major pilot projects in 1980s. By the 1990s, the changes in technologies resulted in several large and many small projects at various utilities [33–35].

In recent years, in response to the growing demand to improve reliability and efficiency of the power system, more automation is being implemented in the distribution system. Reference [36] presents a survey of some utilities in U.S. on the present status of DA implementation and future plans. For instance, Southern California Edison has automated 2,400 distribution switches, 960 remote reclosers, and 7,500 switched capacitor (SC) banks, and also implemented load interruption programs targeted to large customers. Pacific Gas & Electric has substation Supervisory Control and Data Acquisition (SCADA) systems, an extensive capacitor control system, a system to automatically operate reclosers for

reconfiguration, and other DA technologies. The survey [36] reveals the current status of DA, some of which can be summarized as follows:

- Most utilities have SCADA systems which provide information and control at the substation level.

- The next generation of DA systems is expanding automation and reconfiguration of distribution circuits at the component level such as switches, SCs, and Load Tap Changers (LTCs). Most utilities have already carried out some demonstration projects.

- Capacitor automation and coordination with voltage regulators for Volt/var Control (VVC) are becoming relatively common, mostly based on radio links.

Some of the plans of the surveyed utilities toward the implementation of DA technologies can be summarized as follows [36]:

- Automation of circuit reconfiguration.

- Implementation of faster communication and continuous advanced monitoring.

- Integration of AMI, which allows integration of customer load control and load response.

- Automation to facilitate integration of DERs.

## 1.2.3   Distribution System Operation

Conventional distribution system operation has been treated as a VVC problem over the years, dealing with regulation of distribution system voltage and reactive power (var). Distribution transformers are equipped with LTCs for voltage control purposes, while

SCs and fixed capacitors installed at various locations assist in voltage and reactive power control. Although, the primary objective of VVC is to regulate the voltage and reactive power in distribution systems, with availability of additional control equipment, VVC can add flexibility in distribution system operations to achieve certain optimization objectives. Traditionally, distribution loss minimization has been the optimization criterion in most cases [37–41].

The integer control of LTCs and SCs renders the VVC problem a mixed-integer non-linear programming (MINLP) problem. Extensive work has been carried out regarding the solution approaches to VVC problems [37–39, 42–44], which can be broadly categorized as rule-based and network-based methods [45]. In [39], the authors propose a simple rule-based method for VVC, in which the control problem is decoupled into two sub-problems: voltage control by LTCs and var control by SCs, on the basis that the coupling is weak as explained in [46]. The authors propose a solution for the VVC problem for varying level of communication and measurement capabilities in distribution system.

In the rule-based methods, the operation of LTCs and SCs is based on a set of rules and operator's experience, but it does not require distribution network information. Hence, such methods are common where wide-area measurements are not available and VVC controls are based on local measurements of electrical quantities [47]. However, it is observed in [42] that a VVC based on local measurements require frequent revision of controller settings for seasonal load variations and network configuration changes. Also, the rule-based method does not yield an optimal solution to the VVC problem.

The network-based solution methods typically comprise a Distribution Load Flow (DLF) solution and an iterative optimization procedure. Solutions to DLF are usually obtained using a Newton-Raphson method [48, 49], or a fast-decoupled method adapted to distribution systems [50]. Special ladder network methods have also been proposed [51, 52], which employ forward and backward sweeps providing faster convergence in radial network configurations. In the earlier approaches, enumerative

techniques were considered to be an effective optimization procedure, as distribution systems had limited number of LTCs and SCs. However, for a larger system, the combinatorial solution approaches are computationally costly; thus, heuristic approaches as proposed in [37, 38, 42] are considered to solve VVC problems. In [37], the authors propose a relaxed integer programming technique to solve VVC problem, which substantially reduces computational time. Reference in [42] proposes a combinatorial method for the VVC problem based on a "fast power flow" technique to reduce the computational efforts. In [38], the authors combine artificial neural network (ANN) and fuzzy dynamic programming techniques to reduce computational time in solving VVC problem. In [41], the authors decouple the VVC problem into voltage and var control sub-problems, and use dynamic programming techniques to solve them in order to reduce the computational burden. In [53], the authors propose a heuristic method to solve a var control problem based on a "simplified network approach", which reduces the computational time and is suitable for real-time application. More recently, integrated optimization models and solution approaches have been proposed [43, 44], in which DLF model is treated as a constraint in the optimization model and solution. The present research proposes a distribution optimal power flow (DOPF) model in a similar integrated manner.

The implementation of real-time information systems, AMI, improved communication capabilities, more sensors, and improved infrastructure for control systems is envisaged to transform the conventional distribution system into a Smart Grid [21–28]. This will bring in flexibility in distribution system operations via centralized control of components such as LTCs and SCs [30, 54]. In this context, in [55], the authors propose a coordinated, centralized, and real-time voltage control scheme, which is based on the measurement and communication infrastructure available in Smart Grids. Moreover, the Smart Grid infrastructure would allow real-time control of distribution system components with various operational objectives related to economy, efficiency, reliability, environmental concerns, etc. [56], which is an improvement over predominantly existent VVC schemes based on local

measurements. Some of the distribution system operational objectives are discussed in [45], which include maintaining a unity power factor along the feeder, minimizing the power drawn from the substation, maximizing the revenue for systems with DERs, and others. A "conservation biased" voltage control concept is proposed in [57] to reduce the power demand by reducing distribution system voltage within acceptable ranges. In a centralized and coordinated control environment in Smart Grids, schedules to control its components can be obtained similarly to the centralized VVC problems discussed in [37, 38, 42]. The solution approaches are based on the network topology, real-time measurements and power flow equations [45]; thus, a DOPF model, such as the one proposed in this research is at the core of such centralized distribution system operations.

Accurate and comprehensive modeling of components and efficient computational methods are critical requirements for real-time operation and control of distribution systems. The large number of nodes, components and measurements encountered in practical distribution systems require significant data handling and impose a large computational burden [41], rendering the real-time continuous control of distribution system components practically impossible [56]. However, real-time analysis in 15 to 30 minute intervals under normal operating conditions are more manageable from a practical stand-point [56, 58]. In distribution system analyses, computational burden is typically reduced by assuming the distribution system to be a balanced three-phase system, and hence considering a single-phase equivalent model [40–44]. However, these models are not suitable for precise real-time operation and control applications, because of existence of untransposed three-phase feeders, single-phase laterals, and single-phase loads. A comprehensive three-phase feeder model with phase specific and voltage dependent load models need to be considered, as is the case of this research.

In distribution system optimization problems, a DLF [59, 60], and any of the MINLP solution methods discussed in [61–67], can be readily implemented to solve the three-phase DOPF problems. The optimal three-phase DLF problem reported in [58] is

solved in the range of 3-40s for a practical sized distribution system, which makes it applicable to real-time control. However, in [58], the control variables are modeled as continuous variables, which renders the problem a Non-linear Programming (NLP) problem. The computational times reported in [59, 60] for three-phase DLF problems are also promising for real-time applications. However, the issues pertaining to computational robustness and burden of MINLP solution methods are the main challenges for solving the three-phase DOPF for real-time control purposes. Moreover, complexity increases substantially for a 24-hour horizon because of the increased number of variables and the presence of inter-temporal constraints. Commercially available solvers (particularly BARON [68] and DICOPT [69]) are also not viable options, as these solvers are computationally inefficient to solve three-phase DOPF problems both in terms of robustness and CPU time [44]. This necessitates development of a heuristic solution method for the three-phase DOPF problem to reduce the computational burden, so as to make the solution process suitable for real-time applications in distribution system operation, as proposed in this work.

## 1.2.4 Demand Side Management (DSM) and Demand Response (DR)

DSM refers to the set of activities which result in a modification of the utilities' load profiles, bring about a reduction in energy and peak demand, and hence result in reduction of long-term generation capacity needs. DSM includes all sort of activities which leads to load shape modification including load control and DR at the utility level, and other activities behind the meter [70–72]. The IEEE DSM/CDM Techniques Working Group categorized all the different DSM/CDM alternatives, and developed guidelines for utilities to understand all the available options. A comprehensive description of the alternatives are presented in [73], which includes DSM through end-user and utility equipment control. The present research is based on these two alternatives.

The earliest DSM activities were carried out by U.S. utilities in the 1960s, and were directed to control residential costumers' specific appliances; however, successful large scale programs were implemented during the 1980s. In the 1990s, several million North American homes and commercial loads had a control receiver on one or more electrical appliances [74, 75]. Substantial efforts have been made in direct load control, which are implemented to achieve peak load reduction in residential, commercial, and industrial customers. These rely primarily on one-way-communication technologies (radio or power-line carrier) and receivers installed at the customer's end [76]. Most of the reported works on DSM are focused on air conditioning, water heater, and pool pumps in the residential sector [77–80], while in the commercial and industrial sectors, the activities are mainly focused on the control of heating, ventilation, air conditioning, and refrigeration systems [81, 82].

DR programs are designed to induce customers to change their energy usage behavior based on dynamic pricing, such as Time-of-Use (TOU) and Real-time Pricing (RTP), or other incentive signals from the utilities [75, 83, 84]. The effect of dynamic pricing combined with energy management approaches on load profiles have been studied for different customer sectors in [5, 18, 85, 86]. In [85], the authors argue that the use of TOU pricing and load shifting strategies may bring about 45% reduction in average monthly costs and 50% reduction in peak demand for residential customers. In [18], it is shown that energy costs and peak demand may by reduced by 13% and 35% respectively in residential customers through TOU pricing and an optimal energy management system. In [18], it is also shown that total costs (energy and demand charges) for a commercial produce storage and agricultural green house facility can be reduced by 40% through an optimal energy management system in an RTP regime. In [5], it is shown that for an industrial customer (flour mill), total costs can be reduced nearly by 7% using load shifting under a TOU tariff.

Most of the DSM activities in the industrial sector focus on voltage optimization and load shifting at the aggregated load level [87–91]. Voltage optimization is a way of

reducing power demand of loads by varying the voltage within limits prescribed by standards such as American National Standards Institute (ANSI) [92]. A Pacific Northwest study reveals that operating a distribution system in such a way can bring about 3% reduction in energy consumption [57]. In a separate study carried out in [88] for an industrial customer (fiberboard production facility), it is demonstrated that voltage optimization can yield about 5% reduction in energy consumption. Similarly, load shifting activities are discussed in [89–91], in the context of aggregated load profiles for industrial customers, demonstrating the possible reduction of peak demand, energy costs, and demand charges in the industrial sector through DSM activities.

The benefits that can be achieved from DSM programs mainly rely on customer's willingness for controlling its loads, and the availability of communication and control infrastructure. Because of the lack of two-way communication between a customer and the LDC control centre, and the lack of necessary infrastructure at the cutomer's premise for automated, optimal, and coordinated control of various loads, the DSM activities have been limited to a single objective, i.e., peak reduction, and to a few loads, but ignored the end user's preferences [77–82, 87–91]. With the advent of two-way communications (possible through Smart Meters and AMI) and home automation systems in Smart Grids, the realization of advanced DSM programs, such as the EHMS proposed in [18], becomes possible. Such DSM programs in Smart Grids can optimize the energy consumption based on a variety of objectives, fully accounting for the end user's preferences and comfort, and also the requirements of the LDC system operator. The present work tries to address some of these issues.

## 1.2.5  Energy Hub Management Systems (EHMSs)

Energy hub can be defined as a node in an electric power system through which the exchanges of energy and information with energy sources, loads, and the external system occur [93–95]. Thus, EHMS is another novel concept in Smart Grids which manages such

hubs for real-time management of energy activities such as production, consumption, storage, and conservation at the customer level for the benefit of both customers and utilities [17, 18].

The energy hub can range from aggregation of loads and energy sources at customer level to the aggregation of cluster of customers and DERs. In [18], four customer types: residential, commercial and institutional, agricultural, and industrial, are identified. In such EHMSs, the objectives of the customers and the utilities are different, thus a two-tier hierarchical scheme to distinguish between the different objectives of the customers and the utilities is used. At the lower level (referred to as micro-hub), the energy activities are optimized according to the customer's preferences. At the higher level (referred as macro-hub), on the other hand, the energy activities of a group of micro-hubs are optimized for the benefit of both the customers and utilities.

Some examples of possible objectives identified in [18] for micro-hub optimization are minimization of customers' energy cost, minimization of $CO_2$ emissions, or maximizing comfort level of the customers. Energy prices, system emission profile, and weather forecasts are examples of external information that the micro-hubs require as inputs (Figure 1.2). Among the objectives that utilities are interested in EHMS are load-shape modification and peak reduction, which are identified as possible objectives at the macro-hub level. The energy activities and the different objectives functions set at the micro-hubs in the EHMS would lead to load shape modifications which are responsive to price signals, weather, system emission profiles, customers' comfort, and incentive signals from utilities.

In [18], mathematical models required for the EHMSs for residential, commercial and agricultural customers are proposed, which yield optimal operational decisions on scheduling their major loads to achieve desired objectives related to energy cost, emissions, and comfort. In [96–98], mathematical models of various residential loads and energy sources are proposed in a similar context. This research proposes a similar general approach as [18] with an emphasis on mathematical models required for industrial
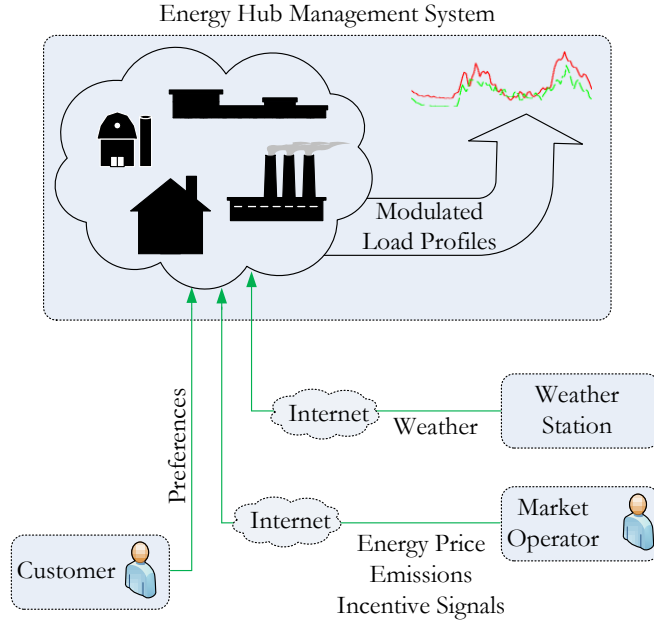
Figure 1.2: EHMS at micro-hub level.

EHMSs.

Mathematical models developed in [89–91] for DSM activities for industrial customers consider aggregated loads, ignoring the behavior of individual industrial processes and their interdependencies. Such models do not serve the main requirements of EHMSs, i.e., end-user preferences, and hence are not suitable for industrial EHMSs. On the other hand, the multi-objective optimization model for operational scheduling of water pumps [7], considers modeling of five independent centrifugal pumps. In [5], process dependencies in the modeling of a flour mill are presented, which, if generalized, can be applied to any process industry. In [99], the idea is extended to a petrochemical industry for optimal operation of a co-generation system considering the models of individual industrial processes. However, the mathematical models in [5, 7, 99] are very specific to the particular industry being modeled, where the industrial processes are simply represented by fixed active power loads independent of applied voltage and material flow

15

rates, ignoring interaction with the distribution system operation and other process variables. The proposed research focus on developing mathematical models required by industrial EHMS to achieve DSM benefits through load control and voltage optimization approaches. Consideration of customer behaviors and load interdependencies is an essential feature of the proposed EHMS modeling.

## 1.3 Research Overview and Objectives

The implementation of real-time information systems, AMI, improved communication capabilities, and improved infrastructure for control systems is envisaged to transform the existing distribution systems into Smart Grids [22]. These Smart Grids, because of environmental concerns and incentives from regulators, are expected to accommodate high levels of penetration of DERs and EVs [23]. Furthermore, dynamic pricing schemes and increasing environmental awareness is expected to encourage customers to participate in energy and demand management programs [23–25]. Similarly, at the customers' end, technologies such as smart meters, home/building automation, and industrial process automation render the electrical loads more manageable, controllable, and responsive to external signals [21–28]. Such Smart Grid technologies facilitate realization of customer's participation on utility's DSM, DR, and demand control programs at system and customer levels, and transform distribution systems into smart grids, where intelligent operation and management of various resources will result in enhanced benefits to customers and LDCs [14, 15].

This research proposes new features for Smart Grids relevant to LDC system operators and industrial customers, based on the optimal operation of distribution systems and industrial EHMSs.

## 1.3.1 Optimal Operation of Distribution Systems

In a Smart Grid environment, LDC system operators need to consider various operational objectives related to economy, efficiency, reliability, environmental concerns, etc. [56]. This research proposes a general mathematical framework from the perspective of LDCs, which incorporates various objectives and constraints related to optimal distribution system operation. Figure 1.3 presents a schematic of the proposed framework depicting control and information exchange among the distribution system, the LDC control centre, EHMS, and other external entities.

The optimization engine, shown in Figure 1.3, consists of a mathematical model along with an appropriate solution method suitable for real-time applications. Observe that real-time information systems will allow customers access to information such as energy price, emissions, incentives signals and weather; these data are essential components of the customer's EHMS. The optimization engine can readily gather information on distribution system status and customers' load profiles, possibly optimized by EHMSs, through Smart Meters and AMI technologies. This information becomes then an essential part for the mathematical model, which yields optimal schedules for the control of distribution system equipment. The infrastructure in Smart Grids would allow the LDC system operator to send the optimal schedules in real-time, in a coordinated and centralized manner, to dispatch the control equipment.

It is important to mention here that the proposed research is not focused on the development of distribution system optimization models considering the devices and customers' particular interests; it rather focuses on the development of models to optimize the operation of distribution systems as viewed by the LDC system operator. However, the behavior of customers with EHMSs is considered here to reflect their effect on distribution system operation.
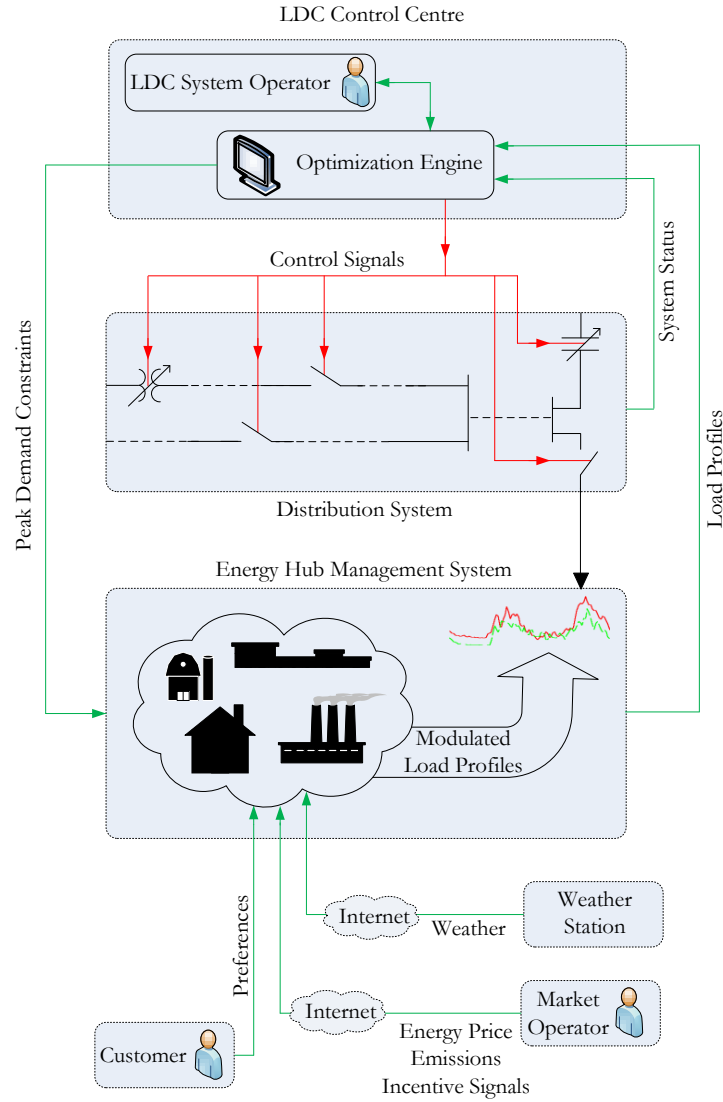
Figure 1.3: Schematic of the proposed distribution system operation in Smart Grid.

## 1.3.2 Optimal Operation of Industrial EHMSs

Figure 1.4 presents the proposed schematic of an industrial customer's EHMS and its integration with the transmission system and the distribution grid as part of a Smart
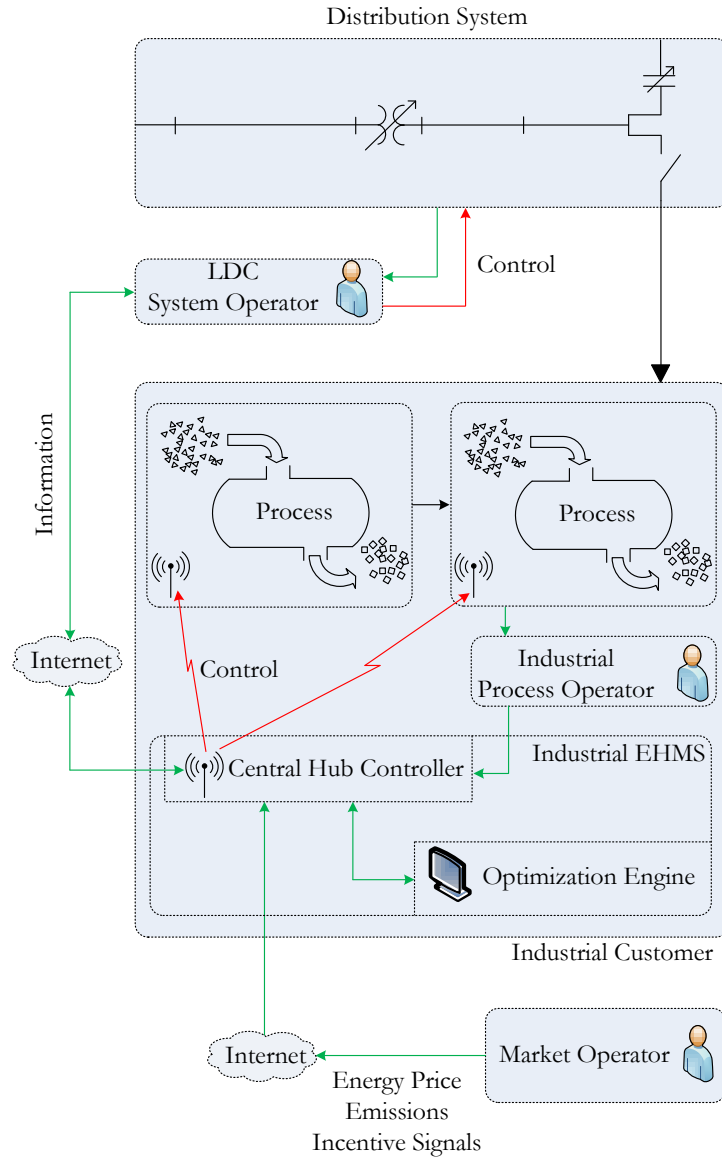
Figure 1.4: Schematic of the industrial EHMS and external system.

Grids. The proposed EHMS configuration consists of two main components: a central hub controller and an optimization engine. Real-time information systems and communication infrastructure in Smart Grids allow the central hub controller access to information such

as energy price, emissions, and incentive signals related to DR from the market operator. The central hub controller also receives information on the industrial processes and their operating preferences from an industrial process operator, and exchanges information on aggregated load profiles with an LDC system operator for proper coordination with the corresponding distribution feeder operation and control of LTCs and SCs.

The optimization engine, shown in Figure 1.4, consists of an industrial load management model and a solution method suitable for real-time applications. The information gathered by the central hub controller is communicated to the optimization engine, which includes the system parameters and models required for load management. The optimization engine yields optimal schedules for the industrial processes, which are then communicated to the processes by the central hub controller to dispatch them.

## 1.3.3 Research Objectives

In light of the literature review and discussions presented in the previous sections, the main novel objectives of the present research can be formulated as follows:

- Develop a mathematical framework for the optimal operation of distribution systems considering comprehensive models of unbalanced three-phase distribution system components and voltage dependent loads. The novel modeling framework, referred to as three-phase DOPF model, will have the possibility to consider various operational objectives in distribution systems, such as the proposed objective of minimizing the energy purchased from the external grid and the number of switching operations of LTCs and SCs.

- The proposed three-phase DOPF model will be an MINPL problem, because of the presence of integer variables associated with the discrete nature of LTCs and SCs. Therefore, with the aim of obtaining a practical and useful solution for real-time applications, a heuristic method will be developed to solve the three-phase DOPF

model based on the "Quadratic Penalty" used in [43, 44]. The proposed solution technique will be benchmarked against a Genetic Algorithm (GA) based method to compare its performance in terms of computational burden and solution optimality.

- Develop a generic Optimal Industrial Load Management (OILM) model that can be readily incorporated into the EHMSs for industrial customers for real-time automated and optimal scheduling of their processes. The OILM model will seek to minimize the total energy costs and/or demand charges for industrial customers, including a set of equality and inequality constraints to represent the industrial process, storage units, operator's requirements, and other relevant constraints. The OILM model will then be integrated with the DOPF model by using the available distribution system information and control expected in Smart Grids so that maximum savings can be obtained by optimally managing the loads and distribution system voltage control components such as LTCs and SCs.

## 1.4 Thesis Outline

The remainder of the thesis is organized as follows: Chapter 2 briefly discusses the main background topics and tools pertaining to the proposed research. Thus, a background to distribution system components and operations is presented first, followed by a discussion on smart distribution grid infrastructure. The chapter also presents the basics of mathematical programming models, modeling tools, and curve fitting technique that are relevant to the present research.

Chapter 3 presents distribution system components modeling and a novel three-phase DOPF. The proposed heuristic and GA-based solution methods for the three-phase DOPF model are discussed next. The chapter also demonstrates the applicability of the proposed three-phase DOPF model and solution methods through case studies

considering two different realistic distribution feeders. Comparative studies of the two solution methods in terms of optimality and computational burden are presented as well.

Chapter 4 presents the proposed OILM model for industrial EHMSs. The estimation of model parameters and results of case studies considering two industrial customers and their distribution feeders are also presented, demonstrating the applicability of the proposed OILM and DOPF models.

Chapter 5 presents the main conclusions and contributions of the research, and some directions for the future work. Finally, the Appendix provides relevant data required for the simulation case studies presented in Chapter 4.

# Chapter 2

# Background

## 2.1  Introduction

This chapter presents a background review of the main concepts and tools pertaining to the research presented in this thesis. First, some aspects of distribution system components, infrastructure, and operations are discussed in Section 2.2. This is followed, in Section 2.3, by an overview of mathematical programming, solution methods, and available tools that are closely related to the present research. Finally, in Section 2.4 the basics of curve fitting technique relevant to this work are discussed.

## 2.2  Distribution Systems

Distribution system refers to the section of an electric power system between the sub-transmission system and the customer's end. Distribution systems are generally considered to be electricity supply network operating at voltage levels of 132 kV and below; the typical distribution voltages in North America are 4.16 kV, 7.2 kV, 12.47 kV, 13.2 kV, 14.4 kV, 23.9 kV, 34.5 kV, and others [2].

## 2.2.1   Distribution System Components

A schematic diagram depicting various components of a distribution system are shown in Figure 2.1 [2, 3]; these components are:

- Feeders: These are the main three-phase wires which originate from the substation transformers to supply energy to the load centers. The feeders often branch out to three-phase, two-phase and single-phase laterals. The wires could be overhead conductors or underground cables.

- Transformers: These step down the voltage to a distribution system voltage level. Three-phase as well as single-phase transformers are found in distribution systems. The three-phase transformer connections could be a wye grounded-wye grounded, delta-wye grounded, open delta-wye grounded, and others.

- Control and Protection Devices: Distribution systems have control devices such as voltage regulators, SCs, switches, etc. Voltage regulating elements such as LTCs may be available in some transformers to regulate the customer end voltage. SCs are used for reactive power supply. Devices such as circuit breakers, reclosers, sectionalizers and fuses are used for the system and equipment protection. Switches and sectionalizers are often used to reconfigure the distribution system feeders.

- Other Components: These include the customer loads, fixed capacitors, and DERs connected at various nodes. Distribution systems are also equipped with metering equipment at substation and feeder levels. Present day distribution systems are also equipped with a communication infrastructure and the various components that make up the AMI.
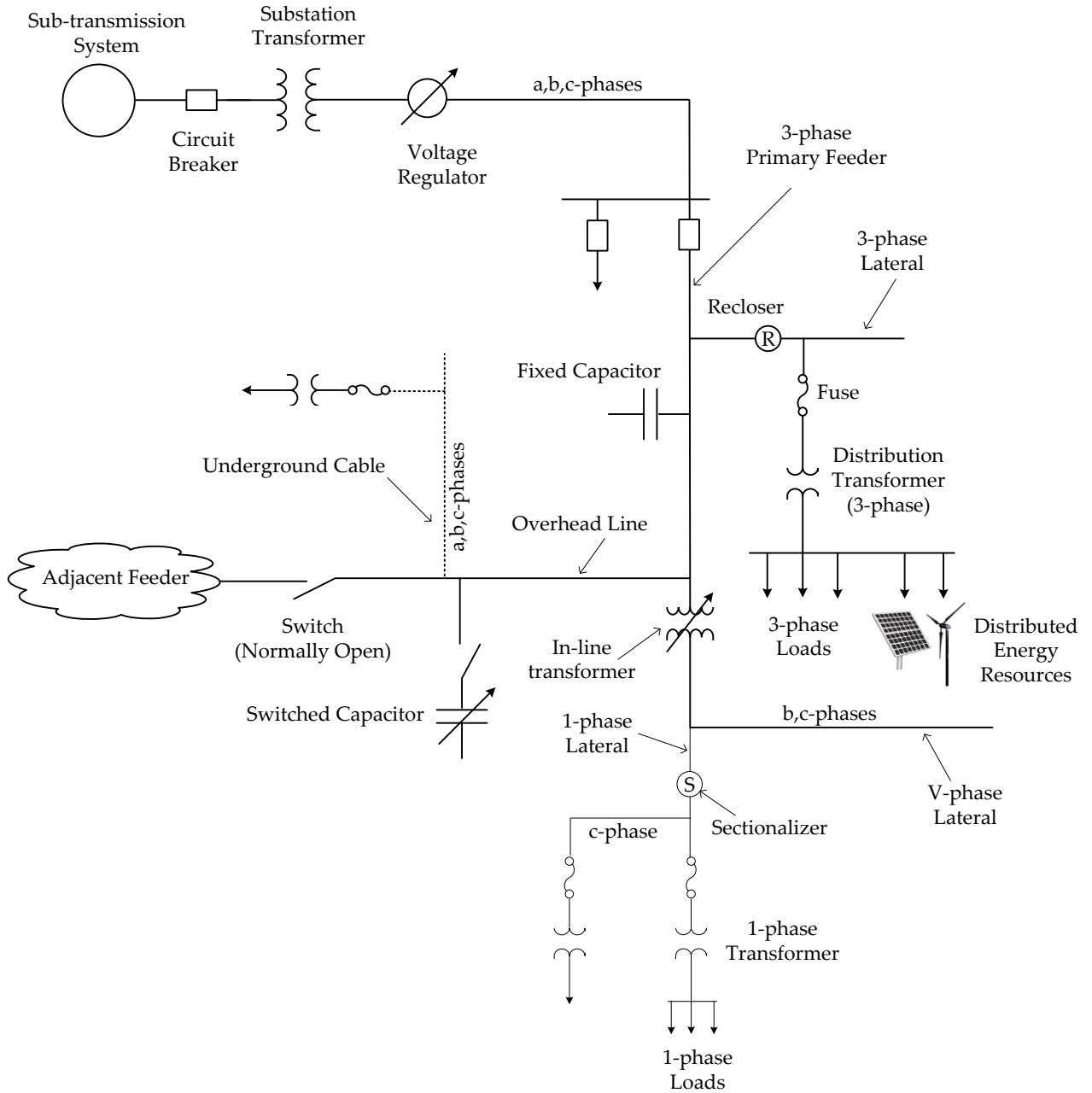
Figure 2.1: A typical distribution system and its components [2, 3].

## 2.2.2 Distribution System Infrastructure

The electric power transmission system has experienced significant infrastructure development over the past years. Communication and control technologies, wide-area measurements, integrated control, SCADA, open access information systems have been or are being integrated into the transmission systems. On the other hand, no significant developments have occurred in the distribution system infrastructure over the years [36]. The distribution system, for the most part, has remained a non-intelligent system still functioning with traditional technologies, operating practices, and relying on operator experience. Some of the critical limitations of existing distribution systems are: limited communication capability; local control, instead of central control; not enough sensors for measurements; and no wide-area measurement provisions.

Conventional distribution systems are equipped with local controllers, as shown in Figure 2.2, which operate the distribution system components based on some measurements and settings. As communication infrastructure is limited and exists at substation levels only, the required measurements are obtained from sensors placed near the devices which measures electrical (e.g. voltage, current) or non-electrical (e.g. temperature) quantities [47]. For the controllers, which operate based on local measurements, there are three required settings [100]:

- Set Point: The reference point to calculate the deviation of measured signals.

- Bandwidth Limit: The maximum allowed deviation, after which the controller starts to operate.

- Time Delay: This is required to prevent frequent operation of the equipment and also to properly coordinate the equipment which respond to the same input quantities.

Lack of infrastructure in communication, control and measurement technologies are barriers to flexible and optimal operation of distribution systems. A major change in
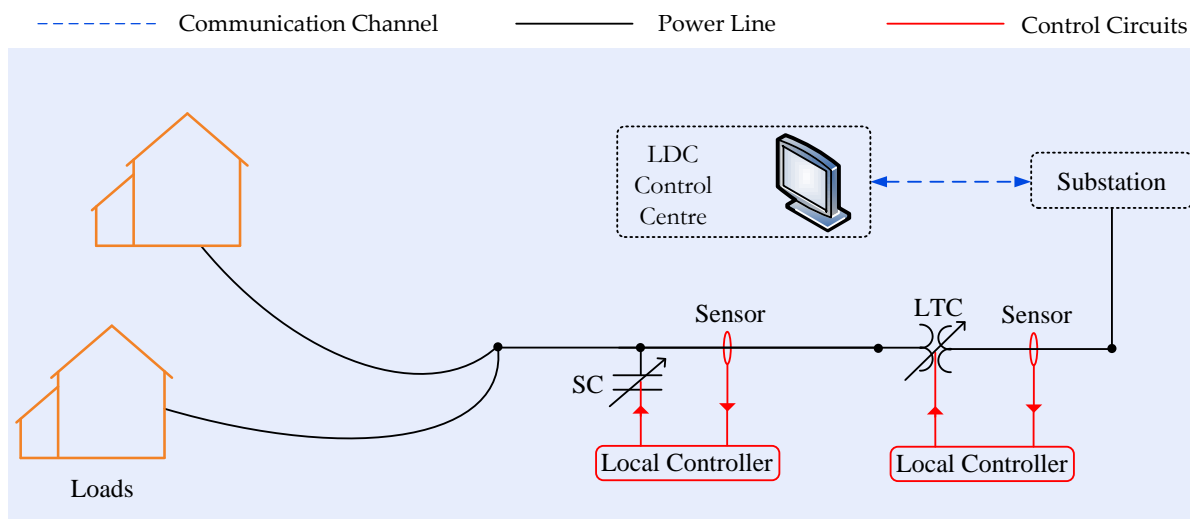
Figure 2.2: A typical communication and control infrastructure in a conventional distribution system.

distribution system infrastructure is required to realize a Smart Grid; thus, it is envisaged that the systems will gradually adopt advanced communication, control and measurement technologies at both customer and system levels.

Figure 2.3 depicts an evolving communication infrastructure at customers' premises, exchanging information and control signals among the major appliances, the utility's smart meter, and other internal and external entities through a central controller; this is referred as a HAN. The central controller in a HAN receives measurement data through various sensors (such as temperature sensor, occupancy sensor, etc.) and sends control signals to smart plugs which can turn ON/OFF the switches or rotate the "knobs" to control power consumption of the appliances. The controller may receive exogenous information such as weather, energy prices typically via the internet, and send measurement data (such as power, voltage, etc.) to the LDC control centre through the smart meter and AMI on the utility's Wide Area Network (WAN). The smart meters of neighboring customers may communicate with each other forming a Neighborhood Area Network (NAN), as shown in Figure 2.3. The HAN or a similar network at the customers'
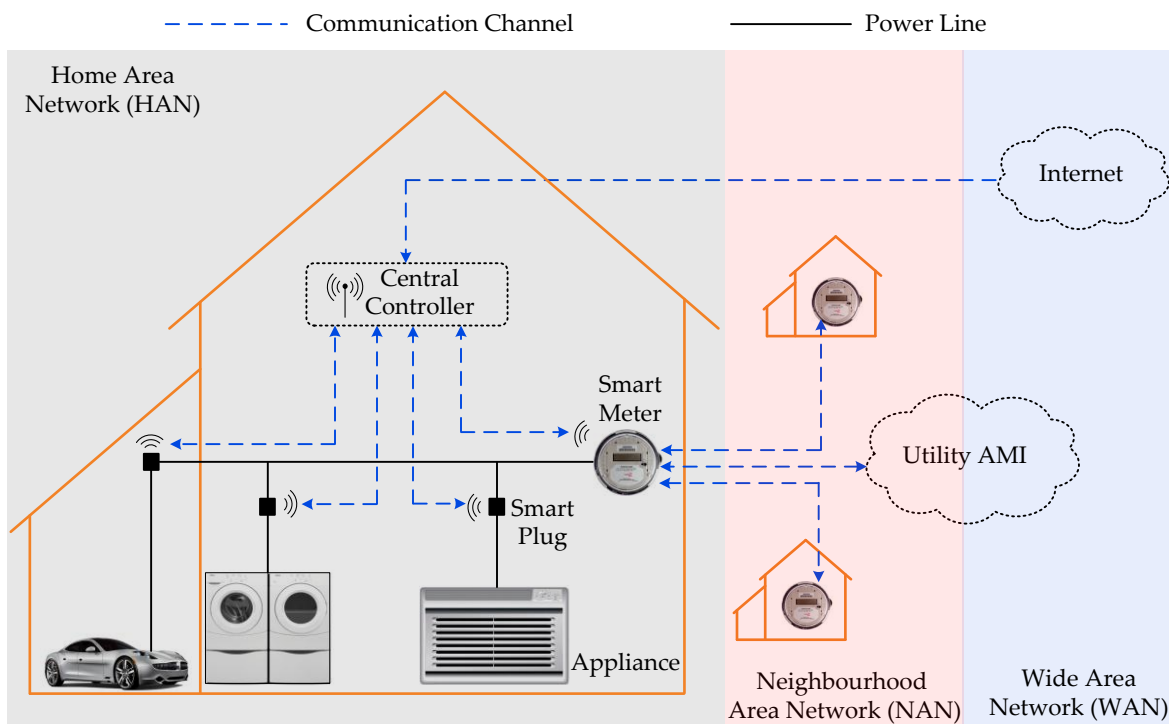
Figure 2.3: A typical communication infrastructure at customer's premise.

premises facilitates realization of various energy management concepts and technologies such as Home-to-Grid, industrial/commercial Building-to-Grid [101], and the proposed EHMS. Communication protocols such as Z-Wave, ZigBee, Wi-Fi, BACnet, and ModBus are common in HANs [102–105].

Figure 2.4 depicts the evolving communication and control infrastructure at distribution system level in a Smart Grid. The LDC control centre receives measurements from each customers via HAN, NAN, and signal "relaying units" installed at various places along the distribution system. These components are the parts of the AMI, which in turn is part of the utility's WAN. The relaying unit also communicates the control signals generated by the LDC control centre to the local controllers to dispatch the distribution system components located at various places along the feeder. However, as proposed in [45], the LDC control centre may bypass the local controllers completely, with the latter operating as back up.
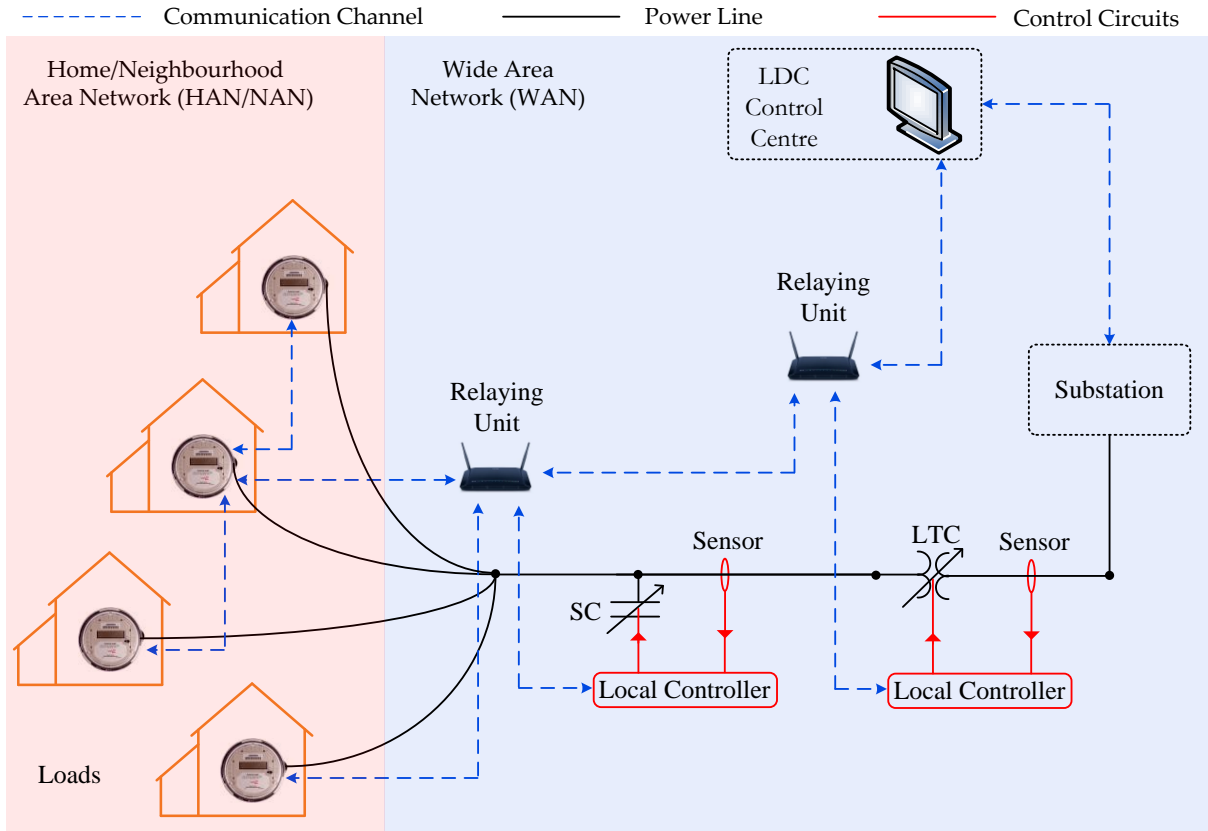
Figure 2.4: A typical communication infrastructure for distribution system operation and control.

As reported in [106–108], communication technologies such as private-radio, public cellular networks, or power-line carrier communication are some of the feasible options for WANs in distribution systems. Also, protocols such as Modbus, IEC 60870-5-101, DNP3, IEC 61850 are commonly used for the WAN communications in distribution systems [106–108].

## 2.3   Voltage Regulation (VR) and Reactive Power Control

### 2.3.1   Overview

Voltage regulation (VR) and reactive power control are the primary operational objectives in distribution systems [109]. VR refers to the means of regulating the distribution system voltage so that every customers' voltage remains within an acceptable limit. VR is important because unregulated voltages can have adverse impacts on system components and on customers' appliances. For example, large voltage fluctuations affect the performance and life of electrical equipment; low voltages cause low illumination, slow heating, etc.; and high voltages may cause premature device failure and reduced device life [100]. The ANSI standard C84.1 defines the acceptable voltage ranges for distribution systems [92]; for example, for residential services with nominal voltage of 120V, voltage variations in the range of 114-126V are acceptable under normal operating conditions. Similarly, reactive power flows in distribution circuits are undesirable as they cause large voltage drops, increased losses and reduced power delivery capability [57]. The problem of VR and reactive power control has been dealt together and is referred as VVC.

For VR purposes, distribution transformers are equipped with LTCs. Fixed capacitors and SCs are also used for VVC. Usually, fixed capacitor banks are used to offset the minimum reactive power requirements, while SCs are added as the load changes.

In addition to the primary objective of VVC to regulate the distribution voltages and the reactive power drawn from the transmission system, it can bring additional advantages to distribution system operations. However, the benefits that can be achieved through VVC depend on the existing communication, measurement and control infrastructure. A VVC based on local controllers may not have the same advantages as a centralized VVC, but both must perform the primary objective of VR and reactive power control [45].

## 2.3.2  Centralized Volt/Var Control (VVC)

A general VVC optimization problem structure is as follows [37, 38, 42, 110, 111]:

Minimize :
$$J = \sum f(I_{br}, V_i, Tap_{br}, Cap_i) \tag{2.1a}$$

Subjected to :

Power flow equations :
$$Pg_i - Pd_i = \sum_{j=1}^{N} |V_i| \cdot |V_j| \cdot |Y_{ij}| \cdot cos(\theta_{ij} + \delta_j - \delta_i) \tag{2.1b}$$

$$Qg_i - Qd_i = -\sum_{j=1}^{N} |V_i| \cdot |V_j| \cdot |Y_{ij}| \cdot sin(\theta_{ij} + \delta_j - \delta_i) \tag{2.1c}$$

Node voltage limits :
$$|V_i^{min}| \le |V_i| \le |V_i^{max}| \tag{2.1d}$$

Branch current limits :
$$|I_{br}| \le |I_{br}^{max}| \tag{2.1e}$$

LTC tap limits :
$$Tap_{br}^{min} \le Tap_{br} \le Tap_{br}^{max} \tag{2.1f}$$

Capacitor limits :
$$Cap_i^{min} \le Cap_i \le Cap_i^{max} \tag{2.1g}$$

where index $br$ represents the branches; indices $i$ and $j$ represent the nodes; $N$ represents the total number of nodes; $I_{br}$ is the current in the branch $br$; $V_i$ is the voltage at node $i$; $Y_{ij}$ is the admittance of the line $ij$; $\theta_{ij}$ is the angle of the admittance of line $ij$; $\delta_i$ and $\delta_j$ are the voltage phase angles at node $i$ and $j$, respectively; $Tap_{br}$ is the LTC tap position in branch $br$; $Cap_i$ is the number of capacitors switched at the node $i$; $Pg_i$ and $Pd_i$ represent active power generation and demand at node $i$ respectively; and $Qg_i$ and $Qd_i$ represent reactive power generation and demand at node $i$ respectively. Typical objective functions are the minimization of losses [37–41], optimal dispatch of LTC and SCs [111], and the maximization of power factor at the substation [45].

The VVC problem (2.1a)-(2.1g) is an MINLP optimization problem, where the non-linearity is introduced by the objective function and the power flow equations, and the integer variables correspond to the discrete LTC and SC controls. Extensive research has been carried out in the past examining solution approaches to this class of problem; a review of this problem is presented next.

## 2.4  Mathematical Programming

Mathematical programming refers to the formulation of an optimization problem and the suitable solution technique to solve it. An optimization problem refers to finding a set of values for the variables that yield the minimum or maximum of a given objective function, subject to a set of constraints. In general, minimization of the objective function is the same as maximization of negative of this function. The set of values of the variables yielding the minimum (or maximum) of the objective function is the optimal solution. Depending on the nature of the problem and the solution technique adopted, optimization problems may arrive at either local and/or global optimum solutions [112].

The general structure of the optimization problem comprises an objective function, and a set of equality and inequality constraints as follows:

Minimize : $\qquad f(x)$

Subjected to : $\qquad g_k(x) = 0; \ \ k = 1, 2, ..., p$ $\qquad\qquad$ (2.2)

$\qquad\qquad\qquad\qquad h_j(x) \leq 0; \ \ j = 1, 2, ..., m$

where $x$ is the set of $n$ decision variables, $f(x)$ is the objective function, and $g_k(x)$ and $h_j(x)$ are the sets of equality and inequality constraints, respectively. Depending on the nature of the objective function and the constraints, the optimization problems can be

categorized as linear or non-linear. Similarly, depending on the nature of decision variables the problem could be a continuous or an integer problem.

## 2.4.1   Linear Programming (LP) and Mixed Integer LP (MILP)

Linear programming (LP) is a form of mathematical programming, which is characterized by a linear objective function and a set of linear equality and inequality constraints. Thus, LP problems have the following general form:

Minimize : $\qquad\qquad\qquad c^T x$

Subjected to : $\qquad\qquad\quad A\,x \leq b$ $\qquad\qquad\qquad\qquad\qquad\qquad$ (2.3)

where $x$ represents the vector of variables to be determined, $A$ is coefficient matrix, $b$ is a vector of known values, and $c$ is a coefficient vector of the objective function.

The LP problems can be categorized as Mixed Integer LP (MILP) problems when at least one of the decision variables is an integer. The general mathematical structure of an MILP problem is as follows:

Minimize : $\qquad\qquad\qquad c^T x + d^T y$

Subjected to : $\qquad\qquad\quad A\,x + B\,y \leq b$ $\qquad\qquad\qquad\qquad\qquad\qquad$ (2.4)

where $x$ represents the vector of integer variables, and $y$ represents the vector of continuous variables.

In LP problems, the inequalities define a polyhedron of feasible solutions, and the optimal solution is typically at one of the vertices. The most popular solution methods for LP problems are the Simplex and Interior-point methods. The Simplex method is a systematic procedure for generating and testing the vertices of the polyhedron. It begins at

an arbitrary vertex as a candidate solution and at each iteration the candidate solution is moved to a new vertex in a direction which yields the largest improvement in the objective function [112]. On the other hand, in the Interior-point method, the candidate solution traverses through the interior of the polyhedron to arrive at the optimal solution. For large LP problems, the number of iterations in the Simplex method are significant; in such cases, the Interior-point method is a better option in terms of reduced computational costs [113].

MILP problems are challenging because of the presence of integer variables. Methods such as complete enumeration can yield a global optimal solution, but are not suitable for problems where the number of integer variables is high [112]. Other common methods to solve the MILP problem are Cutting Plane and Branch and Bound (B&B) methods. The idea behind the Cutting Plane technique is to add constraints to the MILP problem until the vertices of the feasible space are integers. These additional constraints are called "cuts", which remove the non-integer portion of the feasible space, while the integer points are preserved. There are two ways to generate cuts: the first, called Gomory cuts, generates cuts from any LP tableau; this has the advantage of solving any MILP problem, but the method can be very slow. The second approach is to use the structure of the problem to generate "good" cuts; this approach is problem dependent but can be very efficient [114]. The B&B methods, on the other hand, are based on an intelligent enumeration of candidate solutions with large subsets of useless candidates being discarded by using upper and lower estimated bounds of the optimization problem [112].

## 2.4.2 Non-linear Programming (NLP) and Mixed Integer NLP (MINLP)

When the objective function or at least one of the constraints in (2.2) is a non-linear function of its decision variables, then the problem is referred to as an NLP problem. NLP problems could be MINLP if there exists at least one integer variable.

The solution methods for NLP problems are problem specific. The most common solution methods are the Gradient methods, Newton-based methods and Interior-point methods [112]. Gradient methods use information about the slope of the function to determine the search direction where the optimal solution is expected to lie. These methods are very general and can solve NLP problems of any size, but they perform poorly in the neighborhood of the optimal solution, may only yield a local optimal solution, and/or may zigzag before reaching the optimal solution [115]. The Newton-based methods are also Gradient methods, but use second order gradient (Hessian) information; in this case, the objective function is approximately expressed by the second-order Taylor series, and in each iteration the solution is moved towards a new point which yields zero gradient. The advantage of the Newton-based methods is their fast convergence, but these methods require computation of the Hessian matrix and its inverse, which leads to increased computational burden [115]. The Interior-point methods traverse through the interior of the feasible space and uses some barrier functions to arrive at the optimal solution; the logarithmic barrier function method and the primal-dual interior-point method are popular for solving NLP problems [113].

MINLP problems are rather challenging problems because of the presence of non-linear functions and integer variables. Combinatorial optimization methods, which examine all possible candidate solutions can yield a global optimal solution to MINLP problems. The solution methods proposed in [42, 116] for the VVC problem use this Combinatorial approach, but these are not suitable for large problems where the number of integer variables are high [112]. The popular Branch-and-Cut, and B&B methods have been explored extensively for the solution of MINLP problems. The solution method for a distribution system feeder reconfiguration problem proposed in [117] is based on the B&B method, yielding a global optimal solution at a high computational cost. Heuristic methods are also popular solution methods for the MINLP problems. Various problem specific heuristic methods have been proposed in the literature specific to the VVC problem [38, 111, 118], and feeder reconfiguration problem [119–122].

More recently, Evolutionary Algorithms (EA) such as GA and Particle Swarm Optimization (PSO) methods have been used to solve the NLP and MINLP problems, as these methods have non-zero probability of providing global optimum solutions [123], and are relatively easy to implement, but they are computationally costly [112, 115, 124]. In GA-based methods, an optimal solution is reached from a population of solutions called "chromosomes" that are iteratively improved using "cross-over" and "mutation" operations. This algorithm uses multi-path searches in parallel, so as to reduce the local minimum trapping; it only examines the fitness of each solution instead of the objective function to guide its search, and explores the search area where the probability of finding the optimal solution is high [115]. GA-based methods have been applied in [63] to an optimal feeder reconfiguration problem, to an optimal capacitor planning problem [64], and to distribution planning problems [65, 66].

In the PSO method, the system is initialized with a population of random solutions and the method searches for the optima by updating generations. However, unlike the GA, PSO has no evolution operators such as crossover or mutation. In PSO, the potential solutions, called particles, fly through the problem space by following the current optimum particles. Compared to the GA, the advantages of PSO are that it is easy to implement and there are only a few parameters to adjust. However, compared to the GA, convergence of PSO is more sensitive to its parameters. The PSO method has been applied to the feeder reconfiguration problem in [62]. Other methods such as Ant Colony [125], Tabu Search [126], and Simulated Annealing [127] are also reported in the literature for solving MINLP and NLP problems related to distribution system planning.

A reactive power and voltage control optimization problem is solved in [43, 44] by relaxing the MINLP problem so that it becomes an NLP problem, using a quadratic penalty function approach. Such methods reduce the computational burden but do not guarantee a global or local optimum of the original MINLP problem, thus providing a sub-optimal solution.

### 2.4.3   Tools and Solvers

There are many commercial modeling tools and solvers for LP and NLP problems. The General Algebraic Modeling Systems (GAMS) is a popular commercially available mathematical modeling platform, and is used in this research [128]. Various solvers are also available commercially to solve the optimization models developed in GAMS. In this research the MINOS [129] and KNITRO [130] solvers are used to solve the NLP and MINLP problems, respectively. Other solvers, such as BARON [68] and DICOPT [69], were also examined for solving MINLP problems.

In MINOS, NLP problems are solved using a method that iteratively solves subproblems with linearized constraints and an augmented Lagrangian objective function [129]. BARON is capable of solving NLP and MINLP problems and yielding the global optima, and is based on a Branch and Reduce technique [68]. DICOPT is a framework for solving MINLP problems using other standard MILP and NLP solvers to solve the associated MILP and NLP subproblems generated by the algorithm; thus, some standard MILP solvers (e.g. CPLEX [131]) and NLP solvers (e.g. MINOS) are required for solving MINLP problems using DICOPT [69]. KNITRO is a specialized solver for nonlinear optimization (NLP and MINLP), but it can also be used to solve LP and MILP problems [130]; this solver uses three different optimization algorithms for solving optimization problems: two algorithms are of the Interior-point type, and one is of the Active-set type.

## 2.5   Curve Fitting

Curve fitting, also known as regression analysis, is a mathematical modeling approach where the system being modeled is represented by a "best fit" curve or mathematical function obtained from a series of data points. The data points represent the set of dependent and independent variables that describe the system [132, 133].

Curve fitting requires a set of data points, a pre-defined mathematical function, and at least one statistical index to measure the fitness. Curve fitting may yield a linear or polynomial curve depending on the degree of the mathematical function used to describe the system. Based on the measure of fitness, the most common curve fitting methods use the "least square error" criterion, which yields a curve that is minimally deviated from all the data points considered [133].

The least square error method is explained next, which is relevant to the present research. The following polynomial function of degree $M$, in two variables $x$ and $y$, is considered here:

$$z = f(x, y) = \sum_{m=0}^{M} \sum_{p=0}^{M-m} a_{m,p} \, x^m \, y^p \tag{2.5}$$

To estimate the coefficients $a_{m,p}$, a set of data points $(x_1, y_1, z_1)$, $(x_2, y_2, z_2)$, .... $(x_N, y_N, z_N)$ are required, where $N$ represents the total number of data points. For an $M$ degree polynomial in two variables, the following relation gives the minimal data set required:

$$N \geq \frac{M(M+1)}{2} \tag{2.6}$$

The best fit curve $f(x, y)$ has the least square error $\Pi$, which is given as:

$$\Pi = \sum_{i=1}^{N} \left[ z_i - \sum_{m=0}^{M} \sum_{p=0}^{M-m} a_{m,p} \, x_i^m \, y_i^p \right]^2 \tag{2.7}$$

Here, coefficients $a_{m,p}$ are unknown while all $x_i$, $y_i$, and $z_i$ are known. To obtain the least

square error, the unknown coefficients $a_{m,p}$ must yield zero first derivatives, i.e.,

$$\frac{\partial \Pi}{\partial a_{m,p}} = 2 \sum_{i=1}^{N} x_i^m \, y_i^p \left[ z_i - \sum_{m=0}^{M} \sum_{p=0}^{M-m} a_{m,p} \, x_i^m \, y_i^p \right] = 0$$

$$\forall \, m = \{0, ..., M\} \wedge p = \{0, ..., M - m\} \qquad (2.8)$$

The unknown coefficients $a_{m,p}$ can be obtained by solving the $\frac{M\,(M+1)}{2}$ number of linear equations (2.8).

## 2.6  Summary

In this chapter, a review of distribution system components and infrastructure was first presented. The VVC problem, which is an essential distribution system operational objective relevant to this research, was briefly discussed along with its basic mathematical model. A brief review of mathematical programming methods, which are used in this research, were also presented. The mathematical programming solvers and tools that are used in the present research work were briefly discussed as well. Finally, a brief overview of the least square method for curve fitting and its solution process used here was discussed.

# Chapter 3

# Optimal Energy Management of Distribution Systems

## 3.1  Introduction

This chapter presents a generic and comprehensive DOPF model that can be used by LDCs to facilitate the integration of their distribution system feeders into a Smart Grid. The proposed three-phase DOPF framework incorporates detailed modeling of distribution system components and allows use of various operational objectives. Phase specific models would allow LDC to determine realistic operating strategies that can improve the overall feeder efficiency.

The realistic distribution system operational objectives proposed in this work minimize the energy drawn from the substation and the number of switching operations of LTCs and SCs. A heuristic method for solving the three-phase DOPF model by transforming the MINLP problem into an NLP problem is proposed, which reduces the computational burden and facilitates its real-time implementation. A GA-based method is also used to determine the "global" optimal solution to the three-phase DOPF

problem, to evaluate the proposed heuristic solution in terms of both optimality and computational burden. Two distribution feeders namely, the IEEE 13-node test feeder and a practical feeder from Hydro One are considered to test and demonstrate the features of the proposed models and solution methods.

The remainder of the chapter is structured as follows: Section 3.2 presents the nomenclature of all the parameters, indices, and variables used in the modeling of the three-phase DOPF. Modeling details of distribution system components, network equations and operating limits are presented in Sections 3.3, 3.4, and 3.5, respectively. Sections 3.6 and Section 3.7 describe the mathematical model of the three-phase DOPF and the solution methods utilized, respectively. The developed DOPF model is validated using two standard test feeders, i.e., the IEEE-4 node and the IEEE 13-node test feeders, in Section 3.8. The performance of the mathematical model and the solution methods is evaluated based on various case studies for two distribution feeders, i.e, the IEEE 13-node test feeder and an actual Hydro One distribution feeder, in Section 3.9. Finally, Section 3.10 summarizes the chapter.

## 3.2   Nomenclature

*Parameters*

| | |
|---|---|
| $\alpha, \beta, \gamma$ | Scalar weights of the objective function components. |
| $A, B, C, D$ | Three-phase ABCD parameter matrices; $A$ unitless, $B$ in $\Omega$, $C$ in $\mho$, $D$ unitless. |
| $CR$ | Cross-over rate. |
| $CX$ | Chromosomes. |
| $\Delta H$ | Time interval in hour. |
| $\Delta Q$ | Size of each capacitor block in capacitor banks in Var. |
| $\Delta S$ | Percentage voltage change for each LTC tap. |
| $G$ | Number of generations in Genetic Algorithm. |

| | |
|---|---|
| $H$ | Total number of time intervals. |
| $I^{max}$ | Maximum current limits of conductors and cables in A. |
| $I^{sp}$ | Load current at specified power and nominal voltage in A. |
| $K$ | A constant multiplier. |
| $M$ | A $3 \times 3$ constant vector marix. |
| $MR$ | Mutation rate. |
| $Nc^{max}$ | Total number of capacitor blocks available in capacitor banks. |
| $Nt$ | Transformer turn ratio. |
| $P$ | Specified active power of load in W. |
| $Q$ | Specified reactive power of load/capacitor banks in Var. |
| $S$ | Population size. |
| $\theta$ | Specified load power factor angle in rad. |
| $Tap^{max}$ | Maximum tap changer position. |
| $Tap^{min}$ | Minimum tap changer position. |
| $U_3$ | The $3 \times 3$ identity matrix. |
| $V^{max}$ | Maximum voltage limit as per standards in V. |
| $V^{min}$ | Minimum voltage limit as per standards in V. |
| $V^{sp}$ | Specified nominal voltage in V. |
| $X$ | Reactance of capacitor in $\Omega$. |
| $Yc$ | Phase admittance matrix of conductors and cables in ℧. |
| $Z$ | Load impedance at specified power and nominal voltage in $\Omega$. |
| $Zc$ | Phase impedance matrix of conductors and cables in $\Omega$. |
| $Zc_{012}$ | Sequence impedance matrix of conductors and cables in $\Omega$. |
| $Zt$ | Phase impedance matrix of transformers refereed to the secondary side in $\Omega$. |

*Indices*

| | |
|---|---|
| $a, b, c$ | Phases. |
| $C_1$ | Wye-connected fixed capacitors. |

| | |
|---|---|
| $C_2$ | Wye-connected controllable capacitor banks. |
| $C_3$ | Delta-connected fixed capacitors. |
| $C_4$ | Delta-connected controllable capacitor banks. |
| $cd$ | Conductors and cables, $cd \in l$. |
| $d$ | Row of candidate solution matrix. |
| $h$ | Number of intervals, $h = 1, 2..., H$. |
| $l$ | Series elements. |
| $L_1$ | Wye-connected constant power loads. |
| $L_2$ | Wye-connected constant impedance loads. |
| $L_3$ | Wye-connected constant current loads. |
| $L_4$ | Delta-connected constant power loads. |
| $L_5$ | Delta-connected constant impedance loads. |
| $L_6$ | Delta-connected constant current loads. |
| $L_\Delta$ | Delta-connected loads and capacitors, $L_\Delta = L_4, L_5, L_6, C_3, C_4$. |
| $L_Y$ | Wye-connected loads and capacitors, $L_Y = L_1, L_2, L_3, C_1, C_2$. |
| $l_{1n}$ | Series elements whose receiving ends are connected to node $n$, $l_{1n} \in l$. |
| $l_{2n}$ | Series elements whose sending ends are connected to node $n$, $l_{2n} \in l$. |
| $ls$ | Series elements which is connected to substation node $ns$, $ls \in l$. |
| $n$ | Nodes. |
| $n_\Delta$ | Nodes where delta-connected loads are connected, $n_\Delta \in n$. |
| $n_Y$ | Nodes where single phase loads or wye-connected loads are connected, $n_Y \in n$. |
| $ni$ | Integer variables. |
| $ns$ | Substation node, $ns \in n$. |
| $p$ | Phases, $p = a, b, c$. |
| $pp$ | Phase to phase, $pp = ab, bc, ca$. |
| $r$ | Receiving-end. |
| $s$ | Sending-end. |
| $sw$ | Switches, $sw \in l$. |

| | |
|---|---|
| $t_1$ | Delta-wye grounded step down transformers, $t_1 \in l$. |
| $t_2$ | wye grounded-wye grounded transformers, $t_2 \in l$. |
| $t_3$ | Three-phase group controlled tap changers, $t_3 \in t_c$. |
| $t_c$ | Controllable tap changers, $t_c \in l$. |

*Variables*

| | |
|---|---|
| $cap$ | Number of capacitor blocks switched in capacitor banks. |
| $Ess$ | Energy drawn from substation. |
| $F$ | Fitness function. |
| $i$ | Current phasor in A. |
| $J, J'$ | Objective functions. |
| $tap$ | Tap position. |
| $v$ | Voltage phasor in V. |
| $w$ | Continuous variables. |
| $x_o$ | Initial solution set. |
| $x_1, x_2, ..., x_{ni}$ | Elements of $x_o$. |
| $\overline{x}$ | Set of upper bound integers close to $x_o$. |
| $\overline{x_1}, \overline{x_2}, ..., \overline{x_{ni}}$ | Elements of $\overline{x}$. |
| $\underline{x}$ | Set of lower bound integers close to $x_o$. |
| $\underline{x_1}, \underline{x_2}, ..., \underline{x_{ni}}$ | Elements of $\underline{x}$. |
| $X_1, X_2$ | Optimal solutions obtained from the local search technique. |
| $X_B$ | Candidate solution matrix. |
| $X_{Bd}$ | $d^{th}$ row of $X_B$. |
| $X_F$ | Feasible solution matrix. |
| $X_{Fh}$ | $h^{th}$ row of $X_F$. |

## 3.3   Component Models

Commonly found distribution system components, i.e., conductors/cables, transformers, LTCs, switches, capacitors and loads are modeled in the present work to develop the proposed DOPF framework. These models are explained in detail next.

### 3.3.1   Series Components

For each series component, a set of equations are developed using their ABCD parameters that relate the three-phase voltages and currents of the sending-end and receiving-end, as follows:

$$
\begin{bmatrix}
v_{s,a,l,h} \\
v_{s,b,l,h} \\
v_{s,c,l,h} \\
i_{s,a,l,h} \\
i_{s,b,l,h} \\
i_{s,c,l,h}
\end{bmatrix}
=
\begin{bmatrix}
A_l & B_l \\
C_l & D_l
\end{bmatrix}
\begin{bmatrix}
v_{r,a,l,h} \\
v_{r,b,l,h} \\
v_{r,c,l,h} \\
i_{r,a,l,h} \\
i_{r,b,l,h} \\
i_{r,c,l,h}
\end{bmatrix}
\qquad \forall\, l, \forall\, h \qquad (3.1)
$$

where $A_l$, $B_l$, $C_l$, and $D_l$ are $3 \times 3$ matrices. The ABCD parameters of the series elements modeled here are discussed next; more details of which can be found in [2]. All variables, parameters, and indices in (3.1) and other equations in this chapter are defined in Section 3.2.

**Conductors/Cables**

Conductors and cables are modeled as $\pi$-equivalent circuits, and their general ABCD parameters are:

$$A_{cd} = D_{cd} = U_3 + \frac{1}{2} \, Zc_{cd} \, Yc_{cd} \qquad\qquad \forall \, cd \qquad (3.2\text{a})$$

$$B_{cd} = Zc_{cd} \qquad\qquad \forall \, cd \qquad (3.2\text{b})$$

$$C_{cd} = Yc_{cd} + \frac{1}{4} \, Yc_{cd} \, Zc_{cd} \, Yc_{cd} \qquad\qquad \forall \, cd \qquad (3.2\text{c})$$

where $Zc_{cd}$ and $Yc_{cd}$ are $3 \times 3$ matrices in which the diagonal elements represent the self impedance and shunt admittance of each phase, and the off-diagonal elements represent the mutual impedance and shunt admittance between two phases. If the values of self and mutual impedances and/or admittances are not known, these can be readily calculated from conductors' configuration using the modified Carson's equations [2].

Conductors and cables could be single-phase, two-phase, four wire three-phase or three wire three-phase. In the case of single-phase and two-phase conductors and cables, the corresponding self and mutual impedances and admittances become zero in $Zc_{cd}$ and $Yc_{cd}$. Four wire three-phase conductors and cables can be represented by $3 \times 3$ impedance and admittance matrices using Kron's reduction [2].

Instead of self and mutual impedances and shunt admittances in the phase frame, sometimes the parameters are expressed in the sequence frame. In this case, the following equations relate the sequence components to phase components, and similar equations can

be used for the shunt admittance matrix:

$$Zc_{012} = M^{-1} \ Zc \ M \tag{3.3a}$$

$$M = \begin{bmatrix} 1 & 1 & 1 \\ 1 & e^{-j\frac{2}{3}\pi} & e^{j\frac{2}{3}\pi} \\ 1 & e^{j\frac{2}{3}\pi} & e^{-j\frac{2}{3}\pi} \end{bmatrix} \tag{3.3b}$$

where for an unbalanced system, all elements of $Zc_{012}$ are non-zero. In the case where only diagonal elements of $Zc_{012}$ are known, i.e., zero sequence and positive sequence components of the conductors, the three diagonal elements in $Zc$ are identical and all of the off-diagonal elements are also identical; such $Zc$ represents conductors with transposed phases.

## Switches

Switches are modeled as zero impedance series elements. The ABCD parameters in this case are:

$$A_{sw} = D_{sw} = U_3 \qquad\qquad \forall\, sw \qquad (3.4\text{a})$$

$$B_{sw} = C_{sw} = 0 \qquad\qquad \forall\, sw \qquad (3.4\text{b})$$

## Transformers

The ABCD parameters of transformers depend on the connection, i.e., wye or delta. The ABCD parameters for a delta-wye grounded step-down transformer (with American

Standard Connection of 30° negative angular displacement) are:

$$A_{t_1} = \frac{-Nt}{3} \begin{bmatrix} 0 & 2 & 1 \\ 1 & 0 & 2 \\ 2 & 1 & 0 \end{bmatrix} \qquad \forall\, t_1 \qquad (3.5a)$$

$$B_{t_1} = A_{t_1}\, Zt \qquad \forall\, t_1 \qquad (3.5b)$$

$$C_{t_1} = 0 \qquad \forall\, t_1 \qquad (3.5c)$$

$$D_{t_1} = \frac{1}{Nt} \begin{bmatrix} 1 & -1 & 0 \\ 0 & 1 & -1 \\ -1 & 0 & 1 \end{bmatrix} \qquad \forall\, t_1 \qquad (3.5d)$$

where $Zt$ is a $3 \times 3$ diagonal matrix in which diagonal elements represent the impedance of each phase referred to the secondary side.

For a wye grounded-wye grounded connection:

$$A_{t_2} = Nt\, U_3 \qquad \forall\, t_2 \qquad (3.6a)$$

$$B_{t_2} = Nt\, Zt \qquad \forall\, t_2 \qquad (3.6b)$$

$$C_{t_2} = 0 \qquad \forall\, t_2 \qquad (3.6c)$$

$$D_{t_2} = \frac{1}{Nt}\, U_3 \qquad \forall\, t_2 \qquad (3.6d)$$

Single phase transformers can be represented by (3.6a)-(3.6d), where $A$, $B$ and $D$ consist of only one element corresponding to the phase in which the transformer is connected.

**Load Tap Changers (LTCs)**

Voltage regulating transformers in distribution systems are equipped with LTCs. The ABCD parameters in LTCs are not constant, as these depend on the setting of tap positions during operation. The following additional set of equations is needed to represent the ABCD parameters for each LTC:

$$
A_{t_c,h} = \begin{bmatrix} 1 + \Delta S_{t_c} \ tap_{a,t_c,h} & 0 & 0 \\ 0 & 1 + \Delta S_{t_c} \ tap_{b,t_c,h} & 0 \\ 0 & 0 & 1 + \Delta S_{t_c} \ tap_{c,t_c,h} \end{bmatrix} \qquad \forall\, t_c, \forall\, h \quad (3.7a)
$$

$$
B_{t_c,h} = C_{t_c,h} = 0 \qquad\qquad \forall\, t_c, \forall\, h \quad (3.7b)
$$

$$
D_{t_c,h} = A_{t_c,h}^{-1} \qquad\qquad \forall\, t_c, \forall\, h \quad (3.7c)
$$

where the variables $tap_{a,t_c,h}$, $tap_{b,t_c,h}$, and $tap_{c,t_c,h}$ take only integer values from $Tap_{p,t_c,h}^{min}$ to $Tap_{p,t_c,h}^{max}$ (e.g., -16 to +16 for a 32-step LTC). Equations (3.7a)-(3.7c) are for a tap changer with per-phase tap controls. For a three-phase group controlled tap changer, the following additional equation is used to make sure that all tap operations are identical:

$$
tap_{a,t_3,h} = tap_{b,t_3,h} = tap_{c,t_3,h} \qquad\qquad \forall\, t_3, \forall\, h \qquad (3.8)
$$

## 3.3.2 Shunt Components

Shunt components (loads and capacitors) are modeled for individual phases separately to represent unbalanced three-phase loads, since single-phase loads and single phase capacitors are common in distribution feeders. A polynomial load model is adopted, where each load is modeled as a mix of constant impedance, constant current, and constant power components. Capacitors are modeled as constant impedance loads. Capacitor banks are modeled as multiple capacitor blocks with switching options.

Wye-connected and delta-connected loads and capacitors are both represented.

## Wye-connected Loads and Capacitors

The next set of equations is used to represent each type of wye-connected load and capacitors on a per-phase basis; thus, for constant power loads:

$$v_{n,p,h} \, i^*_{L_1,n,p,h} = P_{L_1,n,p,h} + j \, Q_{L_1,n,p,h} \qquad \forall \, n, \forall \, p, \forall \, h \qquad (3.9)$$

For constant impedance loads:

$$Z_{L_2,n,p,h} = \frac{V^{sp\,2}_{n,p}}{P_{L_2,n,p,h} + j \, Q_{L_2,n,p,h}} \qquad \forall \, n, \forall \, p, \forall \, h \qquad (3.10a)$$

$$v_{n,p,h} = Z_{L_2,n,p,h} \, i_{L_2,n,p,h} \qquad \forall \, n, \forall \, p, \forall \, h \qquad (3.10b)$$

For constant current loads:

$$\left| I^{sp}_{L_3,n,p,h} \right| = \left| \frac{V^{sp}_{n,p}}{P_{L_3,n,p,h} + j \, Q_{L_3,n,p,h}} \right| \qquad \forall \, n, \forall \, p, \forall \, h \qquad (3.11a)$$

$$\theta_{L_3,n,p,h} = tan^{-1} \left( \frac{Q_{L_3,n,p,h}}{P_{L_3,n,p,h}} \right) \qquad \forall \, n, \forall \, p, \forall \, h \qquad (3.11b)$$

$$\left| i_{L_3,n,p,h} \right| e^{j \left( \angle v_{n,p,h} - \angle i_{L_3,n,p,h} \right)} = \left| I^{sp}_{L_3,n,p,h} \right| e^{j \, \theta_{L_3,n,p,h}} \qquad \forall \, n, \forall \, p, \forall \, h \qquad (3.11c)$$

For fixed capacitors:

$$X_{C_1,n,p,h} = \frac{-j \, V^{sp\,2}_{n,p}}{Q_{C_1,n,p,h}} \qquad \forall \, n, \forall \, p, \forall \, h \qquad (3.12a)$$

$$v_{n,p,h} = X_{C_1,n,p,h} \, i_{C_1,n,p,h} \qquad \forall \, n, \forall \, p, \forall \, h \qquad (3.12b)$$

For capacitor banks with SCs:

$$X_{C_2,n,p,h} = \frac{-j\,V_{n,p}^{sp\,2}}{cap_{C_2,n,p,h}\,\Delta Q_{C_2,n,p,h}} \qquad\qquad \forall\,n,\forall\,p,\forall\,h \qquad\qquad (3.13\text{a})$$

$$v_{n,p,h} = X_{C_2,n,p,h}\;i_{C_2,n,p,h} \qquad\qquad\qquad \forall\,n,\forall\,p,\forall\,h \qquad\qquad (3.13\text{b})$$

where the variables $cap_{C_2,n,p,h}$ take only positive integer values in the range 0 to $Nc_{C_2,n,p,h}^{max}$.

## Delta-connected Loads and Capacitors

For delta-connected loads and capacitors banks, line-to-line voltages and currents are needed. Thus, the following equations are required to properly relate the line-to-line variables to line variables:

$$\begin{bmatrix} v_{n,ab,h} \\ v_{n,bc,h} \\ v_{n,ca,h} \end{bmatrix} = \begin{bmatrix} 1 & -1 & 0 \\ 0 & 1 & -1 \\ -1 & 0 & 1 \end{bmatrix} \begin{bmatrix} v_{n,a,h} \\ v_{n,b,h} \\ v_{n,c,h} \end{bmatrix} \qquad\qquad \forall\,n,\forall\,h \qquad\qquad (3.14\text{a})$$

$$\begin{bmatrix} i_{L_\Delta,n,a,h} \\ i_{L_\Delta,n,b,h} \\ i_{L_\Delta,n,c,h} \end{bmatrix} = \begin{bmatrix} -1 & 1 & 0 \\ 0 & -1 & 1 \\ 1 & 0 & -1 \end{bmatrix} \begin{bmatrix} i_{L_\Delta,n,ca,h} \\ i_{L_\Delta,n,ab,h} \\ i_{L_\Delta,n,bc,h} \end{bmatrix} \qquad\qquad \forall\,L_\Delta,\forall\,n,\forall\,h \qquad\qquad (3.14\text{b})$$

Equations similar to (3.9)-(3.13b) can be used to represent delta-connected loads and capacitors banks by replacing the line variables with the line-to-line variables calculated in (3.14a) and (3.14b). Thus, for constant power loads:

$$v_{n,pp,h}\,i_{L_4,n,pp,h}^{*} = P_{L_4,n,pp,h} + j\,Q_{L_4,n,pp,h} \qquad\qquad \forall\,n,\forall\,pp,\forall\,h \qquad\qquad (3.15)$$

For constant impedance loads:

$$Z_{L_5,n,pp,h} = \frac{V_{n,pp}^{sp\ 2}}{P_{L_5,n,pp,h} + j\,Q_{L_5,n,pp,h}} \qquad\qquad \forall\,n, \forall\,pp, \forall\,h \qquad (3.16a)$$

$$v_{n,pp,h} = Z_{L_5,n,pp,h}\ i_{L_5,n,pp,h} \qquad\qquad \forall\,n, \forall\,pp, \forall\,h \qquad (3.16b)$$

For constant current loads:

$$\left|I_{L_6,n,pp,h}^{sp}\right| = \left|\frac{V_{n,pp}^{sp}}{P_{L_6,n,pp,h} + j\,Q_{L_6,n,pp,h}}\right| \qquad\qquad \forall\,n, \forall\,pp, \forall\,h \qquad (3.17a)$$

$$\theta_{L_6,n,pp,h} = tan^{-1}\left(\frac{Q_{L_6,n,pp,h}}{P_{L_6,n,pp,h}}\right) \qquad\qquad \forall\,n, \forall\,pp, \forall\,h \qquad (3.17b)$$

$$\left|i_{L_6,n,pp,h}\right| e^{j\left(\angle v_{n,pp,h} - \angle i_{L_6,n,pp,h}\right)} = \left|I_{L_6,n,pp,h}^{sp}\right| e^{j\,\theta_{L_6,n,pp,h}} \qquad\qquad \forall\,n, \forall\,pp, \forall\,h \qquad (3.17c)$$

For fixed capacitors:

$$X_{C_3,n,pp,h} = \frac{-j\,V_{n,pp}^{sp\ 2}}{Q_{C_3,n,pp,h}} \qquad\qquad \forall\,n, \forall\,pp, \forall\,h \qquad (3.18a)$$

$$v_{n,pp,h} = X_{C_3,n,pp,h}\ i_{C_3,n,pp,h} \qquad\qquad \forall\,n, \forall\,pp, \forall\,h \qquad (3.18b)$$

For capacitor banks with SCs:

$$X_{C_4,n,pp,h} = \frac{-j\,V_{n,pp}^{sp\ 2}}{cap_{C_4,n,pp,h}\ \Delta Q_{C_4,n,pp,h}} \qquad\qquad \forall\,n, \forall\,pp, \forall\,h \qquad (3.19a)$$

$$v_{n,pp,h} = X_{C_4,n,pp,h}\ i_{C_4,n,pp,h} \qquad\qquad \forall\,n, \forall\,pp, \forall\,h \qquad (3.19b)$$

where the variables $cap_{C_4,n,pp,h}$ take only positive integer values in the range 0 to $Nc_{C_4,n,pp,h}^{max}$.

## 3.4   Network Equations

The following equation corresponds to the line current balance at each node and phase:

$$\sum_{l_{n1}} i_{r,p,l,h} = \sum_{l_{n2}} i_{s,p,l,h} + \sum_{L_Y} i_{L_Y,n,p,h} + \sum_{L_\Delta} i_{L_\Delta,n,p,h} \qquad \forall\, n, \forall\, p, \forall\, h \qquad (3.20)$$

Also, at each node and phase, the voltages of the elements connected to that node are equal to the corresponding nodal voltage:

$$v_{r,p,l_{n1},h} = v_{s,p,l_{n2},h} = v_{n,p,h} \qquad \forall\, l, \forall\, n, \forall\, p, \forall\, h \qquad (3.21)$$

## 3.5   Operating Limits

Distribution system operating limits, such as voltage limits, feeder current limits, etc., need to be modeled. Thus, distribution voltages at the point of load connection are required to be maintained within a limit prescribed by standards such as ANSI, which can be mathematically represented as:

$$V_{n,p}^{min} \leq v_{n,p,h} \leq V_{n,p}^{max} \qquad \forall\, n_Y, \forall\, p, \forall\, h \qquad (3.22a)$$

$$V_{n,pp}^{min} \leq v_{n,pp,h} \leq V_{n,pp}^{max} \qquad \forall\, n_\Delta, \forall\, pp, \forall\, h \qquad (3.22b)$$

Similarly, feeder current limits can be represented as:

$$i_{r,p,l,h} \leq I_{p,l}^{max} \qquad \forall\, p, \forall\, cd, \forall\, h \qquad (3.23a)$$

$$i_{s,p,l,h} \leq I_{p,l}^{max} \qquad \forall\, p, \forall\, cd, \forall\, h \qquad (3.23b)$$

Limits on transformer capacity, number of switching operations of LTCs and SCs, and others can also be readily represented explicitly.

## 3.6 Three-phase Distribution Optimal Power Flow (DOPF) Model

A three-phase DOPF model is developed based on the component models, network equations, and operating limits described earlier. The developed model is a generic optimization framework where any objective function can be selected for distribution system operations.

Electrical loads in a distribution system are voltage dependent. By operating the distribution system within acceptable voltage limits, the total energy consumption and system peak demand can be reduced [57, 87]. The available LTCs and capacitor banks can be employed to maintain the distribution system voltage within the acceptable limits prescribed by standards [92]. Hence, as demand changes over a day, the LTCs and capacitors are required to switch frequently to maintain the voltages within the limits. However, since switching of these devices is associated with maintenance costs, frequent switching operations are not desirable.

As per the above discussions, a novel objective function is defined here to minimize the energy drawn from the substation as well as the number of switching operations of LTCs

and capacitors. This function can be defined as follows:

$$
J = \alpha \overbrace{\sum_h \Delta H \sum_p Real\left(v_{ns,p,h}\ i^*_{s,p,ls,h}\right)}^{\text{Energy drawn from Substation}}
$$

$$
+ \beta \overbrace{\sum_{h=2}^{H} \sum_p \sum_{t_c} |tap_{p,t_c,h} - tap_{p,t_c,h-1}|}^{\text{Number of LTC switching operations}}
$$

$$
+ \gamma \overbrace{\sum_{h=2}^{H} \sum_n \left( \sum_p |cap_{C_2,n,p,h} - cap_{C_2,n,p,h-1}| + \sum_{pp} |cap_{C_4,n,pp,h} - cap_{C_4,n,pp,h-1}| \right)}^{\text{Number of SC switching operations}} \quad (3.24)
$$

where the parameters $\alpha$, $\beta$ and $\gamma$ are the weights attached to the respective components: energy drawn from the substation, LTC switchings, and capacitor switchings. The selection of these weights depends on the priority given to energy cost and control effort by the distribution system operators. Therefore, equation (3.24) represents the objective function, whereas equations (3.1)-(3.23b) define the equality and inequality constraints of the proposed three-phase DOPF model.

The objective function (3.24) is in line with the past and recent practices of Conservation Voltage Regulation (CVR) to reduce power and energy consumption by controlling voltages in utilities' feeders. Although some utilities have deployed CVR pilot projects to evaluate possible savings, some utilities have been reluctant to implement full-scale CVR because of the resulting revenue reductions [134, 135]. It seems counter-intuitive that some electric utilities are making efforts to reduce energy consumption by encouraging their customers to participate in energy management and energy efficiency activities. However, this is true for utilities whose profits are regulated, which is the case in most places, wherein profits are ensured by regulators if the utilities help achieve system cost savings by reducing electricity demand. In the context of

Ontario, regulations have been enacted pursuant to the GEA [13] to implement energy management and conservation programs at the utilities' feeder level. Recently, the Independent Electricity System Operator (IESO) in coordination with Ontario's LDCs initiated system-wide voltage reduction exercise to demonstrate its effect on power demand [136]. As reported in [135], regulators are realizing the benefits of CVR and thus "enticing" LDCs to implement such energy management programs.

The objective function proposed in this research helps utilities to achieve their goal of reducing energy consumption at the system level. In addition, by minimizing energy consumption, the peak demand and emissions are reduced, which are also of interests to utilities as it leads to deferral of capacity expansions and also showcases their corporate commitment to sustainability [137]. Large customers who operate their own feeders (such as industries and universities) may also benefit by implementing the proposed DOPF model.

## 3.7 DOPF Solution Methods

### 3.7.1 Heuristic Method

In the three-phase DOPF model, LTC and capacitor switching actions are discrete operations, which essentially render the proposed model an MINLP problem. The number of continuous and integer variables increase with the size of the distribution system. The number of variables also increases significantly when distribution system operation decisions are optimized over a 24-hour timeframe.

Commercially available solvers for MINLP problems, in particular BARON [68] and DICOPT [69], did not perform well when used to solve the proposed problem, in terms of solution time and convergence characteristics. Therefore, a method proposed in [43, 44] is adopted in this work that avoids the use of integer variables and transforms the three-phase DOPF into an NLP problem. Hence, a quadratic penalty term is augmented to the

objective function (3.24), resulting in the following modified objective function:

$$J' = J + \sum_{ni} K_{ni} \Big( w_{ni} - round(w_{ni}) \Big)^2 \tag{3.25}$$

where $w_{ni}$ represents the *tap* and *cap* variables used in (3.24). The quadratic term adds a high penalty value to the objective function at non-integer solutions, and thus drives $w_{ni}$ to its closest integer value $round(w_{ni})$. By employing the above method, the MINLP problem is converted into an NLP problem. The parameter $K_{ni}$ needs to be carefully selected, as discussed in [43, 44], to obtain an optimal integer solution to the NLP problem (3.25).

Commercially available NLP solvers (e.g. MINOS [129]), do not guarantee reaching a feasible solution of the three-phase DOPF problem with NLP approximation, because of the presence of the discontinuous quadratic penalty term in (3.25). In Figure 3.1, Scenario 1 depicts a case when the optimal integer solution $X_1$ is obtained using the quadratic penalty function. To obtain an optimal integer solution, both $\omega_{ni}$ and $round(\omega_{ni})$ must lie inside the feasible region of the optimization problem. However, it is possible that $round(\omega_{ni})$ may lie outside the feasible region, as depicted in Scenario 2 in Figure 3.1, in particular when $\omega_{ni}$ is close to the boundary of the feasible region. To address this problem, a local search technique is proposed to ensure that an integer solution $X_2$ is in the feasible region of the optimization problem, as depicted in Figure 3.2.

The proposed three-phase DOPF, with the NLP approximation and local search procedure, is still computationally intensive because of the size of the search space. For example, for a 24-hour timeframe analysis (i.e., $H = 24$) with an interval of one hour (i.e., $\Delta H = 1$), the search combination becomes $2^{24\,ni}$ when the search is restricted to the two integers nearest to $round(\omega_{ni})$. To reduce such a large search space, an hourly local search approach is implemented as explained in Figure 3.2; thereby, the search combination is substantially reduced to $2^{ni} \times 24$. In this process, mathematical precision is somewhat compromised at the cost of reducing the computational burden. However, in practical applications, this is a reasonable sub-optimal approach that allows for the
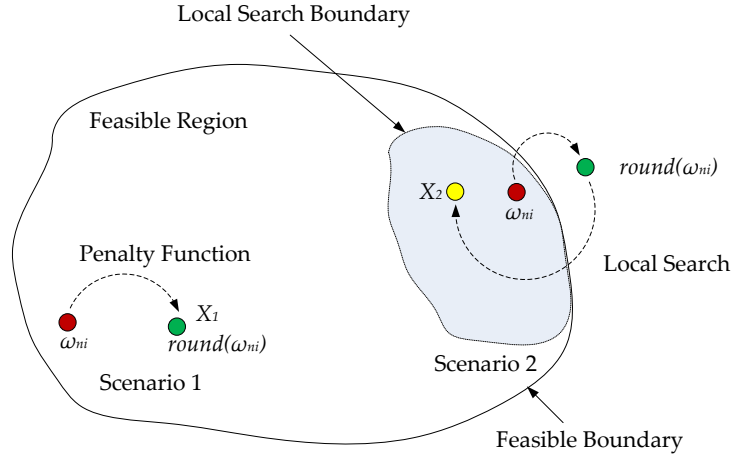
Figure 3.1: Optimal and infeasible cases encountered in the solution process based on a quadratic penalty function method.

implementation of the proposed technique in real-time.

## 3.7.2   Genetic Algorithm (GA) based Method

A GA-based method, similar to the one discussed in [63], is implemented to solve the three-phase DOPF, so that comparisons of the optimal solutions and associated CPU times can be made with respect to the proposed heuristic method. A brief overview of the generic GA-based solution method is presented in Section 2.4, details of which can be found in [124]. Figure 3.3 depicts a pseudo-code of the GA-based solution method for the three-phase DOPF problem, whose parameters are:

- Generations ($G$): The proposed GA-based method is set for 100 generations.

- Chromosome ($CX$): The controllable variables *tap* and *cap* associated with LTCs and SCs in the three-phase DOPF model are integer variables, each represented by a chromosome, which is a 6-bit binary number.
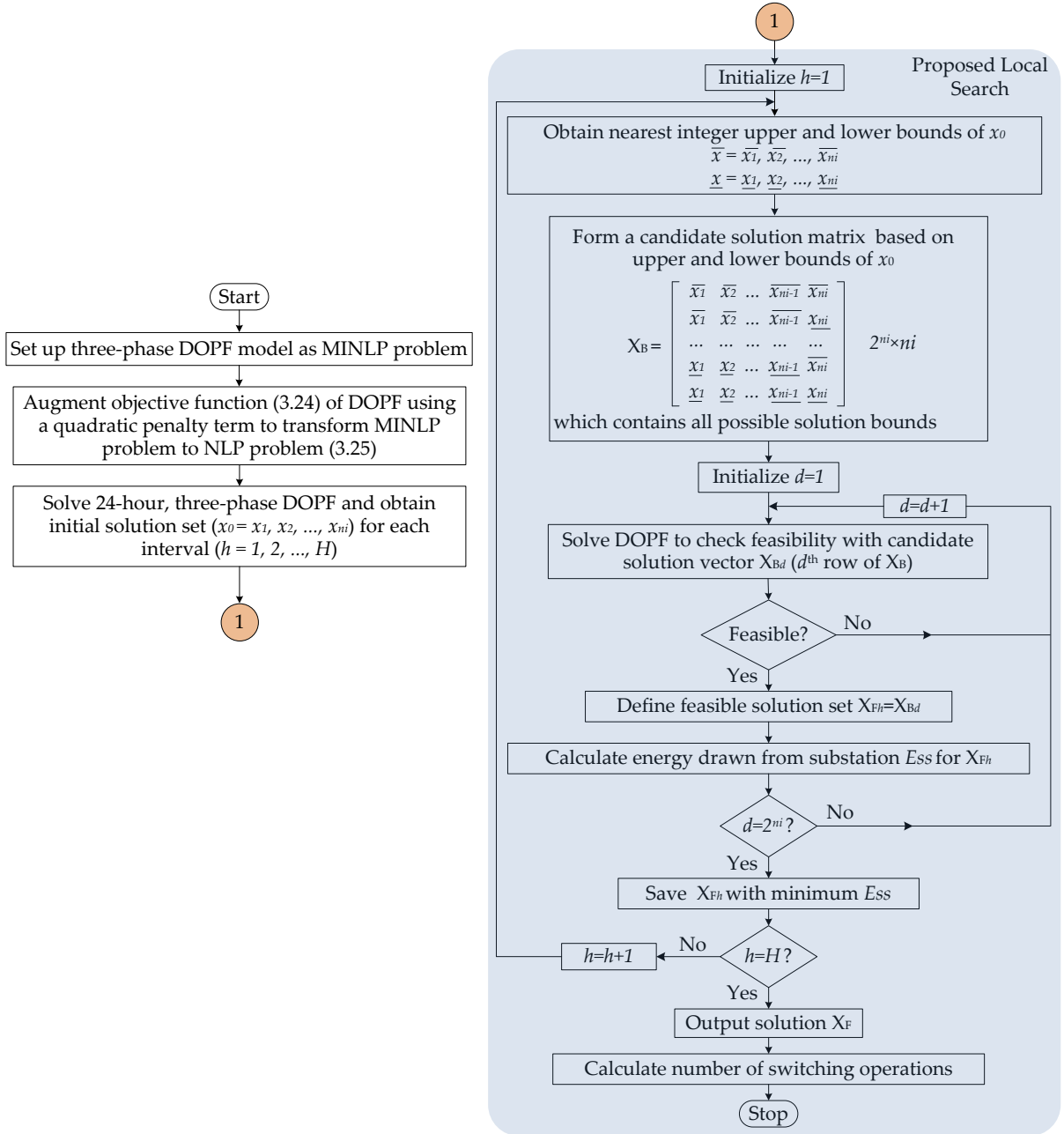
Figure 3.2: Flowchart of the proposed DOPF solution procedure with local search restricted to the two nearest integers.

- Population Size ($S$): A population size of 25 individuals is considered, where individuals mean binary values assigned to the chromosomes represent all *tap* and *cap* variables for $H$ intervals. To start, 25 individuals that satisfy the equality and inequality constraints (3.1)-(3.23b) of the three-phase DOPF are chosen arbitrarily.

- Fitness Function ($F$): The objective function in (3.24) is used to evaluate the fitness of the initial population and offspring. To avoid infeasible cases, any offspring that does not satisfy the equality and inequality constraints (3.1)-(3.23b) is assigned a very high value of $F$ and considered unfit.

- Cross-over and Mutation: A cross-over rate ($CR$) of 80% and a mutation rate ($MR$) of 1% are used. A two-point cross over (after $2^{nd}$ and $4^{th}$ bits) is employed.

Note that in Figure 3.3, the three-phase DLF model is represented by the equality and inequality constraints (3.1)-(3.23b).

The performance of the GA-based method considerably depends on the selection of its parameters. Note that the GA parameters chosen here are not optimally tuned. Optimal parameter tuning of GA require exhaustive heuristic searches and are problem specific [138], and is therefore beyond the scope of this thesis. Furthermore, there is no reported standard or optimal method of GA-parameter settings in the literature for the kind of problem solved in this thesis.

## 3.8 Model Validation

The proposed three-phase DOPF model is developed in GAMS [128], a high-level optimization modeling tool. The constraints of the three-phase DOPF, which represent a DLF model, are solved using the MINOS solver [129]. The developed models are validated using the IEEE 4-node and 13-node test feeders; the network diagrams of these

*begin*
define CX, *F*
choose *G*, *S*, *CR*, *MR*
choose individuals of *S*
solve three-phase DLF for individuals in *S*
evaluate *F* for individuals in *S*
    *repeat*
      rank individuals of *S* based on *F*
        *repeat*
          create a pool of individuals, based on *CR*,  for mating
          choose parents based on two random numbers
          apply cross-over operator to reproduce offspring
          apply mutation operator to offspring based on *MR*
          solve three-phase DLF for offspring
          evaluate *F* for offspring
          discard unfit offspring
        *until*  *S* number of offspring are reproduced
      choose best *S* fit individuals among parents and offspring
    *until*  generation *G* is reached
*end*

Figure 3.3: Pseudo-code illustrating the GA-based solution method for the three-phase DOPF.

feeders are shown in Figure 3.4 and 3.5 respectively (the number of phases in the feeders are depicted with cross bars). Details of the system parameters can be found in [4].

Simulations are carried out to obtain the base DLF solutions and compared them with the results in [4]. Table 3.1 shows a comparison of the results for the IEEE 4-node system with unbalanced loading and delta-wye grounded step down transformer connection (with American Standard Connection of 30° negative angular displacement), showing a maximum error of 1.25% in the voltage angle on phase *a* at node 3. Table 3.2 shows a comparison of the results for the IEEE 13-node test feeder (only node voltages are shown), obtaining a maximum error of 0.3% in the voltage angle on phase *a* at node 634. Observe
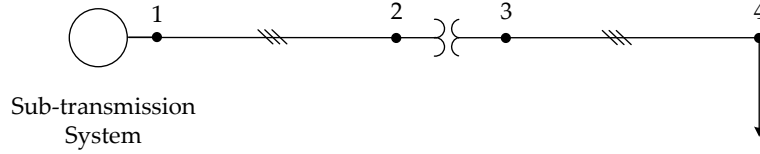
Figure 3.4: IEEE 4-node test feeder [4].
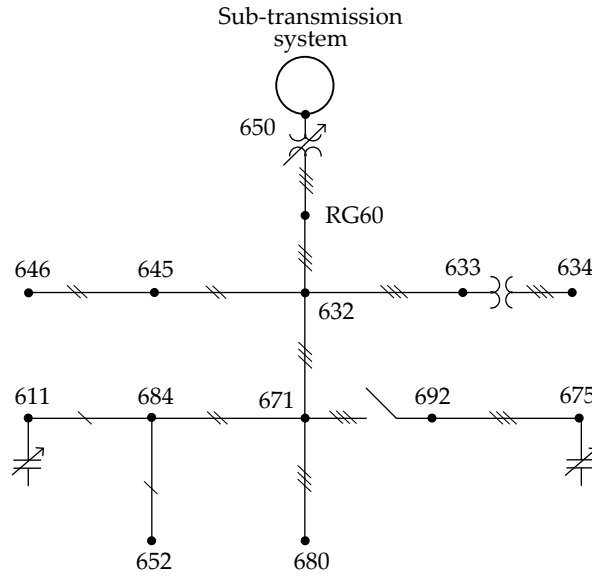


Figure 3.5: IEEE 13-node test feeder [4].

that the results obtained from the DLF solution closely matches the results provided in [4]. The base case DLF solutions thus obtained, verify and validate the developed component models and network equations used to represent a distribution system.

## 3.9   Case Studies

In addition to the three-phase DOPF model, the heuristic method and the GA-based method were also implemented in GAMS [128]. Both the heuristic and GA-based methods require solutions to the three-phase DLF, which is an NLP problem; for this purpose,

Table 3.1: Results comparison for IEEE 4-node test feeder.

| Node | Phase | GAMS Model | | IEEE Report [4] | |
|------|-------|------------|---------|-----------------|---------|
| | | Voltage, V | Angle, ° | Voltage, V | Angle, ° |
| 1 | a | 12470.00 | 30.00 | 12470.00 | 30.00 |
| | b | 12470.00 | -90.00 | 12470.00 | -90.00 |
| | c | 12470.00 | -150.00 | 12470.00 | -150.00 |
| 2 | a | 12350.28 | 29.60 | 12350.00 | 29.60 |
| | b | 12313.89 | -90.39 | 12314.00 | -90.40 |
| | c | 12332.73 | 149.75 | 12333.00 | 149.80 |
| 3 | a | 2291.21 | -32.39 | 2290.00 | -32.80 |
| | b | 2261.31 | -153.79 | 2261.00 | -153.80 |
| | c | 2213.89 | 85.16 | 2214.00 | 85.20 |
| 4 | a | 2157.77 | -34.23 | 2157.00 | -34.20 |
| | b | 1935.88 | -157.01 | 1936.00 | -157.00 |
| | c | 1849.30 | 73.38 | 1849.00 | 73.40 |
| | | Current, A | Angle, ° | Current, A | Angle, ° |
| 1-2 | a | 285.60 | -27.58 | 285.70 | -27.60 |
| | b | 402.76 | -149.59 | 402.70 | -149.60 |
| | c | 349.06 | 74.33 | 349.10 | 74.40 |
| 3-4 | a | 695.15 | -66.02 | 695.50 | -66.00 |
| | b | 1033.11 | 177.14 | 1033.00 | 177.10 |
| | c | 1351.85 | 55.18 | 1352.00 | 55.20 |

the MINOS solver was used [129].

## 3.9.1   IEEE 13-node Test Feeder

To demonstrate and test the proposed three-phase DOPF, an optimal solution is obtained by considering the loss minimization objective on the IEEE 13-node test feeder for a given hour, allowing the LTC positions to vary, while keeping the capacitor banks fixed. As expected, the simulation result shows that losses can be reduced to 107.79 kW from a value

Table 3.2: Results comparison for IEEE 13-node test feeder.

| Node | Phase | GAMS Model | | IEEE Report [4] | |
|------|-------|------------|----------|-----------------|----------|
|      |       | Voltage, p.u. | Angle, ° | Voltage, p.u. | Angle, ° |
| 650  | a     | 1.0000 | 0.00 | 1.0000 | 0.00 |
|      | b     | 1.0000 | -120.00 | 1.0000 | -120.00 |
|      | c     | 1.0000 | 120.00 | 1.0000 | 120.00 |
| RG60 | a     | 1.0625 | 0.00 | 1.0625 | 0.00 |
|      | b     | 1.0500 | -120.00 | 1.0500 | -120.00 |
|      | c     | 1.0687 | 120.00 | 1.0687 | 120.00 |
| 632  | a     | 1.0210 | -2.49 | 1.0210 | -2.49 |
|      | b     | 1.0420 | -121.72 | 1.0420 | -121.72 |
|      | c     | 1.0174 | 117.83 | 1.0174 | 117.83 |
| 633  | a     | 1.0179 | -2.56 | 1.0180 | -2.56 |
|      | b     | 1.0401 | -121.77 | 1.0401 | -121.77 |
|      | c     | 1.0148 | 117.82 | 1.0148 | 117.82 |
| 634  | a     | 0.9932 | -3.24 | 0.9940 | -3.23 |
|      | b     | 1.0210 | -122.22 | 1.0218 | -122.22 |
|      | c     | 0.9952 | 117.34 | 0.9960 | 117.34 |
| 645  | b     | 1.0328 | -121.90 | 1.0329 | -121.90 |
|      | c     | 1.0154 | 117.85 | 1.0155 | 117.86 |
| 645  | b     | 1.0311 | -121.98 | 1.0311 | -121.98 |
|      | c     | 1.0134 | 117.90 | 1.0134 | 117.90 |
| 671  | a     | 0.9899 | -5.30 | 0.9900 | -5.30 |
|      | b     | 1.0529 | -122.35 | 1.0529 | -122.34 |
|      | c     | 0.9778 | 116.02 | 0.9778 | 116.02 |
| 680  | a     | 0.9899 | -5.30 | 0.9900 | -5.30 |
|      | b     | 1.0529 | -122.35 | 1.0529 | -122.34 |
|      | c     | 0.9778 | 116.02 | 0.9778 | 116.02 |
| 684  | a     | 0.9879 | -5.33 | 0.9881 | -5.32 |
|      | c     | 0.9758 | 115.92 | 0.9758 | 115.92 |
| 611  | c     | 0.9738 | 115.77 | 0.9738 | 115.78 |
| 652  | a     | 0.9824 | -5.25 | 0.9825 | -5.25 |
| 692  | a     | 0.9899 | -5.30 | 0.9900 | -5.31 |
|      | b     | 1.0529 | -122.35 | 1.0529 | -122.34 |
|      | c     | 0.9778 | 116.02 | 0.9777 | 116.02 |
| 675  | a     | 0.9834 | -5.55 | 0.9835 | -5.56 |
|      | b     | 1.0553 | -122.52 | 1.0553 | -122.52 |
|      | c     | 0.9759 | 116.03 | 0.9758 | 116.03 |

of 111.06 kW obtained from the base DLF solution provided in [4]. The LTC positions for each tap obtained in this case are 16, -1, and 16, respectively. The node voltages obtained from the three-phase DOPF model are compared with the base DLF solutions, in Figure 3.6. Observe that in the base DLF solution, the phase $b$ voltage at node 675 is above the upper limit of 1.05 p.u.; this can be attributed to the conventional voltage control procedures used in distribution systems, where LTCs are switched to control the voltage at a fictitious load center rather than maintaining voltages at all load nodes. In contrast, the load voltages obtained from the three-phase DOPF model are all within the range of 0.95-1.05 p.u.

To demonstrate the application of the proposed three-phase DOPF model in a 24-hour timeframe in the context of Smart Grids, the load behavior is assumed to respond to external inputs and hence it is different at each node, which is not typically the case in "standard" distribution system studies; thus, twenty-four, hourly, randomly generated load profiles at each node are considered. Each bus load representation comprises constant impedance, constant current, and constant power load models as per [4]. The load data provided in [4] are assumed to correspond peak loads, and the load profile reported in [139] is used. The random load scenarios are generated using a typical load profile and a normal distribution function; at each hour, a random number is generated to scale the load profiles below or above the nominal value using a normal distribution function ($\mu$=1, $\sigma$=0.1). To shift the load profiles in time, discrete random numbers that take integer values from -2 to +2 using a uniform distribution function are used; the load is then shifted forward or backward on the time axis, where the integer number represents the number of hours to be shifted. This yields random changes in magnitude and time in the load profiles; some of the load profiles are depicted in Figure 3.7.

The capacitors available in the IEEE-13 node test feeders are single units with fixed values. To demonstrate the applicability of the proposed method considering SCs, the given capacitor data are modified assuming that five blocks of 100 kVar capacitors are connected at node 675 in each phase, and five blocks of 50 kVar capacitors are connected
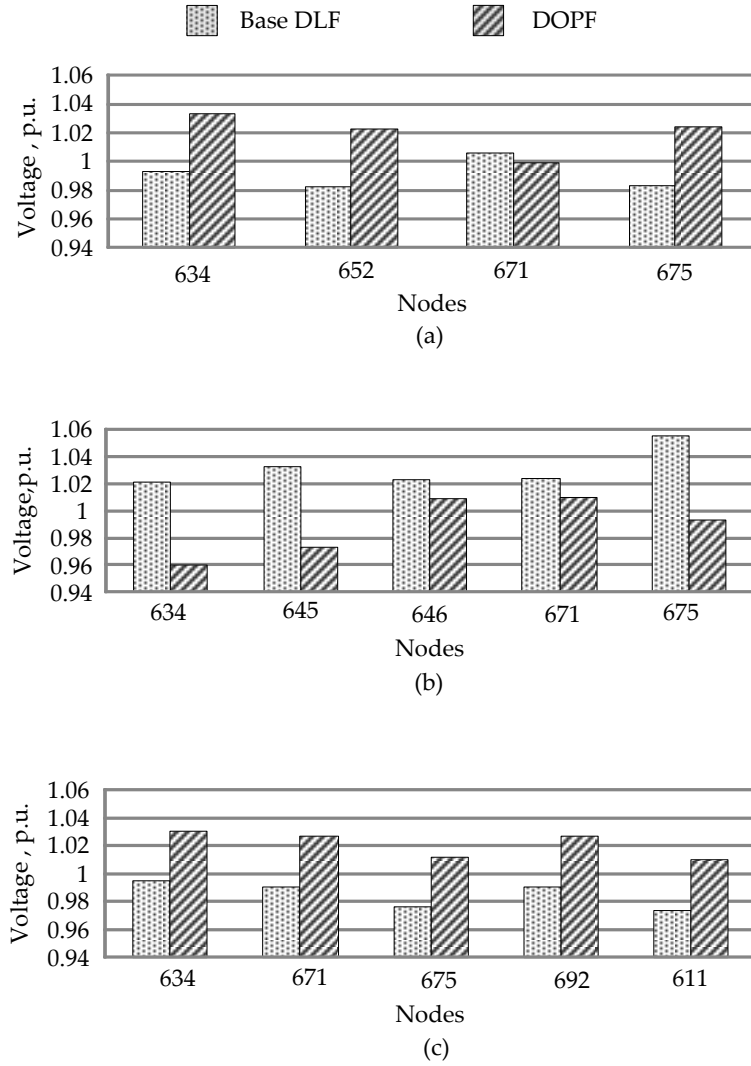
Figure 3.6: Three-phase load voltage profiles for IEEE 13-node test feeder: (a) phase
$a$, (b) phase $b$, and (c) phase $c$.

at node 611 in phase $c$. The LTC and the two assumed capacitor banks are considered to
be controllable. In the proposed objective function (3.24), equal weights are attached to
the switching operations of LTC and capacitors, and these are considered complementary

66
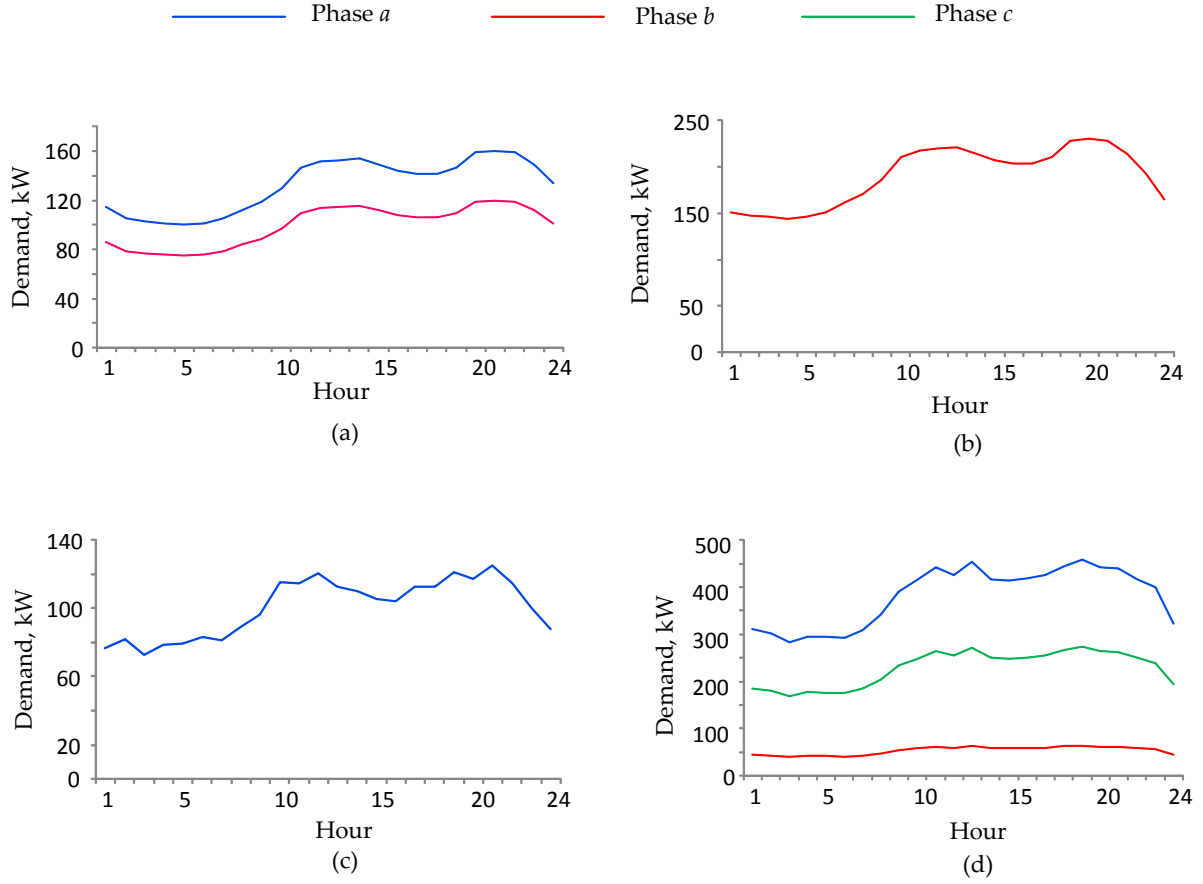
Figure 3.7: Load profiles for IEEE 13-node test feeder: (a) three-phase at node 634, (b) one-phase at node 646, (c) one-phase at node 652, and (d) three-phase at node 675.

to the weight attached to the energy drawn from substation, i.e.,

$$\beta = \gamma = 1 - \alpha \qquad (3.26)$$

Table 3.3 presents the results from the simulation cases considering different values of $\alpha$. In this table, Case 1 corresponds to a base DLF solution, so that appropriate comparisons can be made. Case 2 represents the minimization of energy drawn from the substation; in this case, the energy drawn from the substation is reduced by 7.09% compared to the base

case, while the number of switching operations is reduced only by 6.25%. Case 4 represents the minimization of switching operations, thus resulting in a total of 12 switching operations of LTC and capacitors; in this case, the load voltages are not maintained near the lower limit of 0.95 p.u., thus the energy drawn from the substation is increased to 67.73 MWh. Compared to the base case, Case 4 requires 62.5% less switching operations while there is a 0.07% increase in the energy drawn from the substation, which is to be expected given the DOPF objective used. Case 3 represents a mixed minimization of the energy drawn from the substation and the total number of switching operations. This case is a compromise solution between Case 2 and Case 4 based on the weight $\alpha$ provided, and thus, as expected, yields a higher energy than Case 2 and more switching operations than Case 4. The choice of $\alpha$ depends on the distribution system operator's preference, based on the energy price and maintenance cost of LTC and capacitor switching mechanisms, so that the overall operating cost can be optimized.

It is important to mention that given the practical solution procedure used to deal with the integer variables, one cannot guarantee that the obtained solution is the local optimum. There might be better solutions in terms of both energy and number of operations as $\alpha$ changes; this is the trade-off between mathematical precision and computational effort. However, at least for $\alpha = 1$ and $\alpha = 0$, no better solutions than the minimum energy and minimum number of switching operations, respectively, can be found.

Figure 3.8 shows the comparison of load voltages at peak load for two cases $\alpha = 1$ and $\alpha = 0$. Observe that, for $\alpha = 1$, when the distribution system operator is minimizing the energy drawn from the substation, the voltages are close to 0.95 p.u.; this is because of the frequent LTC and capacitor switchings carried out to maintain the voltage close to the lower acceptable boundary to reduce power demand. For $\alpha = 0$, the operator seeks to minimize the number of switching operations, resulting in the voltage profile no longer remaining at the lower bounds, which thereby leads to increased system loading.

Table 3.3: Simulation results for IEEE 13-node test feeder using heuristic algorithm.

| Case | $\alpha$ | Number of Switching Operations | | | | Energy from Substation (MWh) | Energy Loss (MWh) | % Reduction in Energy from Substation | % Reduction in Number of Switching Operations |
|------|----------|--------|--------|--------|-------|------------|-----------|-----------|-----------|
| | | $tap_1$ | $cap_1$ | $cap_2$ | Total | | | | |
| 1 | — | 10 | 8 | 14 | 32 | 67.684 | 2.129 | — | — |
| 2 | 1.0 | 8 | 16 | 6 | 30 | 62.886 | 1.986 | 7.09 | 6.25 |
| 3 | 0.2 | 16 | 2 | 2 | 20 | 67.081 | 2.125 | 0.89 | 37.5 |
| 4 | 0.0 | 12 | 0 | 0 | 12 | 67.730 | 2.138 | -0.07 | 62.5 |

## 3.9.2 Hydro One Distribution Feeder

Simulations are also carried out considering a practical distribution feeder. For this purpose, an unbalanced distribution feeder, which is a part of the distribution network of Hydro One Inc., is used [139]. The system configuration is shown in Figure 3.9.

The provided load data are considered to be peak loads, and 24-hour load profiles at each node are defined using the same random procedure used in the previous test feeder. In this case, a constant impedance load model is considered, directly calculated from the active and reactive powers at nominal voltage.

The system has three three-phase transformers and a single phase transformer. It is assumed then that all three-phase transformers are equipped with LTCs, and that these are the only controllable devices in the network.

Similar to Section 3.9.1, equal weights are attached to the switching operations of LTCs and are assumed to be complementary to the weight attached to the energy drawn from the substation as follows:

$$\beta = 1 - \alpha \tag{3.27}$$
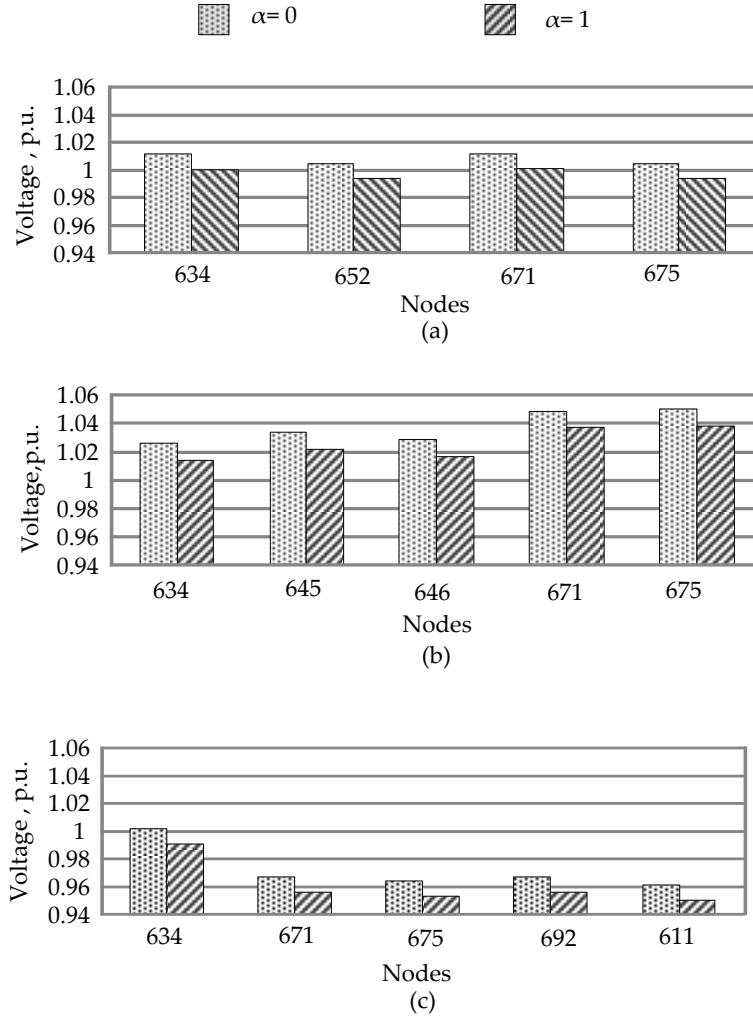
Figure 3.8: Comparison of load voltages at peak load for cases $\alpha = 1$ and $\alpha = 0$: (a) phase $a$, (b) phase $b$, and (c) phase $c$.

Table 3.4 presents the results from the simulation cases considering different values of $\alpha$. In this table, Case 1 corresponds to a non-optimized base case. Case 2 represents the minimization of energy drawn from the substation resulting, as expected, in the maximum reduction of energy compared to the base case. Case 4 represents minimization of switching operations only, leading to the maximum reduction in the number of
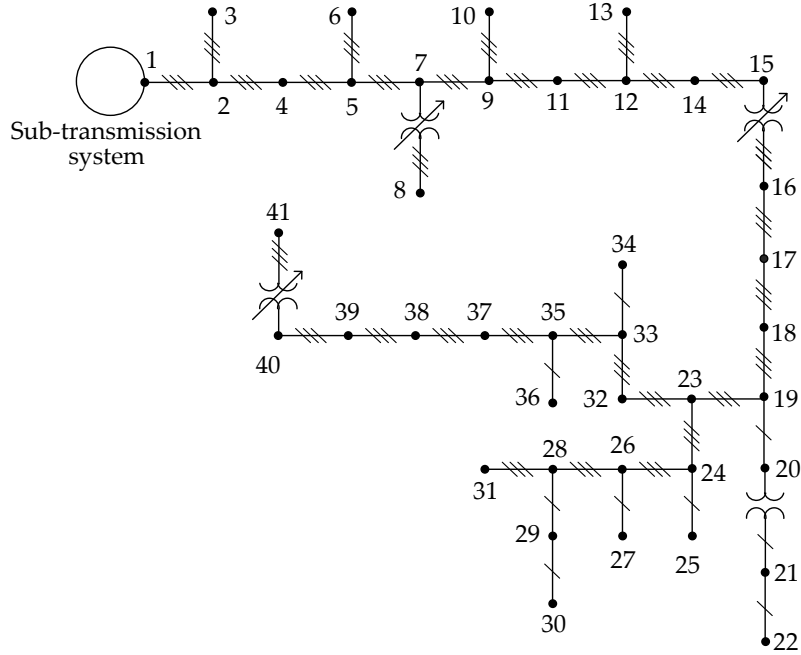
Figure 3.9: Hydro One distribution feeder.

switching operations compared to the base case. Finally, Case 3 is a compromise solution between Case 2 and Case 4.

It should be highlighted from the analysis of the results for the two test feeders that the energy losses in the distribution network are minimum when the operator's objective is to minimize the energy drawn from the substation (Case 2). On the other hand, Case 4 seeks to minimize the LTC and capacitor operations, and hence the losses increase.

### 3.9.3 Optimality versus Computational Burden

For the simulation cases for the IEEE 13-node test feeder and Hydro One Distribution feeder discussed in the previous sections, the performance of the heuristic and the GA-based solution methods are compared here based on the optimal solutions and associated computational burden obtained when solving the three-phase DOPF model.

Table 3.4: Simulation results for Hydro One distribution feeder using heuristic algorithm.

| Case | $\alpha$ | Number of Switching Operations | | | | Energy from Substation (MWh) | Energy Loss (MWh) | % Reduction in Energy from Substation | % Reduction in Number of Switching Operations |
|------|------|------|------|------|------|------|------|------|------|
| | | $tap_1$ | $tap_2$ | $tap_3$ | Total | | | | |
| 1 | — | 12 | 14 | 50 | 76 | 291.619 | 6.090 | — | — |
| 2 | 1 | 28 | 6 | 12 | 46 | 286.976 | 6.058 | 1.59 | 39.47 |
| 3 | 0.6 | 10 | 12 | 20 | 42 | 293.793 | 6.264 | -0.75 | 44.73 |
| 4 | 0 | 4 | 14 | 14 | 32 | 293.987 | 6.265 | -0.81 | 57.89 |

Table 3.5: Variables and search space associated with the two distribution feeders.

| System | | IEEE 13-node Test Feeder | Hydro One Distribution Feeder |
|------|------|------|------|
| NLP Continuous Variables | | 9960 | 27000 |
| MINLP | Continuous Variables | 9792 | 26784 |
| | Integer Variables | 168 | 216 |
| Search Space | 24-Hour | $4.72 \times 10^{21}$ | $4.72 \times 10^{21}$ |
| | Hourly | 192 | 192 |

The GA-based solution method, which uses the complete MINLP model of the IEEE-13 node test feeder in a 24-hour timeframe, involves 9,792 continuous and 168 controllable integer variables, as shown in Table 3.5; the NLP model used in the heuristic method requires a solution of 9,960 continuous variables. In the heuristic solution method, the hourly search technique narrows down the search space to 192 combinations from $4.72 \times 10^{21}$, which would have otherwise been required in case of a 24-hour search.

For $\alpha$=1, similar to the case studies discussed in Section 3.9.1, the optimal energy drawn from the substation obtained using the heuristic method is 62.89 MWh, while for

Table 3.6: Results comparison for IEEE 13-node test feeder using the heuristic and the GA-based solution methods.

| Case | $\alpha$ | Solution Method | Generations | Energy (MWh) | No. of Switchings | Objective Function | Solution Time | % Difference in Objective Function Compared to Heuristic Method |
|------|-----|-----------|------|-------|----|-------|------------|--------|
| 1 | 1 | Heuristic | — | 62.89 | 30 | 62.89 | 4m 46s | — |
|   |   | GA | 1 | 68.88 | 24 | 68.88 | 3m 52s | 9.53 |
|   |   |   | 25 | 62.20 | 35 | 62.20 | 53m 47s | -1.09 |
|   |   |   | 50 | 61.81 | 47 | 61.81 | 1h 47m 32s | -1.71 |
|   |   |   | 100 | 61.23 | 88 | 61.23 | 3h 44m 51s | -2.63 |
| 2 | 0.2 | Heuristic | — | 67.08 | 20 | 29.42 | 3m 39s | — |
|   |   | GA | 1 | 62.55 | 73 | 70.91 | 3m 46s | 141.06 |
|   |   |   | 25 | 65.09 | 42 | 46.62 | 53m 14s | 58.48 |
|   |   |   | 50 | 67.86 | 26 | 34.37 | 1h 46m 58s | 16.85 |
|   |   |   | 100 | 68.18 | 18 | 28.04 | 3h 28m 36s | -4.69 |
| 3 | 0 | Heuristic | — | 67.73 | 12 | 12.00 | 3m 11s | — |
|   |   | GA | 1 | 62.93 | 76 | 76.00 | 3m 44s | 533.33 |
|   |   |   | 25 | 63.75 | 51 | 51.00 | 54m 19s | 325.00 |
|   |   |   | 50 | 66.81 | 28 | 28.00 | 1h 46m 32s | 133.33 |
|   |   |   | 100 | 67.85 | 12 | 12.00 | 3h 28m 39s | 0.00 |

the GA-based method improved solutions are obtained over the generations, starting from 68.88 MWh after the 1st generation to 61.23 MWh at the end of the 100th generation. Observe in Figure 3.10 that the GA-based method starts to yield better solutions after the 16th generation compared to the heuristic method, but requires 39m 17s to complete these 16 generations, which is not a suitable timeframe for real-time applications. Over the subsequent generations, the GA-based method yields better solutions as compared to the heuristic method but at rather large computational cost.
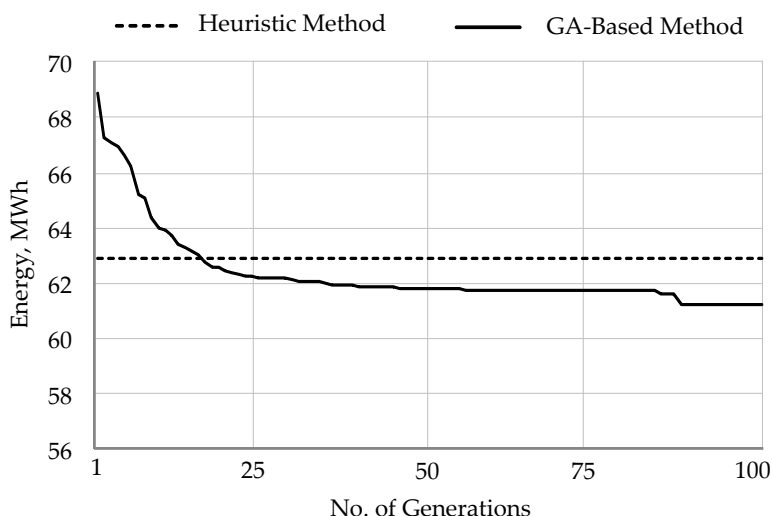
Figure 3.10: Comparison of the heuristic and GA-based solution methods for the IEEE 13-node test feeder for $\alpha = 1$.

For example, after the $50^{\text{th}}$ generation, the optimal solution is improved by 1.71%, as compared to the heuristic method, but requires 1h 47m 32s to arrive at this solution. On the contrary, the heuristic method yields a reasonable solution in 4m 46s, which is suitable for real-time applications, and the solution is close to that obtained from the GA-based method, since the difference in optimality is only 2.63%.

Table 3.6 summarizes the results from the simulation cases considering different values of $\alpha$. Thus, for $\alpha = 0.2$, which represents a weighted sum of energy and switching operations, the GA-based method requires 3h 28m 36s to arrive at the best solution but the difference in optimal value is only 4.69%, compared to the heuristic solution. For $\alpha = 0$, which represents the minimization of switching operations, the GA-based method does not yield any solution better than the one obtained from the heuristic method. These results show that the solutions are obtained in much less time using the heuristic method (not more than 5m), and the solutions are reasonably close to the GA-based method, since the differences in optimality are not more than 4.69%. It is to be noted that the performance of the GA-based method depends on various factors such as the

74

Table 3.7: Results comparison for Hydro One distribution feeder using the heuristic and the GA-based solution methods.

| Case | $\alpha$ | Solution Method | Generations | Energy (MWh) | No. of Switchings | Objective Function | Solution Time | % Difference in Objective Function Compared to Heuristic Method |
|------|------|------|------|------|------|------|------|------|
| 1 | 1 | Heuristic | — | 286.98 | 46 | 286.98 | 10m 5s | — |
| | | GA | 1 | 293.80 | 123 | 293.80 | 5m 7s | 2.38 |
| | | | 25 | 291.26 | 164 | 291.26 | 1h 8m 54s | 1.49 |
| | | | 50 | 291.03 | 147 | 291.03 | 2h 37m 51s | 1.41 |
| | | | 100 | 283.63 | 139 | 283.63 | 5h 17m 29s | -1.17 |
| 2 | 0.6 | Heuristic | — | 293.79 | 42 | 193.08 | 9m 4s | — |
| | | GA | 1 | 292.39 | 136 | 229.83 | 5m 38s | 19.04 |
| | | | 25 | 292.39 | 136 | 229.83 | 1h 21m 50s | 19.04 |
| | | | 50 | 292.03 | 114 | 220.82 | 2h 42m 22s | 14.37 |
| | | | 100 | 292.19 | 42 | 192.11 | 5h 34m 14s | -0.50 |
| 3 | 0 | Heuristic | — | 293.99 | 32 | 32.00 | 7m 9s | — |
| | | GA | 1 | 292.39 | 136 | 136.00 | 5m 50s | 325.00 |
| | | | 25 | 293.39 | 128 | 128.00 | 1h 27m 41s | 300.00 |
| | | | 50 | 292.84 | 57 | 57.00 | 2h 46m 10s | 78.13 |
| | | | 100 | 295.67 | 30 | 30.00 | 5h 55m 57s | -6.25 |

selection of the initial pool of population, cross-over rate, mutation rate, stopping criteria, etc.; however, in general, even though the GA-based method yields a superior optimal solution, the large computational effort involved makes it impractical, particularly for real-time operational and control purposes.

Simulations are also carried out for the Hydro One distribution feeder [139]. The complete MINLP model of the Hydro One feeder in a 24-hour timeframe involves 26,784 continuous and 216 controllable integer variables in the GA-based method, while the

NLP model used for the heuristic method involves 27,000 continuous variables (see Table 3.5). By applying the hourly search technique in the heuristic method, the search space is narrowed down to 192 combinations from the $4.72 \times 10^{21}$ required in the case of a 24-hour search.

Table 3.7 presents the results from the simulation cases considering different values of $\alpha$. The heuristic method requires larger computational times to arrive at the optimal solution as compared to the IEEE 13-node test feeder; however, the maximum computational time required is about 10m, which is significantly less compared to the GA-based method and within a reasonable timeframe for real-time applications. Also, the optimal solutions obtained using both the solution methods are reasonably close, with the differences in optimal values being no more than 6.25%.

The reported results of the proposed algorithm for a real Hydro One distribution feeder demonstrates the practicality of the method; thus, it can be seen that in all cases, the computational time required to solve the problem is such that the real-time application of the proposed methodology is feasible, considering that non-optimized, "over-the-counter" software tools are used. Also, despite yielding sub-optimal solutions, the results are such that it would certainly improve feeder operation.

The simulation results presented in Tables 3.6 and 3.7 are based on an Intel machine with eight 2.83 GHz, 32-bit, virtual processors, and 3 GB memory, running Windows Server 2003.

## 3.10    Summary

In this chapter, a generic three-phase DOPF model was proposed and tested for unbalanced distribution systems. The novel three-phase DOPF model incorporates single-phase, two-phase and three-phase representations for feeder, transformers, switches and LTCs within an optimization framework. Customer loads are realistically modeled as

voltage dependent loads, so that the energy consumption profile can be suitably modulated by optimal control actions. The integer decision variables present in the optimization model are treated as continuous variables using an appropriate solution methodology that transforms the original MINLP problem into an NLP, which is solvable using commercially available solvers. The application of the proposed procedure to two realistic distribution feeders demonstrated that the desired objectives of minimizing the energy drawn from the substation as well as limiting the number of switching operations of the control devices can be feasibly achieved.

This chapter also presented a GA-based solution method to determine the optimal solutions of the three-phase DOPF problem. The proposed heuristic method was compared with respect to the GA results, in terms of both optimality and computational burden, for the two test distribution feeders. A comparison of the two approaches showed that the GA-based method yields superior solutions in terms of optimality, but at a large computational cost. The heuristic method was shown to yield solutions quite close to the global optima at a significantly reduced computational burden. Despite these sub-optimal solutions, the results obtained using the heuristic methods are such that it would certainly improve feeder operation in Smart Grids, with solution times that are suitable for real-time applications.

The mathematical model and solution method presented in this chapter, in conjunction with Smart Grid technologies at the LDC system level, would be beneficial to LDC system operators for real-time, centralized, optimal control of practical distribution feeders.

# Chapter 4

# Optimal Operation of Industrial Energy Hubs

## 4.1   Introduction

This chapter presents the development of a generic OILM model that can be readily incorporated into an EHMS for industrial customers, in coordination with the LDCs, for automated and optimal scheduling of their processes. The mathematical models comprise an objective function that minimizes the total energy costs and/or demand charges, and a set of equality and inequality constraints to represent the industrial process, storage units, distribution system components, operator's requirements, and others. The effectiveness of the proposed OILM model is demonstrated in two industrial customers: a flour mill and a water pumping facility.

The rest of the chapter is organized as follows: Section 4.2 presents the nomenclature of all the parameters, indices, variables, and functions used in the mathematical modeling, Section 4.3 presents the details of the proposed OILM model, Section 4.4 discusses the estimation of the model parameters, and Section 4.5 presents the results of the case studies

carried out for two industrial customers to demonstrate the application of the proposed model. A summary of the chapter is presented in Section 4.6.

## 4.2   Nomenclature

*Parameters:*

| | |
|---|---|
| $a_0 - a_{11}$ | Coefficients of function $f(\,\cdot\,)$. |
| $\Delta T$ | Duration of an interval in hour. |
| $DN$ | Down-time of industrial process in hour. |
| $DP$ | Process inter-dependency matrix. |
| $E$ | Total number of measurements. |
| $F$ | Fixed up-time processes (1 fixed, 0 variable). |
| $GP$ | Gaps between processes in hour. |
| $I_{max}$ | Maximum material inflow rate per hour. |
| $I_{min}$ | Minimum material inflow rate per hour. |
| $IN$ | Total number of input variables. |
| $\lambda$ | Peak demand charge in \$/kW/month prorated per day. |
| $L_0$ | Initial storage level. |
| $L_{cap}$ | Storage capacity. |
| $L_{min}$ | Minimum allowed storage level. |
| $L_{req}$ | Required storage level. |
| $NC$ | Total number of storage units. |
| $NJ$ | Total number of industrial processes. |
| $O_{max}$ | Maximum material outflow rate per hour. |
| $O_{min}$ | Minimum material outflow rate per hour. |
| $OT$ | Total number of output variables. |
| $P_{max}$ | Peak demand requirement set by an LDC. |
| $\tilde{Q}r$ | Measured water discharge rate of the pumps in m$^3$/h. |

| $\rho$ | Energy price in \$/kWh. |
|---|---|
| $R$ | Process I/O matrix. |
| $T$ | Total number of intervals. |
| $T_1$ | First interval of scheduling window. |
| $T_2$ | Last interval of scheduling window. |
| $UP$ | Up-time of industrial processes in hour. |
| $\tilde{V}$ | Measured voltage applied to processes or storage units in kV. |
| $V_{max}$ | Maximum voltage limit as per standard in kV. |
| $V_{min}$ | Minimum voltage limit as per standard in kV. |
| $Y_{max}$ | Maximum limits on non-electrical variables. |
| $Y_{min}$ | Minimum limits on non-electrical variables. |

*Indices:*

| $cf$ | Storage unit number in which final products are stored, $cf \in nc$. |
|---|---|
| $e$ | Number of measurement $1, 2, ..., E$. |
| $in$ | Input variable number $1, 2, ..., IN$. |
| $j, k$ | Industrial process number $1, 2, ..., NJ$. |
| $nc$ | Storage unit number $1, 2, ..., NC$. |
| $ot$ | Output variable number $1, 2, ..., OT$. |
| $\tau, t$ | Time interval $1, 2, ..., T$. |
| $tf$ | Time interval for which the requirements of final products are set, $tf \in t$. |

*Variables:*

| $ir$ | Input flow rates per hour. |
|---|---|
| $nr$ | Auxiliary variable to calculate total number of ON decisions for a process. |
| $nw$ | Auxiliary variable. |
| $or$ | Output flow rates per hour. |
| $P_{peak}$ | Auxiliary variable to model peak demand. |

| | |
|---|---|
| $Pd$ | Active power demand of processes or storage units in kW. |
| $\tilde{P}d$ | Measured active power demand of processes or storage units in kW. |
| $\hat{P}d$ | Estimated active power demand of processes or storage units in kW. |
| $Pt$ | Total power consumption of processes and storage units in kW. |
| $Qd$ | Reactive power demand of processes or storage units in kVAr. |
| $Qr$ | Water discharge rate of the pumps in m$^3$/h. |
| $\hat{Q}r$ | Estimated water discharge rate of the pumps in m$^3$/h. |
| $Qt$ | Total reactive power consumption of processes and storage units in kVAr. |
| $sl$ | Storage level. |
| $st$ | Process ON/OFF status (1 ON, 0 OFF). |
| $ud$ | Decision to turn ON a process (1 ON). |
| $V$ | vector of three phase voltages applied to processes or storage units in kV. |
| $V_{av}$ | Average of three phase voltages applied to processes or storage units in kV. |
| $vd$ | Decision to turn OFF a process (1 OFF). |
| $y$ | Vector of non-electrical variables required to model processes or storage units. |
| $J_{obj}$ | Objective function. |

*Functions:*

| | |
|---|---|
| $f(\,\cdot\,)$ | Load estimation polynomial function to estimate active power demand. |
| $g(\,\cdot\,)$ | Load estimation polynomial function to estimate reactive power demand. |

## 4.3   Mathematical Modeling

This section describes the objective function and the set of equality/inequality constraints representing the industrial processes, storage units, distribution system components, operating limits, and other relevant components that make up the proposed OILM model.

## 4.3.1 Industrial Processes

**Material Inflow/Outflow**

Industrial loads can be modeled as processes, comprising one or multiple devices operating together, and can be considered as a multi-input, multi-output, multi-interval system, as shown in Figure 4.1, where the input and output variables represent the rate of inflow and outflow of material, respectively. For each industrial process $j$, a matrix $R_j$ (referred here as process I/O matrix), relating the material inflow and outflow rates in each time interval, can be defined as follows:

$$\begin{bmatrix} or_{1,j,t} \\ or_{2,j,t} \\ : \\ or_{OT,j,t} \end{bmatrix} = \begin{bmatrix} R_j \end{bmatrix} \begin{bmatrix} ir_{1,j,t} \\ ir_{2,j,t} \\ : \\ ir_{IN,j,t} \end{bmatrix} \qquad \forall j, \forall t \qquad (4.1a)$$

$$\begin{bmatrix} R_j \end{bmatrix} = \begin{bmatrix} R_{1,1,j} & R_{1,2,j} & .. & R_{1,IN,j} \\ R_{2,1,j} & R_{2,2,j} & .. & R_{2,IN,j} \\ : & : & .. & : \\ R_{OT,1,j} & R_{OT,2,j} & .. & R_{OT,IN,j} \end{bmatrix} \qquad \forall j \qquad (4.1b)$$

All variables, parameters, and indices in these and other equations in this chapter are defined in Section 4.2. Here, $R_j$ is a matrix of numbers and its size depends on the number of input/output variables required to model the process. The $R_j$ matrix for an individual process can be determined from historical measurements and the knowledge of the process, as explained in Section 4.4.
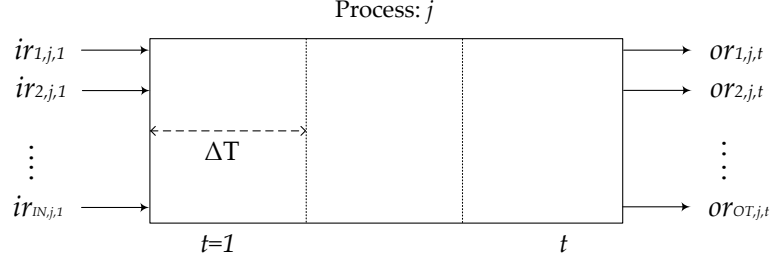
Figure 4.1: Generic input/output model of a process.

**Process Interdependencies**

The status (ON/OFF) of one process may or may not be dependent on the status of another process; hence, a process interdependency model is developed to represent various scenarios. Such interdependencies can broadly be categorized into independent and dependent processes [5], as explained next.

*Independent Processes:* The status of such processes is independent of other processes and can be scheduled at any time interval within a scheduling window ($T_{1,j}$ to $T_{2,j}$). The following equations define an independent process $j$:

$$ud_{j,t} + \sum_{\tau=t+1}^{t+UP_j-1} vd_{j,\tau} \leq 1 \qquad \forall j, T_{1,j} \leq t \leq T_{2,j} - UP_j + 1 \qquad (4.2a)$$

$$vd_{j,t} + \sum_{\tau=t+1}^{t+DN_j-1} ud_{j,\tau} \leq 1 \qquad \forall j, T_{1,j} \leq t \leq T_{2,j} - DN_j + 1 \qquad (4.2b)$$

$$ud_{j,t} + vd_{j,t} \leq 1 \qquad \forall j, T_{1,j} \leq t \leq T_{2,j} \qquad (4.2c)$$

$$ud_{j,t} - vd_{j,t} = st_{j,t} - st_{j,t-1} \qquad \forall j, T_{1,j} \leq t \leq T_{2,j} \qquad (4.2d)$$

$$nr_j = \sum_t ud_{j,t} \qquad \forall j \qquad (4.2e)$$

Equations (4.2a)-(4.2d) enforce the minimum up-time and down-time requirements, while (4.2e) calculates the total number of time intervals the process is ON in the given optimization horizon. Some independent processes have fixed up-time operation requirements, and are distinguished from others by assigning a proper value to a corresponding element of a parameter vector $F$. Thus, the following equation, in addition to (4.2a)-(4.2e), is required to model such processes:

$$\sum_t st_{j,t} = nr_j \, UP_j \qquad\qquad \forall j : F_j = 1 \qquad (4.3)$$

where $F_j = 1$ means that the process $j$ has a fixed time $UP_j$.

*Dependent Processes:* The decision to change the status of dependent processes can be moved along a scheduling window, but their flexibility is limited by the status of other processes. For dependent processes, a parameter matrix $DP$ is defined, and proper values are assigned to its elements to distinguish among various kinds of dependencies. In this work, three dependent processes are modeled, as follows:

- *Sequential Processes ($DP_{j,k} = 1 \ or \ 2$):* Two processes $j$ and $k$ are said to be sequential when the operation of $k$ starts only after the operation of $j$ is complete, and the sequence of operation is predefined, i.e., $k$ follows $j$. The following equations are required to model two sequential processes $j$ and $k$:

$$nw_{j,t} = \sum_{\tau=1}^{t} ud_{j,\tau} \qquad\qquad \forall j, \forall t \qquad (4.4a)$$

$$nw_{k,t} \leq nw_{j,t} \qquad\qquad \forall j, \forall k : DP_{j,k} = 1 \vee 2, \forall t \qquad (4.4b)$$

$$st_{j,t} + st_{k,t} \leq 1 \qquad\qquad \forall j, \forall k : DP_{j,k} = 1 \vee 2, \forall t \qquad (4.4c)$$

Equations (4.4a)-(4.4c) do not require processes $j$ and $k$ to operate for the same

number of time intervals in the optimization horizon. Such sequential processes are distinguished from others by $DP_{j,k} = 2$, and modeled using the following additional equation:

$$nr_j = nr_k \hspace{4cm} \forall j, \forall k : DP_{j,k} = 2 \hspace{1cm} (4.5)$$

- *Interlocked Processes ($DP_{j,k} = 3$):* These processes are special cases of sequential processes in which there is a fixed time gap between the turning ON of the processes $j$ and $k$. For interlocked processes, a parameter matrix $GP$ is defined which contains the required time gaps. The following equation is required to model two interlocked processes $j$ and $k$:

$$ud_{k,t} = ud_{j,t-GP_{j,k}} \hspace{3cm} \forall j, \forall k : DP_{j,k} = 3, \forall t \hspace{0.5cm} (4.6a)$$

$$nr_j = nr_k \hspace{4cm} \forall j, \forall k : DP_{j,k} = 3 \hspace{1cm} (4.6b)$$

- *Parallel Processes ($DP_{j,k} = 4$):* These processes are similar to the interlocked processes, but with no time gap between the turning ON of the processes $j$ and $k$. The following equation is required to model two parallel processes $j$ and $k$:

$$ud_{j,t} = ud_{k,t} \hspace{4cm} \forall j, \forall k : DP_{j,k} = 4, \forall t \hspace{0.5cm} (4.7)$$

## 4.3.2   Storage Units

Storage units are modeled as multi-input, multi-output systems as shown in Figure 4.2. The following mathematical equations model a storage unit *nc*:
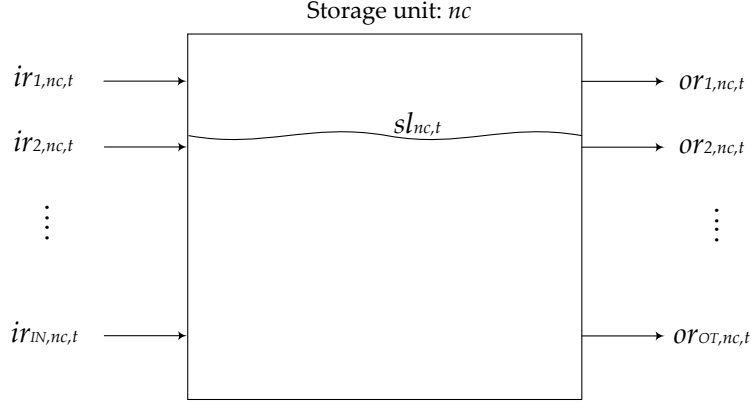
Figure 4.2: A generic model of a storage unit.

$$L_{0,nc} + \sum_{in} ir_{in,nc,t} - \sum_{ot} or_{ot,nc,t} = sl_{nc,t} \qquad\qquad \forall nc, t = 1 \qquad (4.8a)$$

$$sl_{nc,t-1} + \sum_{in} ir_{in,nc,t} - \sum_{ot} or_{ot,nc,t} = sl_{nc,t} \qquad\qquad \forall nc, t \geq 2 \qquad (4.8b)$$

Equation (4.8a) calculates the storage level for the first time interval in the optimization horizon based on the initial storage level, whereas (4.8b) calculates the storage level for subsequent time intervals.

## 4.3.3 Distribution System Components

A detailed mathematical model of the distribution system components are presented and discussed in Chapter 3, and is referred here as three-phase DOPF model. Note that the load control approach considered in the OILM model does not require integration of the three-phase DOPF model into it; however, integration of the two models is necessary when a voltage optimization approach is considered, as explained in more detail in the example discussed in Section 4.5.2.

## 4.3.4 Power Demand

For the OILM model considering both load control and voltage optimization, power demand corresponds to the electrical active and reactive power consumed by the processes and storage units. Power demand of processes can be expressed in terms of input or output material flow rates, voltage, and other non-electrical control variables as follows:

$$Pd_{j,t} = f_j\big(or_{ot,j,t}, V_{av,t}, y_{j,t}\big) \qquad\qquad \forall j, \forall t \qquad (4.9a)$$

$$Qd_{j,t} = g_j\big(or_{ot,j,t}, V_{av,t}, y_{j,t}\big) \qquad\qquad \forall j, \forall t \qquad (4.9b)$$

Note that the voltages used in (4.9a) and (4.9b) are averages of the three phase voltages.

A storage unit may or may not have a power demand, depending on the type of material it contains. If required, active and reactive power demands can be expressed in terms of storage level, voltage and other non-electrical control variables as follows:

$$Pd_{nc,t} = f_{nc}\big(sl_{nc,t}, V_{av,t}, y_{nc,t}\big) \qquad\qquad \forall nc, \forall t \qquad (4.10a)$$

$$Qd_{nc,t} = g_{nc}\big(sl_{nc,t}, V_{av,t}, y_{nc,t}\big) \qquad\qquad \forall nc, \forall t \qquad (4.10b)$$

The polynomial functions $f(\,\cdot\,)$ and $g(\,\cdot\,)$ in (4.9a)-(4.10b), referred here as load estimation polynomial functions, can be determined from the knowledge of the processes/storage units and historical measurements. A detailed explanation on the estimation of these functions is presented in Section 4.4.

The total active and reactive power demands of the industrial load at each time interval can be represented as the sum of the power demands of the processes and storage

units; thus:

$$Pt_t = \sum_j Pd_{j,t} + \sum_{nc} Pd_{nc,t} \qquad\qquad \forall t \qquad (4.11a)$$

$$Qt_t = \sum_j Qd_{j,t} + \sum_{nc} Qd_{nc,t} \qquad\qquad \forall t \qquad (4.11b)$$

For an OILM model considering a load control approach only, the power demand can still be represented by (4.11a) with the voltage fixed at its nominal value.

## 4.3.5 Peak Demand

Industrial customers are also charged for peak demand since this is an important consideration for LDCs. Hence, there is a need to reflect their interests within the model, representing their interaction with customers in the context of a Smart Grid. Modeling of peak demand requires finding the maximum value of $Pt_t$ ($\forall t$), thus rendering the optimization problem discontinuous. To avoid this, an auxiliary variable $P_{peak}$ is minimized in the objective function, and is used to constraint the peak demand as follows:

$$\lambda\, Pt_t \leq \lambda\, P_{peak} \qquad\qquad \forall t \qquad (4.12a)$$

$$\lambda\, P_{peak} \leq \lambda\, P_{max} \qquad\qquad (4.12b)$$

These equations ensure that the demand in each interval is always less than or equal to the value of the auxiliary variable, which in turn should be less than a peak power demand $P_{max}$ predefined by the LDC as part of a DR program, if applicable.

## 4.3.6  Limits on Process/Storage Variables

Each process can have limits on the input and output material flow rates and on the other non-electrical variables associated with it, which are modeled as follows:

$$I_{min,in}\, st_{j,t} \leq ir_{in,j,t} \leq I_{max,in}\, st_{j,t} \qquad\qquad \forall in, \forall j, \forall t \qquad (4.13a)$$

$$O_{min,ot}\, st_{j,t} \leq or_{ot,j,t} \leq O_{max,ot}\, st_{j,t} \qquad\qquad \forall ot, \forall j, \forall t \qquad (4.13b)$$

$$Y_{min,j}\, st_{j,t} \leq y_{j,t} \leq Y_{max,j}\, st_{j,t} \qquad\qquad \forall j, \forall t \qquad (4.13c)$$

When a process is ON ($st_{j,t} = 1$), the flows and all other electrical/non-electrical variables associated with it must be in a range defined by the minimum and maximum limits, and when the process is OFF ($st_{j,t} = 0$), all of them must be zero.

Similarly, limits on storage level and non-electrical variables associated with storage units can be represented as:

$$L_{min,nc} \leq sl_{nc,t} \leq L_{cap,nc} \qquad\qquad \forall nc, \forall t \qquad (4.14a)$$

$$Y_{min,nc} \leq y_{nc,t} \leq Y_{max,nc} \qquad\qquad \forall nc, \forall t \qquad (4.14b)$$

## 4.3.7  Distribution System Operating Limits

When voltage optimization is considered in the OILM model, the voltage applied to the industrial loads would be required to be maintained within limits prescribed by standards such as ANSI [92], as follows:

$$V_{min} \leq V_t \leq V_{max} \qquad\qquad \forall t \qquad (4.15)$$

In this case, limits on other variables associated with distribution system operations, such as feeder current limits and limits on transformer capacities and tap operation of LTCs, may also be considered in the modeling.

## 4.3.8 Production Requirements

Production requirements are enforced in terms of cumulative levels of one or more storage units of final products, at one or more time intervals in the optimization horizon. This can be represented as follows:

$$\sum_{cf} sl_{cf,tf} \geq L_{req,tf} \qquad\qquad \forall tf \qquad (4.16)$$

## 4.3.9 Optimization Objective

Given the importance of cost reduction to industrial customers, the minimization of the customer's energy costs and peak demand charges is considered as the optimization objective. This can be represented as follows:

$$J_{obj} = \overbrace{\Delta T \sum_t \rho_t \ Pt_t}^{\text{Energy costs}} + \overbrace{\lambda \ P_{peak}}^{\text{Peak demand charges}} \qquad (4.17)$$

This objective function can also be used for an industrial customer that chooses to minimize its energy costs only or peak demand charges only, by setting $\lambda = 0$ or $\rho_t = 0$, respectively.

Equality and inequality constraints (4.1)-(4.16) along with (4.17) form the OILM model. Depending on the order of the load estimation polynomial function in (4.9a)-(4.10b), the OILM model can be either an MILP or an MINLP problem, as demonstrated in the case studies discussed in Section 4.5.

## 4.4 Model Parameter Estimations

This section explains the estimation of process I/O matrices discussed in (4.1a) and (4.1b), and the load estimation polynomial functions in (4.9a)-(4.10b). Other model parameters used in (4.1)-(4.17) are straightforward to obtain and are provided in the Appendix for the case studies discussed in Section 4.5.

### 4.4.1 Process I/O Matrix

As explained in Section 4.3, the process I/O matrices relate the material inflow and outflow rates in each time interval. Thus, consider the wheat bran removing machine in Figure 4.3, which is one of the processes used in the flour mill example discussed in Section 4.5. The input to the process is inflow rate of wheat, while the outputs are the outflow rates of bran and skinless wheat. From one set of measurements, the relation between inflow and outflow rates can be determined; for example, if a certain amount of input wheat yields 80% of skinless wheat and 20% bran, the process I/O matrix for the bran removing machine would be:

$$\begin{bmatrix} R \end{bmatrix} = \begin{bmatrix} 0.8 \\ 0.2 \end{bmatrix} \tag{4.18}$$

and the input/output relation for the bran removing machine would be:

$$\begin{bmatrix} or_{1,t} \\ or_{2,t} \end{bmatrix} = \begin{bmatrix} 0.8 \\ 0.2 \end{bmatrix} \begin{bmatrix} ir_{1,t} \end{bmatrix} \qquad \forall t \tag{4.19}$$
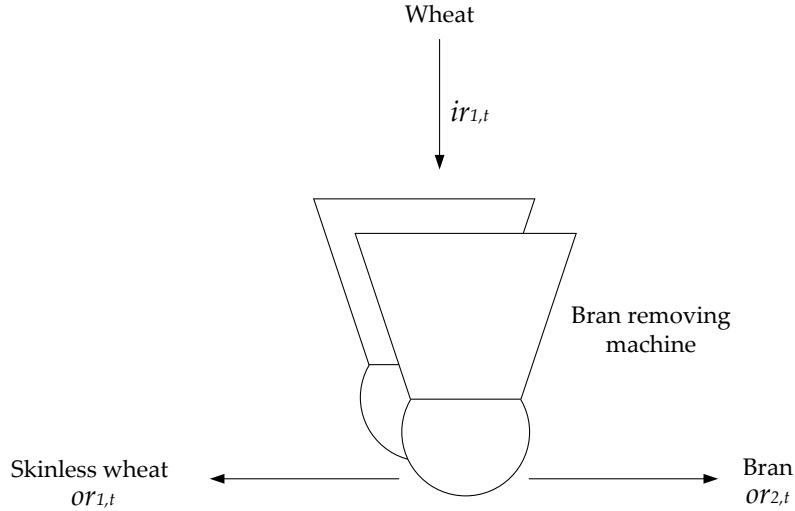
Figure 4.3: A bran removing machine illustrating input and output material flows.

## 4.4.2 Load Estimation Polynomial Functions

The load estimation polynomial functions model the relationship between the electrical active and reactive power demands with the electrical and non-electrical control variables associated with the processes. The estimation can be carried out either from knowledge of the process or using a least square error estimation of historical measurement data; the latter is explained in detail next.

Consider the water pump in Figure 4.4, which is similar to one of the pumps used in the water pumping facility example described in Section 4.5. In this case, the electrical variable (voltage) and non-electrical variable (water discharge) are considered as input control variables, and the active and reactive power demands (outputs) are estimated using (4.9a)-(4.9b). The estimation of the polynomial $f(\,\cdot\,)$ can be carried out based on available measurement data as explained next.

Assume $e$ number of measurements are available for active power demand $\tilde{Pd}_e$, voltage $\tilde{V}_e$, and discharge $\tilde{Qr}_e$. Assume as well, that polynomial $f(\,\cdot\,)$ is a quadratic function in
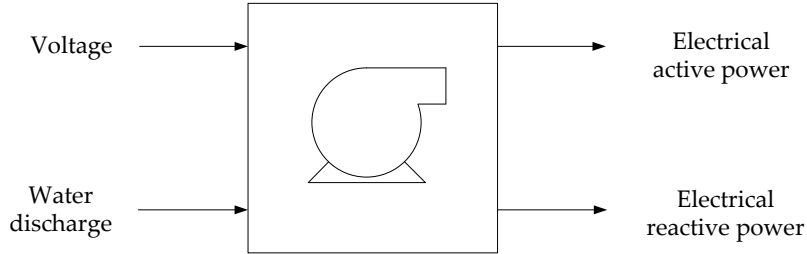
Figure 4.4: A water pump illustrating control and estimated variables.

$\tilde{V}_e$ and $\tilde{Qr}_e$, which properly fits the available data based on a statistical analysis of the root mean square error; this analysis may yield higher degree polynomial depending on the process [132, 133]. The estimated value of $\tilde{Pd}_e$, given by $\hat{Pd}_e$, can be obtained from the measurements of $\tilde{V}_e$ and $\tilde{Qr}_e$ as follows:

$$\hat{Pd}_e = f(\tilde{Qr}_e, \tilde{V}_e) = a_0 + a_{01}\, \tilde{V}_e + a_{10}\, \tilde{Qr}_e + a_{02}\, \tilde{V}_e^{\,2} + a_{20}\, \tilde{Qr}_e^{\,2} + a_{11}\, \tilde{V}_e\, \tilde{Qr}_e \qquad \forall e \quad (4.20)$$

Based on (4.20) and $\tilde{Pd}_e$, the parameters $a_0$ to $a_{11}$ of the polynomial $f(\cdot)$ are estimated using a least square error method as explained in Section 2.5, which can be modeled as an optimization problem as follows:

$$\text{Min.} \quad \sqrt{\frac{1}{E} \sum_e \left( \hat{Pd}_e - \tilde{Pd}_e \right)^2}$$

$$\text{s.t.} \quad \hat{Pd}_e = f(\tilde{Qr}_e, \tilde{V}_e) = a_0 + a_{01}\, \tilde{V}_e + a_{10}\, \tilde{Qr}_e + a_{02}\, \tilde{V}_e^2 + a_{20}\, \tilde{Qr}_e^{\,2} + a_{11}\, \tilde{V}_e\, \tilde{Qr}_e \quad \forall e \quad (4.21)$$

A similar procedure can be applied to estimate the parameters of the reactive power demand polynomial $g(\cdot)$.

## 4.5  Case Studies

In this section, the OILM model proposed in Section 4.3 is applied to two industrial customers: flour mill and water pumping facility. The proposed models are developed in GAMS [128], and solved using the KNITRO solver [130].

### 4.5.1  Flour Mill Load Control

The flour mill depicted in Figure 4.5 is considered here [5]. It consists of 5 processes and 4 storage units. Process 1 is a pump to elevate water from a source to a storage tank. Process 2 and 3 represent washing and drying of raw material (wheat). Process 4 involves removal of bran from wheat, and Process 5 is a grinding machine to produce flour. Information on the electrical distribution system supplying power to the flour mill is not available, and hence the OILM corresponds to the load control approach only.

The only controllable variables in the flour mill facility are material outflow rates; the power demands of the processes are expressed in these terms. The processes are modeled as active power loads; hence, only estimations for $f(\,\cdot\,)$ are needed, which are carried out from the knowledge of the processes. In the estimation process it is assumed that the rated electrical power of the 5 processes are 8 kW, 22 kW, 12.75 kW, 36.5 kW, and 78 kW, respectively [5]. Since no detailed information is available regarding the processes, the active power consumed by each process is arbitrarily and without loss of generality assumed here to vary linearly with the outflow rate, and the process efficiency is assumed not to vary with the change in outflow rates; these relationships can be established from actual/simulated input and output measurements of the processes, as demonstrated for the water pumping facility in Section 4.5.2. The coefficients for the linear polynomial $f(\,\cdot\,)$, thus obtained, are listed in the Appendix.

For the simulation studies, the Hourly Ontario Electricity Price (HOEP) for October 12, 2011 is used as the energy price (Figure 4.6) [6], as per the RTP used for industrial loads in
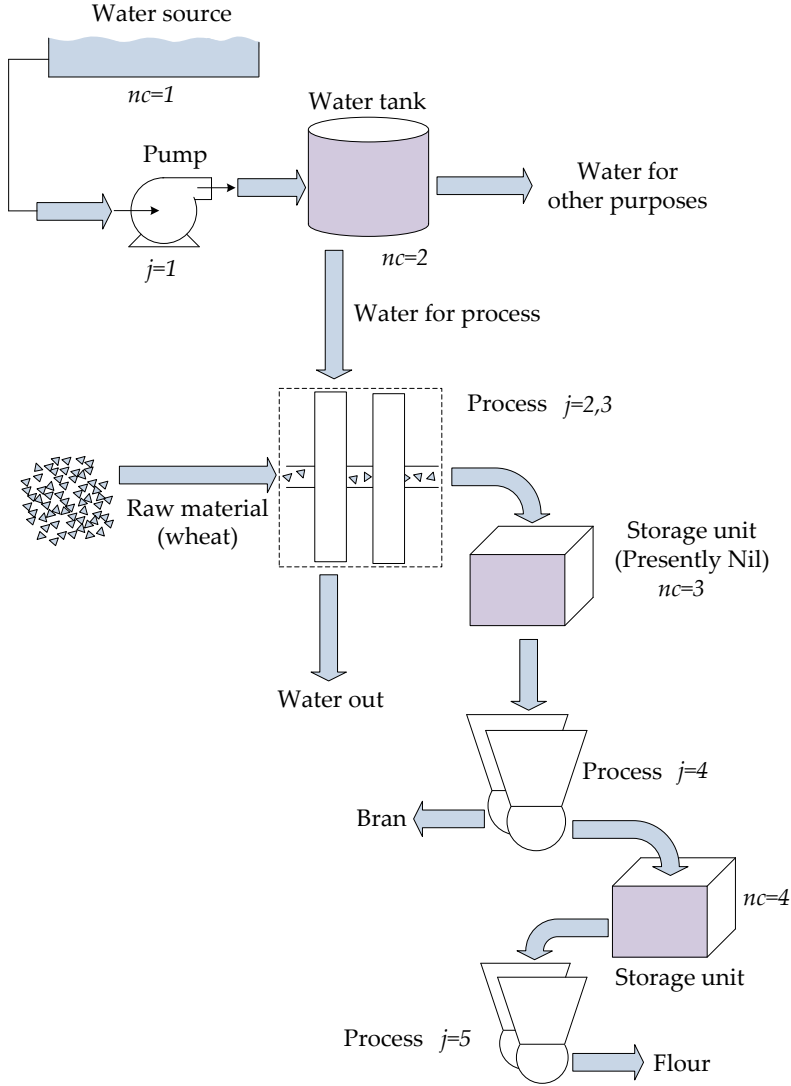
Figure 4.5: Schematic diagram of a flour mill showing its processes and storage units [5].

Ontario, and a demand charge of $7/kW/month is considered, which is the demand charge in Ontario during Fall [140]. It should be noted that the existing "Global Adjustment" mechanism in Ontario is not considered here in the cost calculations [141]. The production requirement is considered to be 25 tons of flour per day. The minimum outflow rates for each process, when the process is ON, are assumed to be 50% of the outflow rates at

Figure 4.6: HOEP on October 12, 2011 [6].

rated power. The various other parameters required for the modeling of the processes and storage units are provided in the Appendix.

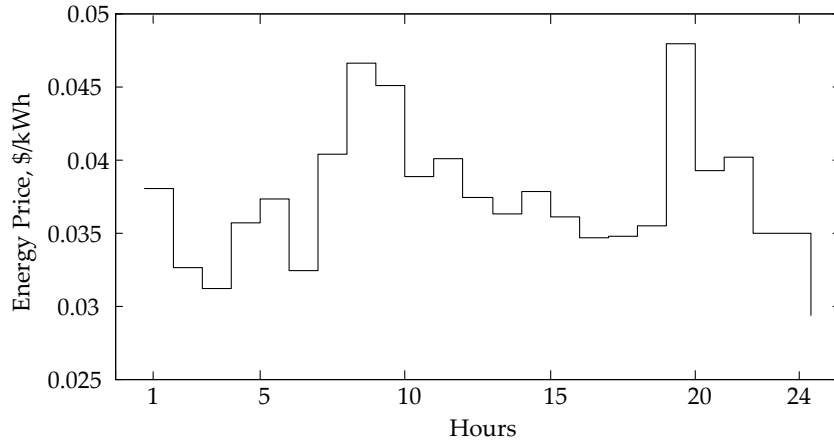Simulations are carried out for three different cases and the results are summarized in Table 4.1. Case 0 is the base case, which corresponds to a non-optimized energy consumption profile of an industrial customer, which is basically a feasible solution of the OILM model, and is used for comparison purposes. Case 1 corresponds to the minimization of energy costs, and Case 2 corresponds to the minimization of both energy costs and demand charges. Observe in Table 4.1 that the developed OILM model yields a ~5% reduction in energy costs and a ~2.8% reduction in total costs (highlighted in the table). However, these figures depend on various factors such as limits on the material flows, variation of process efficiencies with the out-flow rates, initial storage levels, flexibility in scheduling of the processes, energy prices, and demand charges.

The 24-hour power consumption profiles of the three cases are shown in Figure 4.7. Case 1 results in minimum energy cost, and is 5.3% less compared to Case 0. Note that the power consumption profile for Case 1 comply with the HOEP, i.e., when the electricity price is low at hours 3, 6, 16, and 24, an increased power consumption is observed. As a consequence, the peak demand is increased by 43.8% compared to Case 0 (this shifted

96

Table 4.1: Performance of OILM for a Flour Mill

| | | Case 0 | Case 1 | Case 2 |
|---|---|---|---|---|
| Energy Costs [$/day] | | 80.81 | 76.50 | 79.76 |
| Demand Charges† [$/day] | | 23.28 | 33.48 | 21.42 |
| Total Costs [$/day] | | 104.09 | 109.98 | 101.18 |
| Energy [kWh/day] | | 2164.70 | 2149.42 | 2149.42 |
| Peak Demand [kW] | | 99.76 | 143.48 | 91.80 |
| % Difference | Energy Costs | — | -5.33 | -1.30 |
| | Demand Charges | — | 43.82 | -7.98 |
| w.r.t. | Total Costs | — | 5.66 | -2.79 |
| Case 0 | Energy | — | -0.71 | -0.71 |
| | Peak Demand | — | 43.82 | -7.98 |

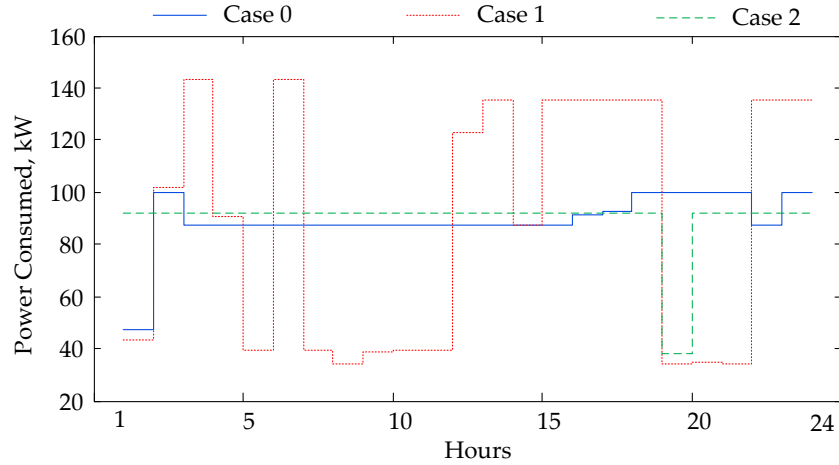† Monthly charges prorated per day.



Figure 4.7: Optimal operation of a flour mill.

peak demand increase has been observed in [18] as well). In Case 2, both energy costs and demand charges are less as compared to Case 0; the reduction in demand charges is 7.9%, while the reduction in energy costs is 1.3%. The resulting flat load profile in

Case 2 is because of the maximum flexibility allowed (of 24 hours) in the scheduling of the processes. The difference in the energy required in the base case and the optimized cases can be attributed to the difference in storage levels at the end of the optimization horizon.

## 4.5.2 Water Pumping Facility Load Control and Voltage Optimization

The water pumping facility considered here is depicted in Figure 4.8 [7], and consists of 5 processes and 2 storage units. Processes 1 through 5 are centrifugal pumps which elevate water from a source to a reservoir. The rated electrical power of Processes 1, 2 and 3 are 595 kW, 445 kW, and 260 kW, respectively; Process 5 is identical to Process 1 and Process 4 is identical to Process 2. The water pumping facility is assumed to be connected to the end of the IEEE 4-node test feeder [4], as depicted in Figure 4.8, to demonstrate the combined effect of load control and voltage optimization in the OILM model. The voltage in the IEEE 4-node test feeder is controlled by an LTC equipped transformer. Hence, the control variables are the voltages applied to the pumps and their water discharge rates.

Because of the lack of historical measurement data in this case, data are generated using PSCAD simulations [142]. The pumps are assumed to be connected to a three-phase voltage source with nominal voltage of 4.16 kV, and multiple simulations are carried out by varying the voltage from 0.95 p.u. to 1.05 p.u., and the speed from 0.97 p.u. to 0.999 p.u. The recorded data from the simulations and pump performance curves are then used to estimate the quadratic polynomials $f(\,\cdot\,)$ and $g(\,\cdot\,)$, as discussed in the Section 4.4.2; the coefficients thus obtained are given in the Appendix.

Similar to the previous studies, the HOEP for October 12, 2011 is considered as the energy price (Figure 4.6) [6], and \$7/kW/month is used as the demand charge [140]. The production requirement is the 24-hour water demand profile shown in Figure 4.9, and the total water required for the city in 24 hours is 54,788 m$^3$ [7]. The minimum outflow rates
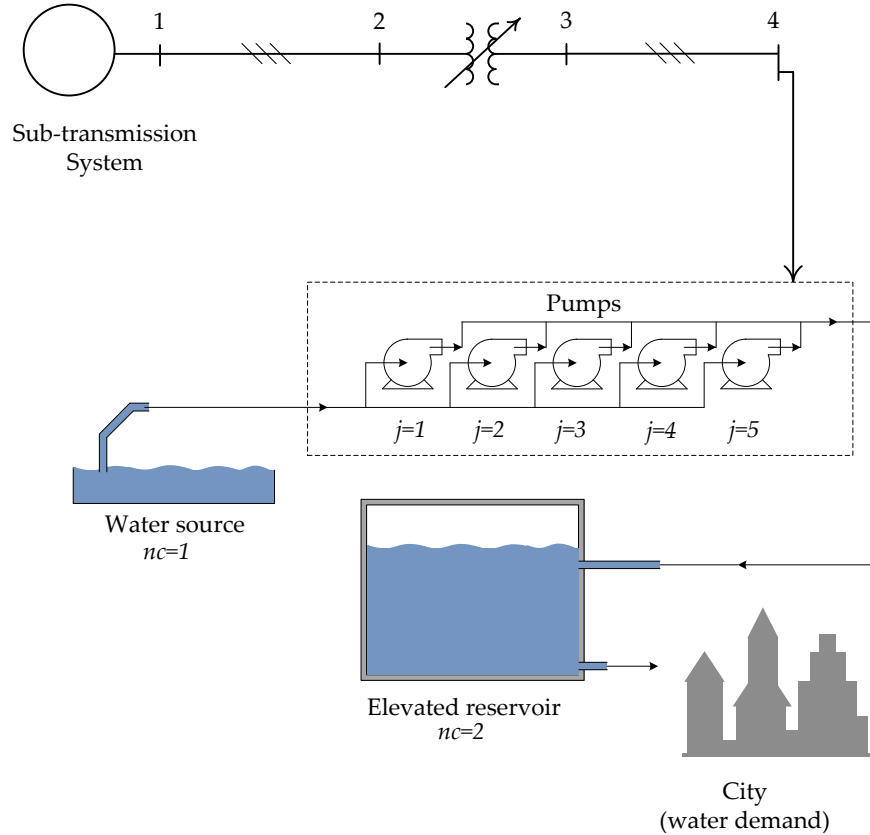
Figure 4.8: Schematic diagram of a water pumping facility with processes and storage units [7], connected to the IEEE 4-node test feeder [4].

for each process, when the process is ON, are assumed to be 50% of the outflow rates at the rated power. The various other parameters required for the modeling of the processes and storage units are given in the Appendix.

Simulations are carried out for three different cases and the results are summarized in Table 4.2; the 24-hour power consumption profiles obtained for the three cases are shown in Figure 4.10. Similar to the previous studies, Case 0 corresponds to a non-optimized, feasible base case; Case 1 corresponds to minimization of energy costs; and Case 2 corresponds to minimization of both energy costs and demand charges. Case 1 results in a 38.1% reduction in energy costs as compared to Case 0 as highlighted in the table, but in a 73.7%
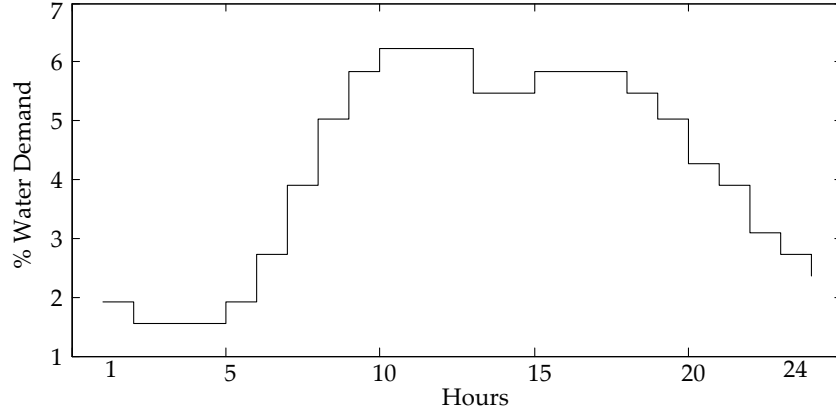
Figure 4.9: City water demand profile for 24-hours [7].

Table 4.2: Performance of OILM for a Water Pumping Facility Connected to the IEEE 4-node Test Feeder.

|  |  | Case 0 | Case 1 | Case 2 |
|---|---|---|---|---|
| Energy Costs [$/day] | | 266.65 | 165.08 | 200.08 |
| Demand Charges$^\dagger$ [$/day] | | 137.91 | 239.52 | 50.26 |
| Total Costs [$/day] | | 404.56 | 404.61 | 250.34 |
| Energy [kWh/day] | | 7085.61 | 5454.60 | 5325.89 |
| Peak Demand [kW] | | 591.05 | 1026.55 | 215.42 |
| % Difference w.r.t. Case 0 | Energy Costs | — | -38.09 | -24.96 |
| | Demand Charges | — | 73.68 | -63.55 |
| | Total Costs | — | 0.01 | -38.12 |
| | Energy | — | -23.02 | -24.84 |
| | Peak Demand | — | 73.68 | -63.55 |

$^\dagger$ Monthly charges prorated per day.

increase in peak demand, which is consistent with the results obtained for the flour mill. In Case 2, both the energy costs and demand charges are less as compared to Case 0, with reductions of 25.0% and 63.6%, respectively, and results in 38.1% savings in total costs as

100

Figure 4.10: Optimal operation of a water pumping facility connected to the IEEE 4-node test feeder (load control and voltage optimization).

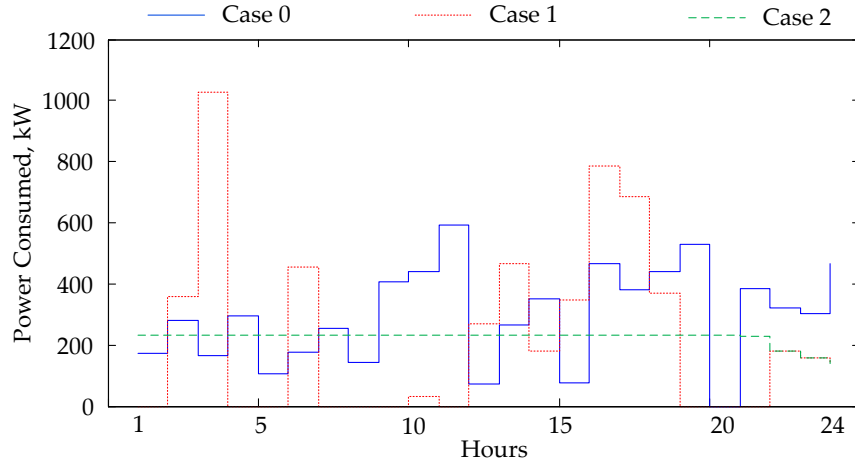highlighted in the table. Note that these figures depend on various factors such as limits on the material flows, variation of process efficiencies with out-flow rates, initial storage levels, flexibility in scheduling of the processes, energy prices, and demand charges. The resulting flat load profile in Case 2 is because of the maximum flexibility (of 24 hours) allowed in the scheduling of the processes. The difference in energy required for the three cases can be attributed to the difference in the optimal storage level profiles, and change in efficiencies of the processes as the water discharge rate and voltage changes.

Another set of case studies are carried out considering only load control, to compare the savings with that obtained with voltage optimization. In this case, only an estimation of the polynomial $f(\cdot)$ is required, which is readily obtained by fixing the voltage at its nominal value of 4.16 kV in the machine equations provided in the Appendix. Thus, the only controllable variables in the system are the water discharge rates of the pumps. In these studies, a base case, i.e., Case 0, is not relevant, since the objective here is to determine the possible savings accrued by means of the voltage optimization approach.

The results of these case studies are summarized in Table 4.3, along with a comparison with respect to the corresponding cases with voltage optimization presented

101

Table 4.3: Comparison of Load Control and Voltage Optimization for Water Pumping Facility.

| | | Case 1 | Case 2 |
|---|---|---|---|
| Energy Costs [$/day] | | 186.86 | 200.51 |
| Demand Charges† [$/day] | | 239.36 | 53.98 |
| Total Costs [$/day] | | 426.22 | 254.49 |
| Energy [kWh/day] | | 5477.36 | 5337.26 |
| Peak Demand [kW] | | 1025.83 | 231.35 |
| % Difference w.r.t. cases in Table 4.2 | Energy Costs | 13.19 | 0.21 |
| | Demand Charges | -0.07 | 7.39 |
| | Total Costs | 5.34 | 1.66 |
| | Energy | 0.42 | 0.21 |
| | Peak Demand | -0.07 | 7.39 |

† Monthly charges prorated per day.

in Table 4.2; the 24-hour power consumption profiles obtained for the three cases are shown in Figure 4.11. Observe that the energy costs increase by 13.2% in Case 1, and total cost increase by 1.7% in Case 2, as highlighted in the table. These figures demonstrate that the voltage optimization approach may yield additional savings for industrial customers, which are consistent with the savings reported in [87] and [88].

## 4.6   Summary

This chapter presented and discussed an OILM model, which can be readily integrated into EHMSs for the benefit of industrial customers and LDC system operators. The developed OILM model incorporates the modeling of processes, process interdependencies, storage units, distribution system components, and various other operating requirements set by the distribution system and industrial process operators. The OILM model is generic and
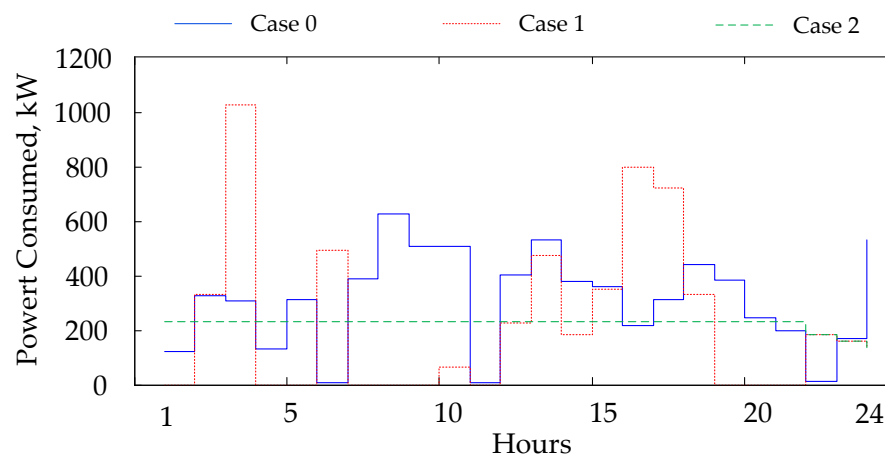
Figure 4.11: Optimal operation of a water pumping facility connected to the IEEE 4-node test feeder (load control only).

applicable to any industrial process, and its effectiveness was demonstrated through case studies carried out on two industrial processes, i.e., a flour mill and a water pumping facility. The results obtained from the case studies show that the OILM model may yield significant savings to the industrial customers in energy costs and demand charges, and may also help LDC system operators to reduce peak demand. Therefore, the proposed mathematical models, in conjunction with Smart Grid technologies at the customer and LDC levels, have the potential to benefit both customers and LDCs. The models are currently being implemented and tested at various industrial facilities in Southern Ontario, Canada.

# Chapter 5

# Conclusions

## 5.1 Summary

The research presented in this thesis focuses on the optimal operation of distribution systems and industrial energy hubs in the context of Smart Grids. The main content and conclusions drawn from the thesis can be summarized as follows:

- Chapter 1 presented the main motivations for the research, outlining the concerns on capacity expansion and environmental emissions, potential benefits from distribution system optimization and EHMSs to LDCs and customers, and the evolving Smart Grid technologies at both the system and customer levels. A literature review of related works, particularly on Smart Grids, DA, distribution system operation, DSM, DR, and EHMSs, was presented. This chapter also presented an overview of the research and the expected contributions.

- Chapter 2 presented the background topics relevant to the present research. Thus, distribution system components such as feeders, transformers, control equipment, metering equipment, etc., were discussed briefly. Some salient features of

communication and control infrastructure in conventional and evolving smart distribution grids were also discussed. This chapter also presented a brief review of VR, reactive power control, and the mathematical model of a generic VVC optimization problem. An overview of mathematical programming, solution methods, tools, and solvers used in this research were discussed as well. A curve fitting technique based on the least square error method and its solution process were also presented.

- Chapter 3 presented the modeling, solution, and results of the proposed three-phase DOPF, which can be readily deployed by an LDC system operator for real-time optimal operation of distribution feeders in Smart Grids. The DOPF incorporates comprehensive modeling of three-phase components, distribution system operating limits, and a novel operational objective of minimizing the electrical energy purchased from the external grid, while limiting the number of switching operations of LTCs and SCs. This chapter also presented a heuristic method to solve the three-phase DOPF, which adopts a quadratic penalty approach to reduce the computational burden so as to make the solution process suitable for real-time applications. In this chapter, a GA-based method for solving the three-phase DOPF model was discussed as well, and the results of applying this method were compared with those obtained from the heuristic method in order to benchmark its performance.

  The results of applying the three-phase DOPF model and the solution methods in two distribution systems, i.e., the IEEE 13-node test feeder and a Hydro One distribution feeder, were discussed. It was shown that the energy purchased from the grid can be reduced by 7% and the number of switching operations by 63%, depending on the objective function. A comparison of the results obtained using the two solution methods showed that the maximum solution time taken by the heuristic method is about 10 minutes, while the GA-based method always required more than 3 hours to arrive at the optimal solutions. These results demonstrate the benefits that

can be obtained by deploying the proposed DOPF model and the heuristic solution method in real-time distribution system operations.

- Chapter 4 presented the modeling, analysis, and results of the proposed OILM, which can be readily deployed by industrial customer into EHMSs for real-time optimal operation and control of industrial loads in Smart Grids. The OILM model is based on a load control approach, and includes comprehensive modeling of industrial processes, process interdependencies, storage units, process operating constraints, production requirements, and an objective function to minimize the energy costs and/or demand charges. This chapter also presented the integration of the OILM model with the DOPF model, incorporating operating constraints of the LDC system operator and combining a voltage optimization approach with load control for additional benefits.

  The results of applying the OILM model on two industrial customers, i.e., a flour mill and a water pumping facility, were also discussed. The load control approach for the flour mill showed that the customer's energy costs and demand charges can be reduced by 5% and 7%, respectively, under an RTP scheme, depending on the objective function. Similarly, from the case studies of a water pumping facility, it was found that the energy costs and demand charges can be reduced by 38% and 63%, respectively. It was also shown that additional 13% and 7% savings can be achieved on energy costs and demand charges, respectively, if voltage optimization is considered in the OILM model. The results demonstrate the benefits to industrial customers and LDCs that can be obtained by deploying OILM and DOPF models in EHMSs.

## 5.2  Contributions

The main contributions of the research presented in this thesis are as follows:

1. A generic three-phase DOPF model has been developed, considering comprehensive models of distribution system series/shunt components and voltage dependent loads. The developed DOPF model may be used to achieve various distribution system operational objectives desired by LDC system operator. Thus, a novel operational objective is proposed that minimizes the energy purchased from the grid while limiting the number of switching operations of LTCs and SCs.

2. A novel heuristic method has been proposed to solve the three-phase DOPF model, which yields an adequate sub-optimal solution in a time frame suitable for real-time applications. A GA-based method has been applied to solve the three-phase DOPF model in order to benchmark the performance of the heuristic method in terms of optimality and computational burden.

3. An novel OILM model has been developed, based on a load control approach considering comprehensive models of industrial processes, process interdependencies, storage units, process operating constraints, production requirements, and an objective function that minimizes the energy costs and/or demand charges. The OILM model may be combined with the three-phase DOPF model in order to consider voltage optimization. The proposed OILM model is generic and applicable to various kinds of process industries. The model is being implemented on some industrial pilots in Southern Ontario, Canada.

The main contents and contributions of Chapter 3 are published in the IEEE Transactions on Industrial Electronics [143] and an IEEE conference proceedings [144]. The contents and contributions of Chapter 4 will be submitted to the IEEE Transactions on Smart Grids shortly, based on [145].

## 5.3  Future Work

The followings are the some possible future directions for the present research:

1. Based on the monitoring and implementation phases of the pilot sites where the OILM model will be applied, some adjustments on mathematical modeling will likely be required.

2. In Chapter 3, the three-phase DOPF model is applied to optimize the distribution system operations assuming some modulated load profiles in Smart Grids. However, such load profiles and the operational objective desired by LDC would be different, especially in the case of high DER and EV penetrations, as these make the operational problem stochastic in nature. The proposed three-phase DOPF and heuristic solution method could be extended to carry out stochastic analyses of distribution system operations where DERs and EVs are significant in the system.

3. The OILM and DOPF models are combined in Chapter 4 and used to optimize the electricity requirements of industrial customers that are being supplied by dedicated feeders. However, in practice, multiple industrial EHMSs may be connected to a single feeder. Thus, a study on optimal operation of multiple industrial EHMSs and their coordination would be necessary from a practical stand point.

4. The OILM and DOPF models are combined in Chapter 4 and used to optimize energy requirement from the customer point of view. Even though the optimization process ensures that the interests of LDC system operators are considered, it may not yield an optimal solution for the LDC. In this case, a mechanism is required that considers a trade-off between the optimal solutions desired by the LDC system operator and the customer, and satisfies the operational requirements set by both.

# APPENDICES

Only non-zero parameters used in the case studies of flour mill and water pumping facility are listed here.

## A.1  Flour Mill Parameters

$$\Delta T = 1; \quad T = 24; \quad T_1 = 1; \quad T_2 = 24$$

$$NC = 4; \quad J = 5$$

$$R_1 = [1]; \quad R_2 = \begin{bmatrix} 1 & 0 \\ 0 & 1 \end{bmatrix}; \quad R_3 = [0.8]; \quad R_4 = [1]$$

$$UP' = \begin{bmatrix} 1 & 1 & 1 & 1 & 1 \end{bmatrix}; \quad DP = \begin{bmatrix} 0 & 0 & 0 & 0 & 0 \\ 0 & 0 & 1 & 0 & 0 \\ 0 & 0 & 0 & 0 & 0 \\ 0 & 0 & 0 & 0 & 0 \\ 0 & 0 & 0 & 0 & 0 \end{bmatrix}$$

$$Pd_{1,t} = f_{1,t}\big(or_{1,1,t}\big) = 0.133 \, or_{1,1,t}$$

$$Pd_{2,t} = f_{2,t}(or_{2,1,t}) = 11.043\,or_{2,1,t}$$

$$Pd_{3,t} = f_{3,t}(or_{3,1,t}) = 11.090\,or_{3,1,t}$$

$$Pd_{4,t} = f_{4,t}(or_{4,1,t}) = 36.650\,or_{4,1,t}$$

$$Pd_{5,t} = f_{5,t}(or_{5,1,t}) = 48.148\,or_{5,1,t}$$

$$O_{max} = \begin{bmatrix} 60.000 \text{ kl/h} \\ 2.330 \text{ tons/h} \\ 1.330 \text{ tons/h} \\ 1.660 \text{ tons/h} \\ 2.000 \text{ tons/h} \end{bmatrix} ; \quad O_{min} = \begin{bmatrix} 30.000 \text{ kl/h} \\ 1.170 \text{ tons/h} \\ 0.665 \text{ tons/h} \\ 0.830 \text{ tons/h} \\ 1.000 \text{ tons/h} \end{bmatrix}$$

$$L_{cap} = \begin{bmatrix} \infty \\ 180 \text{ kl} \\ 0 \\ 6 \text{ tons} \end{bmatrix}$$

## A.2 Water Pumping Facility parameters

$$\Delta T = 1; \quad T = 24; \quad T_1 = 1; \quad T_2 = 24$$

$$NC = 2; \quad J = 5$$

$$R_1 = R_2 = R_3 = R_4 = R_5 = [1]$$

$$V_{max} = 1.05 \times 4.16 \text{ kV}; \quad V_{min} = 0.95 \times 4.16 \text{ kV}$$

$$
O_{max} = \begin{bmatrix} 1800 \text{ m}^3/\text{h} \\ 1440 \text{ m}^3/\text{h} \\ 828 \text{ m}^3/\text{h} \\ 828 \text{ m}^3/\text{h} \\ 1800 \text{ m}^3/\text{h} \end{bmatrix} ; \quad O_{min} = \begin{bmatrix} 900 \text{ m}^3/\text{h} \\ 720 \text{ m}^3/\text{h} \\ 414 \text{ m}^3/\text{h} \\ 414 \text{ m}^3/\text{h} \\ 900 \text{ m}^3/\text{h} \end{bmatrix}
$$

$$
L_0 = \begin{bmatrix} \infty \\ 7800 \text{ m}^3 \end{bmatrix} ; \quad L_{min} = \begin{bmatrix} \infty \\ 2600 \text{ m}^3 \end{bmatrix}
$$

$$
L_{cap} = \begin{bmatrix} \infty \\ 18200 \text{ m}^3 \end{bmatrix} ; \quad UP' = \begin{bmatrix} 1 & 1 & 1 & 1 & 1 \end{bmatrix}
$$

$$
Pd_{1,t} = f_{1,t}\left(V_{av,t}, Qr_{1,t}\right) = -476.633 + 0.527\, Qr_{1,t} + 8.670\, V_{av,t}
$$

$$
- 1.454 \times 10^{-4} Qr_{1,t}^2 - 8.827\, V_{av,t}^2 + 1.257 \times 10^{-5}\, Qr_{1,t}\, V_{av,t}
$$

$$
Pd_{2,t} = f_{2,t}\left(V_{av,t}, Qr_{2,t}\right) = -356.480 + 0.492\, Qr_{2,t} + 6.485\, V_{av,t}
$$

$$
- 1.699 \times 10^{-4}\, Qr_{2,t}^2 - 6.602\, V_{av,t}^2 + 1.175 \times 10^{-5}\, Qr_{2,t}\, V_{av,t}
$$

$$
Pd_{3,t} = f_{3,t}\left(V_{av,t}, Qr_{3,t}\right) = -59.448 + 0.140\, Qr_{3,t} + 2.271\, V_{av,t}
$$

$$
- 8.237 \times 10^{-5}\, Qr_{3,t}^2 - 2.307\, V_{av,t}^2 + 5.817 \times 10^{-6}\, Qr_{3,t}\, V_{av,t}
$$

$$
Pd_{4,t} = f_{4,t}\left(V_{av,t}, Qr_{4,t}\right) = -59.448 + 0.140\, Qr_{4,t} + 2.271\, V_{av,t}
$$

$$
- 8.237 \times 10^{-5}\, Qr_{4,t}^2 - 2.307\, V_{av,t}^2 + 5.817 \times 10^{-6}\, Qr_{4,t}\, V_{av,t}
$$

$$Pd_{5,t} = f_{5,t}\big(V_{av,t}, Qr_{5,t}\big) = -476.633 + 0.527\,Qr_{5,t} + 8.6703\,V_{av,t}$$

$$- 1.454 \times 10^{-4}Qr_{5,t}^2 - 8.827\,V_{av,t}^2 + 1.257 \times 10^{-5}\,Qr_{5,t}\,V_{av,t}$$

$$Qd_{1,t} = g_{1,t}\big(V_{av,t}, Qr_{1,t}\big) = 139.975 - 0.165\,Qr_{1,t} + 6.741\,V_{av,t}$$

$$+ 4.873 \times 10^{-5}\,Qr_{1,t}^2 - 6.876\,V_{av,t}^2 + 9.259 \times 10^{-6}\,Qr_{1,t}\,V_{av,t}$$

$$Qd_{2,t} = g_{2,t}\big(V_{av,t}, Qr_{2,t}\big) = 104.691 - 0.155\,Qr_{2,t} + 5.042\,V_{av,t}$$

$$+ 5.695 \times 10^{-5}\,Qr_{2,t}^2 - 5.143\,V_{av,t}^2 + 8.655 \times 10^{-6}\,Qr_{2,t}\,V_{av,t}$$

$$Qd_{3,t} = g_{3,t}\big(V_{av,t}, Qr_{3,t}\big) = 47.771 - 0.119\,Qr_{3,t} + 0.819\,V_{av,t}$$

$$+ 7.421 \times 10^{-5}\,Qr_{3,t}^2 - 0.849\,V_{av,t}^2 + 5.986 \times 10^{-6}\,Qr_{3,t}\,V_{av,t}$$

$$Qd_{4,t} = g_{4,t}\big(V_{av,t}, Qr_{4,t}\big) = 47.771 - 0.119\,Qr_{4,t} + 0.819\,V_{av,t}$$

$$+ 7.420 \times 10^{-5}\,Qr_{4,t} - 0.849\,V_{av,t}^2 + 5.986 \times 10^{-6}\,Qr_{4,t}\,V_{av,t}$$

$$Qd_{5,t} = g_{5,t}\big(V_{av,t}, Qr_{5,t}\big) = 139.975 - 0.165\,Qr_{5,t} + 6.741\,V_{av,t}$$

$$+ 4.873 \times 10^{-5}\,Qr_{5,t}^2 - 6.876\,V_{av,t}^2 + 9.259 \times 10^{-6}\,Qr_{5,t}\,V_{av,t}$$

# References

[1] "Industrial Energy Use in Canada: Emerging Trends," National Energy Board, Canada, Nov. 2010. [Online]. Available: http://www.neb-one.gc.ca/clf-nsi/ rnrgynfmtn/nrgyrprt/nrgdmnd/ndstrlnrgscnd2010/ndstrlnrgscnd-eng.pdf

[2] W. H. Kersting, *Distribution System Modeling and Analysis*, 2nd ed. Boca Raton: CRC Press, 2006.

[3] T. Gonen, *Electric Power Distribution System Engineering*, 2nd ed. Boca Raton: CRC Press, 2007.

[4] W. H. Kersting, "Radial Distribution Test Feeders," in *Proc. IEEE PES Winter Meeting*, vol. 2, 2001, pp. 908–912.

[5] S. Ashok and R. Banerjee, "An Optimization Mode for Industrial Load Management," *IEEE Trans. Power Syst.*, vol. 16, no. 4, pp. 879–884, Nov. 2001.

[6] "A Guide to Electricity Charges-Market Participants." [Online]. Available: http://www.ieso.ca/imoweb/role/wholesaleCharges.asp

[7] B. Baran, C. V. Lucken, and A. Sotelo, "Multi-objective Pump Scheduling Optimisation Using Evolutionary Strategies," *Journals of Advances in Engineering Software*, vol. 36, no. 1, pp. 39–47, 2005.

REFERENCES

[8] "International Energy Outlook 2009," U. S. Energy Information Administration, May 2009. [Online]. Available: http://www.eia.doe.gov/oiaf/ieo/world.html

[9] "Ontario Electricity Industry: Planning Ahead," Ontario Power Authority (OPA). [Online]. Available: http://www.powerauthority.on.ca

[10] "A Climate Change Plan for the Purposes of the Kyoto Protocol Implementation Act," Environment Canada, May 2009. [Online]. Available: http://www.ec.gc.ca/doc/ed-es/KPIA2009/s2_eng.htm

[11] "Copenhagen Accord," United Nations Framework Convention on Climate Change. [Online]. Available: http://unfccc.int/meetings/copenhagen_dec_2009/items/5262.php

[12] "Copenhagen Accord," Government of Canada, Oct. 2010. [Online]. Available: http://www.climatechange.gc.ca/cdp15-cop15/default.asp?lang=En&n=970E8B07-1

[13] "Ontario's Green Energy Act," Minsitry of Energy and Infrastructure. [Online]. Available: http://www.mei.gov.on.ca/en/energy/gea/

[14] "Renewable Energy Feed-in Tariff Program," Ontario Power Authority. [Online]. Available: http://fit.powerauthority.on.ca

[15] "Ontario Leadership in Renewable Energy," Ontario Ministry of Economic Development and Trade. [Online]. Available: http://www.ontariocanada.com/ontcan/1medt/en/cleantech_en.jsp

[16] "Demand Response Program," Ontario Power Authority (OPA). [Online]. Available: http://www.powerauthority.on.ca/Page.asp?PageID=1212&SiteNodeID=147

[17] "The Energy Hub Management System: Enabling and Empowering Energy Managers Through Increased Information and Control," University of Waterloo. [Online]. Available: http://www.energyhub.uwaterloo.ca/

REFERENCES

[18] M. C. Bozchalui, "Optimal Operation of Energy Hubs in the Context of Smart Grids," PhD Thesis, Department of Electrical and Computer Engineering, University of Waterloo, 2011.

[19] "Enabling Tomorrow's Electricity System," Report of the Ontario Smart Grid Forum, Feb. 2009. [Online]. Available: http://www.ieso.ca/imoweb/pubs/ smart_grid/Smart_Grid_Forum-Report.pdf

[20] "Modernizing Ontario's Electricity System: Next Steps," Report of the Ontario Smart Grid Forum, May 2011. [Online]. Available: http://www.ieso.ca/imoweb/ pubs/smart_grid/Smart_Grid_Forum-Report-May_2011.pdf

[21] A. Bose, "Smart Transmission Grid Applications and Their Supporting Infrastructure," *IEEE Trans. Smart Grid*, vol. 1, no. 1, pp. 11–19, Jun. 2010.

[22] "Smart Grid: an Introduction." [Online]. Available: http://www.oe.energy.gov/ DocumentsandMedia/DOE_SG_Book_Single_Pages.pdf

[23] R. E. Brown, "Impact of Smart Grid on Distribution System Design," in *Proc. IEEE PES General Meeting*, Jul. 2008, pp. 1–4.

[24] F. Goodman and M. McGranaghan, "EPRI Research Plan for Advanced Distribution Automation," in *Proc. IEEE PES General Meeting*, vol. 3, 2005, p. 2620.

[25] J. D. Kueck and B. J. Kirby, "Distribution System of the Future," Oak Ridge National Laboratory. [Online]. Available: http://www.ornl.gov/~webworks/cppr/ y2001/rpt/116950.pdf

[26] G. T. Heydt, "The Next Generation of Power Distribution Systems," *IEEE Trans. Smart Grid*, vol. 1, no. 3, pp. 225–235, Dec. 2010.

REFERENCES

[27] A. S. Bouhouras, G. T. Andreou, D. P. Labridis, and A. G. Bakirtzis, "Selective Automation Upgrade in Distribution Networks Towards a Smarter Grid," *IEEE Trans. Smart Grid*, vol. 1, no. 3, pp. 278–285, Dec. 2010.

[28] A. P. S. Meliopoulos, G. Cokkinides, R. Huang, E. Farantatos, S. Choi, Y. Lee, and X. Yu, "Smart Grid Technologies for Autonomous Operation and Control," *IEEE Trans. on Smart Grid*, vol. 2, no. 1, pp. 1–10, Mar. 2011.

[29] A. Schneider, "The Smart Grid in Review." [Online]. Available: http://www.kema.com/consulting_services/cross_sector/INC/Automation_Insight/ \December_2008/Smart_Grid_Review.asp

[30] "Smart Grid Definitions," Leonardo Energy. [Online]. Available: http://www. leonardo-energy.org/what-definition-smart-grid

[31] H. Farhangi, "The Path of the Smart Grid," *IEEE Power and Energy Magazine*, vol. 8, no. 1, pp. 18–28, Jan.-Feb. 2010.

[32] D. Bassett, K. Clinard, J. Grainger, S. Purucker, and D. Ward, "Tutorial Course: Distribution Automation," *IEEE Tutorial Publication*, 1988.

[33] E. K. Chan and H. Ebenhoh, "The Implementation and Evolution of a SCADA System for a Large Distribution Network," *IEEE Trans. Power Syst.*, vol. 7, no. 1, pp. 320–326, Feb. 1992.

[34] J. Carr, "Considerations in the Adoption of a Full Scale Distribution Automation System," *IEEE Trans. Power App. Syst.*, vol. PAS-100, no. 3, pp. 1167–1172, Mar. 1981.

[35] D. L. Brown, J. W. Skeen, P. Daryani, and F. A. Rahimi, "Prospects for Distribution Automation at Pacific Gas & Electric Company," *IEEE Trans. Power Del.*, vol. 6, no. 4, pp. 1946–1954, Oct. 1991.

REFERENCES

[36] "Value of Distribution Automation Application," California Energy Commission, Apr. 2007. [Online]. Available: http://www.energy.ca.gov/2007publications/ CEC-500-2007-028/CEC-500-2007-028.PDF

[37] R. Baldick and F. F. Wu, "Efficient Integer Optimization Algorithms for Optimal Coordination of Capacitors and Regulators," *IEEE Trans. Power Syst.*, vol. 5, no. 3, pp. 805–812, Aug. 1990.

[38] Y. Y. Hsu and F. C. Lu, "A Combined Artificial Neural Network-fuzzy Dynamic Programming Approach to Reactive Power/voltage Control in a Distribution Substation," *IEEE Trans. Power Syst.*, vol. 13, no. 4, pp. 1265–1271, Nov. 1998.

[39] V. Borozan, M. E. Baran, and D. Novosel, "Integrated Volt/Var Control in Distribution Systems," in *Proc. IEEE PES Winter Meeting*, vol. 3, 2001, pp. 1485–1490.

[40] J. Kearly, A. Y. Chikhani, R. Hackam, M. M. A. Salama, and V. H. Quintana, "Microprocessor Controlled Reactive Power Compensator for Loss Reduction in Radial Distribution Feeders," *IEEE Trans. Power Del.*, vol. 6, no. 4, pp. 1848–1855, Oct. 1991.

[41] M. M. A. Salama, N. Manojlovic, V. H. Quintana, and A. Y. Chikhani, "Real-time Optimal Reactive Power Control for Distribution Networks," *International Journal of Electrical Power & Energy Systems*, vol. 18, no. 3, pp. 185 –193, 1996.

[42] I. Roytelman, B. K. Wee, and R. L. Lugtu, "Volt/var Control Algorithm for Modern Distribution Management System," *IEEE Trans. Power Syst.*, vol. 10, no. 3, pp. 1454–1460, Aug. 1995.

[43] M. Liu, S. K. Tso, and Y. Cheng, "An Extended Nonlinear Primal-dual Interior-Point Algorithm for Reactive-power Optimization of Large-scale Power Systems with

REFERENCES

Discrete Control Variables," *IEEE Trans. Power Syst.*, vol. 17, no. 4, pp. 982–991, Nov. 2002.

[44] M. B. Liu, C. A. Cañizares, and W. Huang, "Reactive Power and Voltage Control in Distribution Systems with Limited Switching Operations," *IEEE Trans. Power Syst.*, vol. 24, no. 2, pp. 889–899, May 2009.

[45] I. Roytelman and V. Ganesan, "Coordinated Local and Centralized Control in Distribution Management Systems," *IEEE Trans. Power Del.*, vol. 15, no. 2, pp. 718–724, Apr. 2000.

[46] J. J. Grainger and S. Civanlar, "Volt/var Control on Distribution Systems with Lateral Branches Using Shunt Capacitors and Voltage Regulators Part I: The Overall Problem," *IEEE Trans. Power App. Syst.*, vol. PAS-104, no. 11, pp. 3278–3283, Nov. 1985.

[47] M. Dixon, "Autodaptive Volt/var Management System," in *Proc. Rural Electric Power Conference*, 2001, pp. D4/1–D4/8.

[48] J. H. Teng and C. Y. Chang, "A Branch Voltage based Three Phase Load Flow Method for Unbalanced Distribution Systems," in *Proc. International Conference on Power System Technology*, vol. 2, 2000, pp. 601–606.

[49] M. R. Irving and M. J. H. Sterling, "Efficient Newton-Raphson Algorithm for Load-flow Calculation in Transmission and Distribution Networks," *IEE Proc. Gen. Tran. and Dist.*, vol. 134, no. 5, pp. 325–330, Sep. 1987.

[50] R. D. Zimmerman and H. D. Chiang, "Fast Decoupled Power Flow for Unbalanced Radial Distribution Systems," *IEEE Trans. Power Syst.*, vol. 10, no. 4, pp. 2045–2052, Nov. 1995.

REFERENCES

[51] W. H. Kersting and D. L. Mendive, "An Application of ladder Network Theory to the Solution of Three Phase Radial Load Flow Problem," in *Proc. IEEE PES Winter Meeting*, 1976.

[52] W. H. Kersting, "A Method to Teach the Design and Operation of a Distribution System," *IEEE Trans. Power App. Syst.*, vol. PAS-103, no. 7, pp. 1945–1952, Jul. 1984.

[53] M. M. A. Salama and A. Y. Chikhani, "A Simplified Network Approach to the VAr Control Problem for Radial Distribution Systems," *IEEE Trans. Power Del.*, vol. 8, no. 3, pp. 1529–1535, Jul. 1993.

[54] E. Santacana, G. Rackliffe, L. Tang, and X. Feng, "Getting Smart," *IEEE Power and Energy Magazine*, vol. 8, no. 2, pp. 41–48, Mar.-Apr. 2010.

[55] M. E. Elkhatib, R. El-Shatshat, and M. M. A. Salama, "Novel Coordinated Voltage Control for Smart Distribution Networks with DG," *IEEE Trans. on Smart Grid*, vol. 2, no. 4, pp. 598–605, Dec. 2011.

[56] J. See, W. Carr, and S. E. Collier, "Real Time Distribution Analysis for Electric Utilities," in *Proc. IEEE Rural Electric Power Conference*, Apr. 2008, pp. B5–B5–8.

[57] E. T. Jauch, "'Conservation Biased' Distribution Volt/Var/(kW) Management," in *Proc. IEEE PES General Meeting*, Jul. 2009, pp. 1–7.

[58] S. Bruno, S. Lamonaca, G. Rotondo, U. Stecchi, and M. La Scala, "Unbalanced Three-Phase Optimal Power Flow for Smart Grids," *IEEE Trans. Ind. Electron.*, vol. 58, no. 10, pp. 4504–4513, Oct. 2011.

[59] M. Abdel-Akher, K. M. Nor, and A. H. A. Rashid, "Improved Three-Phase Power-Flow Methods Using Sequence Components," *IEEE Trans. Power Syst.*, vol. 20, no. 3, pp. 1389–1397, Aug. 2005.

REFERENCES

[60] C. S. Cheng and D. Shirmohammadi, "A Three-phase Power Flow Method for Real-time Distribution System Analysis," *IEEE Trans. Power Syst.*, vol. 10, no. 2, pp. 671–679, May 1995.

[61] Y. T. Hsiao, "Multiobjective Evolution Programming Method for Feeder Reconfiguration," *IEEE Trans. Power Syst.*, vol. 19, no. 1, pp. 594–599, Feb. 2004.

[62] R. F. Chang and C. N. Lu, "Feeder Reconfiguration for Load Factor Improvement," in *Proc. IEEE PES Winter Meeting*, vol. 2, 2002, pp. 980–984.

[63] K. Nara, A. Shiose, M. Kitagawa, and T. Ishihara, "Implementation of Genetic Algorithm for Distribution Systems Loss Minimum Re-configuration," *IEEE Trans. Power Syst.*, vol. 7, no. 3, pp. 1044–1051, Aug. 1992.

[64] S. Sundhararajan and A. Pahwa, "Optimal Selection of Capacitors for Radial Distribution Systems Using a Genetic Algorithm," *IEEE Trans. Power Syst.*, vol. 9, no. 3, pp. 1499–1507, Aug. 1994.

[65] G. Levitin, A. Kalyuzhny, A. Shenkman, and M. Chertkov, "Optimal Capacitor Allocation in Distribution Systems Using a Genetic Algorithm and a Fast Energy Loss Computation Technique," *IEEE Trans. Power Del.*, vol. 15, no. 2, pp. 623–628, Apr. 2000.

[66] P. Nallagownden, L. T. Thin, N. C. Guan, and C. M. H. Mahmud, "Application of Genetic Algorithm for the Reduction of Reactive Power Losses in Radial Distribution System," in *Proc. IEEE Power and Energy Conference*, Nov. 2006, pp. 76–81.

[67] W. M. Lin and H. C. Chin, "Preventive and Corrective Switching for Feeder Contingencies in Distribution Systems with Fuzzy Set Algorithm," *IEEE Trans. Power Del.*, vol. 12, no. 4, pp. 1711–1716, Oct. 1997.

[68] "BARON: Branch and Reduce Optimization Navigator," University of Illinois at Urbana-Champaign. [Online]. Available: http://archimedes.scs.uiuc.edu/

REFERENCES

[69] "DICPOT," GAMS Development Corporation. [Online]. Available: http://archimedes.scs.uiuc.edu/

[70] N. J. Rabadi, M. M. A. Nasr, and M. A. Hijazi, "The Potential and Strategies for Demand-side Management within the Industrial Sector in Jordan–II," *Journals of Energy Conversion and Management*, vol. 32, no. 6, pp. 585–593, 1991.

[71] D. Violette, "Demand-side Management (DSM): Future Role in Energy Markets," Meetings of the National Energy Board Calgary, Alberta, Apr. 2006. [Online]. Available: http://www.summitblue.com/attachments/0000/0441/P48_-_Demand-Side_Management_-_Future_Role_in_Energy_Markets.pdf

[72] K. Johnson and M. D. Group, "The Fundamental of Linking Demand Side Management Strategies with Program Implementation Tactics," Market Development Group. [Online]. Available: www.marketdevelop.com

[73] R. M. Delgado, "Demand-side Management Alternatives," *Proc. of the IEEE*, vol. 73, no. 10, pp. 1471–1488, Oct. 1985.

[74] E. Gardner, "Load management DSM: Past, Present and Future," in *Proc. Rural Electric Power Conference*, 1995, pp. A2/1–A213.

[75] "Primer on Demand Side Management: A Report Prepared for the World Bank," Charles River Associates, Oakland, California, Feb. 2005.

[76] G. Strbac, "Demand Side Management: Benefits and Challenges," *Journals of Energy Policy*, vol. 36, no. 12, pp. 4419–4426, 2008.

[77] H. Saele and O. S. Grande, "Demand Response From Household Customers: Experiences From a Pilot Study in Norway," *IEEE Trans. on Smart Grid*, vol. 2, no. 1, pp. 102–109, Mar. 2011.

REFERENCES

[78] C. M. Chu and T. L. Jong, "A Novel Direct Air-Conditioning Load Control Method," *IEEE Trans. Power Syst.*, vol. 23, no. 3, pp. 1356–1363, Aug. 2008.

[79] D. C. Wei and N. Chen, "Air Conditioner Direct Load Control by Multi-pass Dynamic Programming," *IEEE Trans. Power Syst.*, vol. 10, no. 1, pp. 307–313, Feb. 1995.

[80] S. El-Ferik, S. A. Hussain, and F. M. Al-Sunni, "Identification of Physically Based Models of Residential Air-conditioners for Direct Load Control Management," in *Proc. Asian Control Conference*, vol. 3, Jul. 2004, pp. 2079–2087.

[81] K. F. Fong, V. I. Hanby, and T. T. Chow, "HVAC System Optimization for Energy Management by Evolutionary Programming," *Journals of Energy and Buildings*, vol. 38, no. 3, pp. 220–231, 2006.

[82] W. Z. Huang, M. Zaheeruddin, and S. H. Cho, "Dynamic Simulation of Energy Management Control Functions for HVAC Systems in Buildings," *Journals of Energy Conversion and Management*, vol. 47, no. 78, pp. 926–943, 2006.

[83] "Assessment of Demand Response and Advanced Metering: Staff Report," U.S. Department of Energy: Federal Energy Regulatory Comission, Sep. 2007. [Online]. Available: Available:http://www.ferc.gov/legal/staff-reports/ 09-07-demand-response.pdf

[84] A. T. D. Almeida and A. H. Rosenfeld, "Demand-Side Management and Electricity End-use Efficiency," *Journal of Applied Sciences*, vol. 149, 1988.

[85] A. Moholkar, P. Klinkhachorn, and A. Feliachi, "Effects of Dynamic Pricing on Residential Electricity Bill," in *Proc. IEEE PES Conference and Exposition*, Oct. 2004, pp. 1030–1035.

[86] H. Allcott, "Rethinking Real Time Electricity Pricing," MIT Center for Energy and Environmental Policy Research, Oct. 2009.

REFERENCES

[87] R. Beck, "Distribution Efficiency Initiative," Northwest Energy Alliance, Dec. 2007. [Online]. Available: www.rwbeck.com/neea.pdf

[88] T. Wilson, K. Benson, and D. Bell, "Saving Megawatts with Voltage Optimization," PCS Utilidata. [Online]. Available: http://utilidata.com/userfiles/file/Industrial% 20Voltage%20Optimization\.pdf

[89] A. I. Cohen and C. C. Wang, "An Optimization Method for Load Management Scheduling," *IEEE Trans. Power Syst.*, vol. 3, no. 2, pp. 612–618, May 1988.

[90] C. O. Bjork and B. G. Karlsson, "Load Management Applications for Industrial Loads," *IEEE Trans. Power App. Syst.*, vol. PAS-104, no. 8, pp. 2058–2063, Aug. 1985.

[91] C. N. Kurucz, D. Brandt, and S. Sim, "A Linear Programming Model for Reducing System Peak through Customer Load Control Programs," *IEEE Trans. Power Syst.*, vol. 11, no. 4, pp. 1817–1824, Nov. 1996.

[92] "ANSI C84.1-2006," American National Standard for Electric Power Systems & Equipment-Voltage Rating (60Hz). [Online]. Available: http://www.nema.org/stds/ complimentary-docs/upload/ANSI20C84-1.pdf

[93] M. Geidl and G. Andersson, "Optimal Power Flow of Multiple Energy Carriers," *IEEE Trans. Power Syst.*, vol. 22, no. 1, pp. 145–155, Feb. 2007.

[94] M. Geidl, G. Koeppel, P. Favre-Perrod, B. Klockl, G. Andersson, and K. Frohlich, "Energy Hubs for the Future," *IEEE Power and Energy Magazine*, vol. 5, no. 1, pp. 24–30, Jan.-Feb. 2007.

[95] M. Schulze, L. Friedrich, and M. Gautschi, "Modeling and Optimization of Renewables: Applying the Energy Hub Approach," in *Proc. IEEE International Conference Sustainable Energy Technologies*, Nov. 2008, pp. 83–88.

REFERENCES

[96] X. Guan, Z. Xu, and Q. S. Jia, "Energy-Efficient Buildings Facilitated by Microgrid," *IEEE Trans. Smart Grid*, vol. 1, no. 3, pp. 243–252, Dec. 2010.

[97] A. Molderink, V. Bakker, M. G. C. Bosman, J. L. Hurink, and G. J. M. Smit, "Management and Control of Domestic Smart Grid Technology," *IEEE Trans. Smart Grid*, vol. 1, no. 2, pp. 109–119, Sep. 2010.

[98] M. A. A. Pedrasa, T. D. Spooner, and I. F. MacGill, "Coordinated Scheduling of Residential Distributed Energy Resources to Optimize Smart Home Energy Services," *IEEE Trans. Smart Grid*, vol. 1, no. 2, pp. 134–143, Sep. 2010.

[99] S. Ashok and R. Banerjee, "Optimal Operation of Industrial Cogeneration for Load Management," *IEEE Trans. Power Syst.*, vol. 18, no. 2, pp. 931–937, May. 2003.

[100] M. E. Baran and M. Y. Hsu, "Volt/Var Control at Distribution Substations," *IEEE Trans. Power Syst.*, vol. 14, no. 1, pp. 312–318, Feb. 1999.

[101] G. A. McNaughton and R. Saint, "Enterprise Integration Implications for Home-area Network Technologies," in *Proc. IEEE Innovative Smart Grid Technologies*, Jan. 2010, pp. 1–5.

[102] G. Patricio and L. Gomes, "Smart House Monitoring and Actuating System Development Using Automatic Code Generation," in *Proc. IEEE International Conference on Industrial Informatics*, Jun. 2009, pp. 256–261.

[103] K. Gill, S. H. Yang, F. Yao, and X. Lu, "A ZigBee-based Home Automation System," *IEEE Trans. Consum. Electron.*, vol. 55, no. 2, pp. 422–430, May 2009.

[104] W. Kastner, G. Neugschwandtner, S. Soucek, and H. M. Newmann, "Communication Systems for Building Automation and Control," *Proc. of the IEEE*, vol. 93, no. 6, pp. 1178–1203, Jun. 2005.

REFERENCES

[105] D. Dietrich, D. Bruckner, G. Zucker, and P. Palensky, "Communication and Computation in Buildings: A Short Introduction and Overview," *IEEE Trans. Ind. Electron.*, vol. 57, no. 11, pp. 3577–3584, Nov. 2010.

[106] N. Chari, "Outlining the Communications Behind Distribution Automation," Renew Grid Magazine, Apr. 2011. [Online]. Available: http://gridcom.tropos.com/docs_import/news/Outlining_Communications_Behind.pdf

[107] R. Uluski and G. Gilchrist, "Communications for Distribution Automation." [Online]. Available: http://www.elp.com/index/display/article-display/290248/articles/utility-automation-engineering-td/volume-12/issue-4/features/communications-for-distribution-automation.html

[108] V. Aravinthan, B. Karimi, V. Namboodiri, and W. Jewell, "Wireless Communication for Smart Grid Applications at Distribution level —Feasibility and Requirements," in *Proc. IEEE PES General Meeting*, Jul. 2011, pp. 1–8.

[109] X. Mamo, M. McGranaghan, R. Dugan, J. Maire, and O. Devaux, "A Roadmap for Developing Real Time Distribution System Simulation Tools for the Smart Grid," in *Proc. IET-CIRED Seminar: Smart Grids for Distribution*, Jun. 2008, pp. 1 –7.

[110] M. Fan, Z. Zhang, and C. E. Lin, "Discrete VAR Optimization in a Distribution System Using Mixed-integer Programming with an Expert System," *Journals of Electric Power Systems Research*, vol. 27, no. 3, pp. 191–201, 1993.

[111] R. H. Liang and C. K. Cheng, "Dispatch of Main Transformer ULTC and Capacitors in a Distribution System," *IEEE Trans. Power Syst.*, vol. 16, no. 4, pp. 625–630, Oct. 2001.

[112] S. S. Rao, *Engineering Optimization: Theory and Practice.* New York: John Wiley & Sons, Inc., 1996.

REFERENCES

[113] T. Terlaky, *Interior Point Methods of Mathematical Programming.* Dordrecht, The Netherlands: Kluwer Academic Publishers, 1996.

[114] F. D. Lewis, "Cutting Plane Techniques," University of Kentucky. [Online]. Available: http://www.cs.uky.edu/~lewis/cs-heuristic/text/integer/cutting.html

[115] J. Zhu, *Optimization of Power System Operation.* Hoboken, New Jersey: A John Wiley & Sons Inc. Publication, 2009.

[116] M. Kaplan, "Optimization of Number, Location, Size, Control Type, and Control Setting of Shunt Capacitors on Radial Distribution Feeders," *IEEE Trans. Power App. Syst.*, vol. PAS-103, no. 9, pp. 2659–2665, Sep. 1984.

[117] A. Merlin and H. Back, "Search for a Minimal-loss Operating Spanning Tree Configuration in an Urban Power Distribution System," in *Proc. 5th Power System Computing Conference*, 1975, pp. 1–18.

[118] F. C. Lu and Y. Y. Hsu, "Fuzzy Dynamic Programming Approach to Reactive Power/voltage Control in a Distribution Substation," *IEEE Trans. Power Syst.*, vol. 12, no. 2, pp. 681–688, May 1997.

[119] S. K. Goswami and S. K. Basu, "A New Algorithm for the Reconfiguration of Distribution Feeders for Loss Minimization," *IEEE Trans. Power Del.*, vol. 7, no. 3, pp. 1484–1491, Jul. 1992.

[120] I. Roytelman, V. Melnik, S. S. H. Lee, and R. L. Lugtu, "Multi-objective Feeder Reconfiguration by Distribution Management System," *IEEE Trans. Power Syst.*, vol. 11, no. 2, pp. 661–667, May 1996.

[121] T. E. DcDermott, I. Drezga, and R. P. Broadwater, "A Heuristic Nonlinear Constructive Method for Distribution System Reconfiguration," *IEEE Trans. Power Syst.*, vol. 14, no. 2, pp. 478–483, May 1999.

126

REFERENCES

[122] K. Nara, Y. Mishima, and T. Satoh, "Network Reconfiguration for Loss Minimization and Load Balancing," in *Proc. IEEE PES General Meeting*, vol. 4, Jul. 2003, p. 2418.

[123] A. Kunjur and S. Krishnamurty, "Genetic Algorithms in Mechanism Synthesis," Department of Mechanical Engineering, University of Massachusetts. [Online]. Available: http://www.ecs.umass.edu/mie/labs/mda/mechanism/papers/genetic.html

[124] D. E. Goldberg, *Genetic Algorithms in Search, Optimization and Machine Learning*, 1st ed. Boston: Addison-Wesley Longman Publishing Co, 1989.

[125] J. F. Gomez, H. M. Khodr, P. M. De Oliveira, L. Ocque, J. M. Yusta, R. Villasana, and A. J. Urdaneta, "Ant Colony System Algorithm for the Planning of Primary Distribution Circuits," *IEEE Trans. Power Syst.*, vol. 19, no. 2, pp. 996–1004, May 2004.

[126] Y. C. Huang, H. T. Yang, and C. L. Huang, "Solving the Capacitor Placement Problem in a Radial Distribution System Using Tabu Search Approach," *IEEE Trans. Power Syst.*, vol. 11, no. 4, pp. 1868–1873, Nov. 1996.

[127] Y. J. Jeon, J. C. Kim, J. O. Kim, J. R. Shin, and K. Y. Lee, "An Efficient Simulated Annealing Algorithm for Network Reconfiguration in Large-scale Distribution Systems," *IEEE Trans. Power Del.*, vol. 17, no. 4, pp. 1070–1078, Oct. 2002.

[128] "GAMS Release 2.25," A Users Guide, GAMS Development Corporation, 1998. [Online]. Available: http://www.gams.com/

[129] Stanford Business Software Inc. [Online]. Available: http://sbsi-sol-optimize.com/asp/sol_product_minos.htm

[130] "KNITRO," Electrical and Computer Engineering Department, Northwestern University. [Online]. Available: http://www.gams.com/dd/docs/solvers/knitro.pdf

REFERENCES

[131] "ILOG CPLEX 11.0 Users Manual," ILOG SA, Gentilly, France, 2008.

[132] S. L. Arlinghaus, *Practical Handbook of Curve Fitting*, 1st ed. Boca Raton: CRC Press, 1994.

[133] N. R. Draper and H. Smith, *Applied Regression Analysis*, 3rd ed. New York: Wiley, 1998.

[134] T. L. Wilson, "Measurement and Verification of Distribution Voltage Optimization Results for the IEEE Power & Energy Society," in *Proc. IEEE PES General Meeting*, Jul. 2010, pp. 1–9.

[135] P. Fairley, "An Easy Smart-Grid Upgrade Saves Power [Update]," *IEEE Spectrum*, vol. 47, no. 10, pp. 13–14, Oct. 2010.

[136] "Hydro Ottawa Participates in IESO Voltage Reduction Exercise," Hydro Ottawa News Release. [Online]. Available: http://www.hydroottawa.com/newsevents/ news_display.cfm?LANG=e&act=form&News_ID=228

[137] E. Hirst, "Electric Utilities and Energy Efficiency," Oak Ridge National Laboratory. [Online]. Available: http://www.ornl.gov/info/ornlreview/rev28_2/text/uti.htm

[138] B. Yuan and M. Gallagher, "A Hybrid Approach to Parameter Tuning in Genetic Algorithms," in *Proc. IEEE Congress on Evolutionary Computation*, vol. 2, Sep. 2005, pp. 1096 –1103.

[139] "Integration of storage in electrical distribution systems and its impact on the depth of penetration of DG," Natural Resources Canada. [Online]. Available: http://canmetenergy.nrcan.gc.ca/sites/canmetenergy.nrcan.gc. ca/files/files/pubs/2009-174_RP-TEC_411-IMPACT_Graovac_Wang_Iravani_e.pdf

[140] "A Guide to Electricity Charges for Business." [Online]. Available: http: //www.ieso.ca/imoweb/siteshared/electricity_charges.asp

REFERENCES

[141] "Global Adjustment." [Online]. Available: http://www.ieso.ca/imoweb/b100/b100_ga.asp

[142] "PSCAD," Manitoba-HVDC Research Centre. [Online]. Available: https://pscad.com/

[143] S. Paudyal, C. A. Cañizares, and K. Bhattacharya, "Optimal Operation of Distribution Feeders in Smart Grids," *IEEE Trans. Ind. Electron.*, vol. 58, no. 10, pp. 4495–4503, Oct. 2011.

[144] S. Paudyal, C. A. Cañizares, and K. Bhattacharya, "Three-phase Distribution OPF in Smart Grids: Optimality versus Computational Burden," in *Proc. Innovative Smart Grid Technologies (ISGT Europe)*, Dec. 2011, pp. 1–7.

[145] S. Paudyal, C. A. Cañizares, and K. Bhattacharya, "Optimal Operation of Industrial Energy Hubs in Smart Grids," *IEEE Trans. on Smart Grid*, pp. 1–8, Jul. 2012, submitted for publication.